DISSERTATIONES
MEDICINAE
UNIVERSITATIS
TARTUENSIS
322

LIIS PREEM

Design and characterization of antibacterial electrospun drug delivery systems for wound infections

DISSERTATIONES MEDICINAE UNIVERSITATIS TARTUENSIS
322

DISSERTATIONES MEDICINAE UNIVERSITATIS TARTUENSIS
322

LIIS PREEM

Design and characterization of antibacterial electrospun drug delivery systems for wound infections

UNIVERSITY OF TARTU
Press
1632

Institute of Pharmacy, Faculty of Medicine, University of Tartu, Estonia

Dissertation is accepted for the commencement of the degree of Doctor of Philosophy (in Pharmacy) on 15.12.2021 by the Council of the Faculty of Medicine, University of Tartu, Estonia.

Supervisors: Associate Professor Karin Kogermann, PhD
Institute of Pharmacy, Faculty of Medicine
University of Tartu, Estonia

Associate Professor Andres Meos, PhD
Institute of Pharmacy, Faculty of Medicine
University of Tartu, Estonia

Professor Tanel Tenson, PhD
Institute of Technology, Faculty of Science and Technology
University of Tartu, Estonia

Reviewed by: Associate Professor Niilo Kaldalu, PhD
Institute of Technology, Faculty of Science and Technology
University of Tartu, Estonia

Associate Professor and Lecturer Meeme Utt, PhD
Institute of Biomedicine and Translational Medicine, Faculty of Medicine
Institute of Pharmacy, Faculty of Medicine
University of Tartu, Estonia

Opponent: Professor Hanne Hjorth Tønnesen, PhD
Department of Pharmacy,
University of Oslo, Norway

Commencement: 18.02.2022

Publication of this dissertation is granted by the University of Tartu.

This research was supported by the Estonian Research Council grants ETF7980, PUT1088, IUT-2-22, and PRG335, European Regional Development Fund through the Centre of Excellence for Molecular Cell Technology, Estonian Ministry of Education and Research and European Regional Development Fund (Kristjan Jaak Scholarship, Dora Pluss Programme and University of Tartu ASTRA project PER ASPERA), and L'ORÉAL Baltic "For Women In Science" fellowship 2018 (K. Kogermann).

ISSN 1024-395X
ISBN 978-9949-03-804-6 (print)
ISBN 978-9949-03-805-3 (pdf)

University of Tartu Press
www.tyk.ee

CONTENTS

LIST OF ORIGINAL PUBLICATIONS

Given thesis is based on the following original publications referred to in the text by Roman numerals (I–IV):

I **Preem, L.**, Mahmoudzadeh, M., Putrinš, M., Meos, A., Laidmäe, I., Romann, T., Aruväli, J., Härmas, R., Koivuniemi, A., Bunker, A., Tenson, T., Kogermann, K., 2017. Interactions between Chloramphenicol, Carrier Polymers, and Bacteria-Implications for Designing Electrospun Drug Delivery Systems Countering Wound Infection. *Molecular Pharmaceutics*, 14 (12), 4417−4430.

II Zupančič, Š., **Preem, L.**, Kristl, J., Putrinš, M., Tenson, T., Kocbek, P., Kogermann, K., 2018. Impact of PCL Nanofiber Mat Structural Properties on Hydrophilic Drug Release and Antibacterial Activity on Periodontal Pathogens. *European Journal of Pharmaceutical Sciences*, 122, 347−358.

III **Preem, L.**, Vaarmets, E., Meos, A., Jõgi, I., Putrinš, M., Tenson, T., Kogermann, K., 2019. Effects and Efficacy of Different Sterilization and Disinfection Methods on Electrospun Drug Delivery Systems. *International Journal of Pharmaceutics*, 567, 118450−118450.

IV **Preem, L.**, Bock, F., Hinnu, M., Putrins, M., Sagor, K., Tenson, T., Meos, A., Ostergaard, J., Kogermann, K., 2019. Monitoring of Antimicrobial Drug Chloramphenicol Release from Electrospun Nano- and Microfiber Mats Using UV Imaging and Bacterial Bioreporters. *Pharmaceutics*, 11 (9), 487.

Contribution of Liis Preem to original publications (I–IV):

Publication I: participation in study design; performing majority of the experiments (design and preparation of electrospun matrices, ATR-FTIR, DSC, contact angle measurements, *in vitro* drug release, swelling and weight loss, *in vitro* cytotoxicity testing, antimicrobial activity testing), coordinating experiments and participating in sample preparation for the analyses (SEM, XRPD, HPLC, RSM, MIP, BET analyses), performing data analysis, writing the paper.

Publication II: participation in study design, performing part of the experiments (solid state analyses, *in vitro* cytotoxicity, antimicrobial activity testing), participation in data analysis, co-writing the paper.

Publication III: participation in study design, performing majority of the experiments, coordinating some experiments (gamma sterilization, plasma sterilization), performing data analysis and writing the paper.

Publication IV: participation in study design, performing majority of the experiments (preparation of electrospun matrices, SEM, solid state and HPLC analyses, drug release testing into buffer solution and agar hydrogel, antibacterial activity testing), participating in data analysis, co-writing the paper.

ABBREVATIONS

A. actinomycetemcomitans	*Aggregatibacterium actinomycetemcomitans*
AA	acetic acid
API	active pharmaceutical ingredient
ATR	attenuated total reflection
BET	Brunauer-Emmett-Teller
CAM	chloramphenicol
CF	chloroform
CFU	colony-forming unit
CIP	ciprofloxacin
DDS	drug delivery system
DMEM	Dulbecco's Modified Eagle medium
DMSO	dimethyl sulfoxide
DSC	differential scanning calorimetry
DSM	*Deutsche Sammlung von Mikroorganismen* (German Collection of Microorganisms)
E. coli	*Escherichia coli*
ECM	extracellular matrix
F. nucleatum	*Fusobacterium nucleatum spp polymorphum*
FA	formic acid
FDA	Food and Drug Administration
FTG	fluid thioglycollate medium
FTIR	Fourier transform infrared
HPLC	high-performance liquid chromatography
LB	lysogeny broth
MD	molecular dynamics
MET	methanol
MIC	minimal inhibitory concentration
MIP	mercury intrusion porosimetry
MTZ	metronidazole
P. gingivalis	*Porphyromonas gingivalis*
PBS	phosphate buffered saline
PCL	polycaprolactone
PEO	poly(ethylene oxide)
PLA	polylactic acid
PVP	polyvinylpyrrolidone
RH	relative humidity
rpm	rotations per minute
RSM	Raman scattering microspectroscopy
S. aureus	*Staphylococcus aureus*
S. mutans	*Streptococcus mutans*
SEM	scanning electron microscopy
TSB	tryptic soy broth
UV	ultraviolet
UV-Vis	ultraviolet-visible
XRD	X-ray diffraction

1. INTRODUCTION

Nonhealing wounds represent an escalating socioeconomic problem in modern society (Järbrink et al., 2017). Several factors contribute to the pathological progression of wounds, but it is more and more recognized that biofilm and microbial unbalance that overwhelms host's immune responses play a major part in creating unfavorable wound environment stalling or preventing healing (P. G. Bowler et al., 2001; D. Leaper et al., 2015). Thus, antimicrobial strategies have an irreplaceable part in the management of these wounds (Daeschlein, 2013).

Systemic administration of antibiotics is indicated if the wound is severely infected (Lee et al., 2005), although this poses a risk of toxicity and insufficient local drug levels in the wound (P. G. Bowler et al., 2001; Rhoads et al., 2008). The latter can increase the risk for developing antibiotic resistance and initiate persister formation (Andersson & Hughes, 2014). Alternatively, traditional topical pharmaceutical products, like solutions, ointments, creams, can be used, despite the inconvenience of needing frequent administration, loss of rheological properties due to absorption of wound exudate and lacking effectiveness in the presence of wound exudate or biofilm (J. S. Boateng et al., 2008; Siddiqui & Bernstein, 2010). As a drug needs proper delivery system to fully exhibit its therapeutic potential, incorporating antimicrobial drugs to advanced wound dressings could help to improve therapeutic outcomes (J. Boateng & Catanzano, 2015).

Electrospinning represents a highly flexible and robust method for the production of polymeric nano- and microfiber matrices, allowing relatively easy incorporation of different drugs to create versatile drug delivery systems (DDSs) with a wide range of drug release kinetics (Kajdič et al., 2019). Polymeric DDSs have the capability to deliver drugs to the site of action at a controlled rate and establish localized, clinically relevant drug concentrations for extended periods of time, hence have the potential to improve the therapeutic efficacy, reduce toxicity and enhance patient compliance (Han et al., 2009; Rambhia & Ma, 2015).

In addition, electrospun fibers possess many useful properties for wound care application, including oxygen permeability, high effective surface area and porosity promoting hemostasis and absorption of wound exudate (Rieger et al., 2013). Also, the morphology of electrospun fibers resembles natural skin extracellular matrix (ECM) that promotes cell adhesion, migration and proliferation, and reduces scar formation (Vasita & Katti, 2006; Zahedi et al., 2009). Thus, electrospun fiber matrices have great potential to be used as wound dressings and localized DDSs.

Due to the novelty of electrospinning as a method for creating DDSs, much is still unknown about the impact of different material and process parameters on the structural, physicochemical and biopharmaceutical properties of electrospun fiber matrices and how these affect the *in vivo* performance. Better under-

standing of these relationships would help to guide rational design of safe and effective electrospun fibrous wound dressings.

The present research work aimed to develop antibacterial drug-loaded electrospun matrices intended for the prevention and local treatment of wound infections, using different carrier polymers and antibacterial drugs. The main hypotheses were that differently designed electrospun matrices have different physicochemical and biopharmaceutical properties and depending on the drug release profile, these matrices have different antimicrobial efficacy. Comprehensive characterization of these developed DDSs was carried out to gain understanding of the essential factors contributing to their performance and quality. Insight about the interactions between carrier polymers and drugs at the molecular level and how these affect bulk properties and structural features of the fiber matrices was sought. Novel analytical methods were developed besides established methods to improve understanding and rationalize the drug release behavior and antibacterial activity of electrospun fiber matrices.

2. LITERATURE REVIEW

2.1. Wounds

Skin is the largest single organ of the body, continuous with the mucous membranes, forming a barrier that protects the body from external environment and helps to maintain the internal environment. A wound is a loss of epithelial tissue integrity causing impaired protective functions of the skin and mucous membranes. The damaging factor can be external (e.g., surgery, chemicals, temperature, friction, pressure) or internal (underlying disease, e.g., diabetes, carcinoma). Wounds can be classified in several different ways with a view to their management and healing: etiology, location, timing, depth of the injury, presence or likeliness of developing infection etc. (N. J. Percival, 2002)

Normal wound healing occurs in four overlapping stages: hemostasis, inflammation, proliferation, and remodeling. After injury, platelets are first to arrive at the wound site where they regulate the formation of a blood clot. Pro-inflammatory macrophages, neutrophils and T cells carry out inflammatory response to cleanse the wound from foreign particles. The proliferation stage is characterized by keratinocytes migration for re-epithelialization, rapid proliferation of endothelial cells for angiogenesis and fibroblasts producing ECM proteins and improving wound contraction. Ultimately, remodeling converts the healing wound to a strong and flexible barrier (Guo & DiPietro, 2010).

Disturbances in this well-orchestrated and finely balanced process can cause improper or impaired wound healing. Hypoxia, old age, infection, stress, medication (e.g. glucocorticoid steroids), obesity, alcohol consumption, smoking and poor nutrition are known factors to impair wound healing (Guo & DiPietro, 2010). In oral cavity, wound healing has additional challenges due to bacteria-laden environment and constant physical trauma (Toma et al., 2021). Non-healing wounds are mostly associated with predisposing conditions, like ischemia, diabetes, venous stasis disease or pressure. Due to the growth of elderly population, epidemic obesity and related chronic diseases, non-healing wounds are an escalating burden on the healthcare. The related expenditures are enormous and sharply increasing. For example, in 2016, chronic wounds presented a 5.5% cost to the National Health Service in Wales (Phillips et al., 2016), and an evaluation in 2018 revealed that in Unites States, Medicare spending estimates for all wound types ranged from $28.1 to $96.8 billion (Nussbaum et al., 2018). Reduced quality of life and humanistic burden is an additional cost not only measured in money.

2.2. Wound infection

Skin and mucous membranes that are continuous with it at body openings are colonized by microorganisms that in normal situations do not have access to the underlying tissues. Once the protective barrier is compromised, the wound will

be contaminated by the microbes from the host and the surrounding environment. Depending on the replication status of those microbes and host response, the wound is classified as being contaminated (presence of non-dividing microbial cells), colonized (presence of dividing microbial cells with no harm to the host), critically colonized (an intermediate stage with presence of dividing microbial cells and beginning of local tissue responses) or infected (presence of dividing microbial cells and host injury). This represents a wound infection continuum (Edwards & Harding, 2004). Whereas the first two stages are considered normal, the latter two stages disrupt the orderly wound healing process. Before the wound exhibits the classical signs of infection, more subtle signs exist due to the microbial imbalance, thus already needing antimicrobial intervention. Bacterial load of more than 10^5 bacteria per gram of tissue has been used to diagnose infection and start antimicrobial treatment. However, the validity of this has been questioned as both the hosts' immunological status and underlying pathologies together with microbial phenotype, virulence factors and synergistic effects between some microbial species affect the course of wound healing (Philip G. Bowler, 2003; Howell-Jones et al., 2005).

2.3. Wound microbiology

The diversity of microorganisms present in a wound is affected by several factors, including wound type, location, depth, oxygenation and the conditions of host immune system (P. G. Bowler et al., 2001). Most wound colonizers are endogenous (coming from the skin, gastrointestinal, oropharyngeal or genitourinary mucosae) as most exogenous environmental contaminants are not able to replicate in a wound.

Most common bacteria isolated from skin wounds are *Staphylococcus aureus* and coagulase-negative staphylococci. Other frequent isolates include *Enterococcus faecalis*, *Pseudomonas aeruginosa*, *Escherichia coli*, *Klebsiella spp.*, *Proteus spp.*, *Prevotella spp.*, *Bacteroides spp.*, *Peptostreptococcus spp.*, *Porphyromonas spp.* etc. (Howell-Jones et al., 2005; Siddiqui & Bernstein, 2010). *Porphyromonas gingivalis*, *Parvimonas micra*, *Fusobacterium nucleatum* are associated with oral ulcerations (Laheij et al., 2013). Molecular techniques have shed light on the true complexity and polymicrobial nature of infected wounds, whereas routine microbial cultures largely underestimate the diversity of strict anaerobic bacteria and yeasts (Davies et al., 2001; Steven L Percival et al., 2015; Rhoads et al., 2012). Although the find of certain bacteria, especially in low numbers, may not be clinically relevant, some pathogens are always significant, e.g. group A beta-hemolytic streptococci, mycobacteria and *Clostridium perfringens* (Schraibman, 1990; Siddiqui & Bernstein, 2010). On the other hand, some commensal species may prevent colonization by pathogens and aid the healing process (Ovington, 2003). Wound microbiota is most likely dynamic over the course of wound progression. The longer the wound remains, the higher the number of both aerobic and anaerobic bacteria is. Due to

inadequate perfusion and low oxygen levels of chronic wounds, the growth of anaerobes is facilitated (Siddiqui & Bernstein, 2010). Also, some wound locations, for example periodontal pockets in case of periodontal diseases, have anaerobic environment that favors the growth of anaerobes, e.g., *Porphyromonas gingivalis*, *Treponema denticola,, Tannerella forsythia, Eubacterium spp., Prevotella spp., Peptostreptococcus spp., Fusobacterium spp., Bacteroides spp. and Selemonas spp.* (Alwaeli, 2018; Socransky & Haffajee, 2005).

Microorganisms tend to aggregate on surfaces to form a biofilm. Biofilms are complex communities of bacteria embedded within a matrix of extracellular polymeric substance usually attached to a surface of a substrate (Lam et al., 1980). Biofilm is the most common lifestyle of microorganisms in nature, for example, oral microbiome resides predominantly in the form of complex biofilms (Deo & Deshmukh, 2019). Clinical biofilms can be characterized by the presence of non-attached cell aggregates that are embedded in the secondary matrix composed of host material, including immune cells, that contribute to the chronic state of inflammation (Sønderholm et al., 2017). Sessile and planktonic (free-flowing) bacteria have significant phenotypic differences that make biofilms highly tolerant to hostile environmental conditions, like antibiotic treatments and hosts' immunological responses. In addition to the conventional resistance mechanisms, stationary-phase physiology of sessile bacteria, their slow growth in the center of the biofilm, and possible matrix mediated antibiotic binding and diffusion retardation contribute to the difficulties of biofilm eradication (Høiby et al., 2011). The local ecology of chronic non-healing wounds is supportive of biofilm formation. Biofilm-related infections typically develop slowly and have persistent nature, responding poorly to antimicrobial therapy and are rarely resolved solely by immune defenses (Brady et al., 2008; Stewart et al., 2001). Mature biofilm can also shed fragments of biofilm, planktonic bacteria and microcolonies, which can be the seeds for new biofilm colonies and invasive infection. Thus, special attention needs to be put on finding and implementing preventive and/or treatment strategies to fight against wound biofilm.

2.4. Wound infection management

Management of wound infection and biofilm comprises two major steps: removal of existing biofilm by different debridement techniques, and prevention of biofilm reconstitution by rational use of dressings and antimicrobials (D. J. Leaper et al., 2012).

Debridement for removing biofilm and necrotic tissue is one of the most effective ways to fight or prevent wound infection and enhance healing (S. L. Percival & Suleman, 2015). Non-debrided tissue obscures wound depth and condition, provides a focus for infection, provokes inflammation and interferes with wound granulation, contraction and epithelialization (Ousey & McIntosh, 2010; Steed et al., 1996; Wolcott et al., 2009). Desloughing reduces the potential areas of microbial attachment, thus making the formation of new biofilm

less likely. Moreover, killing the bacteria in biofilm alone is not sufficient as the presence of extracellular polymeric matrix without viable bacteria can still significantly delay wound healing and increase inflammation and risk for biofilm regrowth (Hemmi et al., 2000). It has also been shown that immature biofilm that remains after the debridement is more susceptible to antibiotic treatment (Wolcott et al., 2010). Though autolytic debridement via neutrophil-derived enzymes occurs naturally in early stages of wound healing, assisted surgical, enzymatic, autolytic or mechanical debridement accelerates the healing process (Steed et al., 1996). Irrigation fluids, gels and wound dressings that have an ability to loosen, soften, and sequester debris and necrotic tissue are often used (Steven L. Percival et al., 2019).

Systemic administration of antibiotics is indicated if wound infection is spread to deep tissues, or the infection is systemic. However, systemic antibiotics can only suppress rapidly growing cells and have limited efficacy in treating or preventing wound biofilm formation. Systemic administration is further complicated by poor blood circulation in many chronic wounds, leading to inappropriate antibiotic concentrations at the site of infection and/or systemic side effects. It is important to note that due to the polymicrobial nature of non-healing wounds, genetic exchange between bacteria is likely to take place, as happened with the emergence of vancomycin-resistant *S. aureus*, first isolated from chronic wound patients (Centers for Disease Contol and Prevention (CDC), 2002a, 2002b). Thus, inappropriate antibiotic concentrations at the site of infection can be a growth stage for antibiotic resistance. Fortunately, these problems could be overcome by precise local delivery. Topical antibacterial dressings have been shown to prevent the attachment and maturation of biofilm (Rhoads et al., 2008).

Antiseptics are agents that destroy or inhibit the growth and development of microorganisms in or on living tissue. Unlike antibiotics, antiseptics are not administered systemically, but only applied topically on the intact skin or some on open wounds. However, it has been debated that they can cause some harm to human cells and thus prolong wound healing (Drosou et al., 2003). Still, most contemporary antiseptics, when used with care and not exceeding optimal concentrations, are valuable tools as they have broad spectrum and are thus beneficial for treating polymicrobial wound infections (Roberts et al., 2017). The lack of clinically significant microbial resistance to topical antiseptics due to their less specific action mechanisms is often highlighted as an advantage over topical antibiotics (D. J. Leaper et al., 2012). However, there is an increasing concern that widespread use of topical antiseptics, like chlorhexidine and triclosan, can actually lead to cross-resistance with other clinically relevant antibacterial drugs (Kampf, 2016; McNamara & Levy, 2016). Most common antiseptics used on wounds are silver, polyvinylpyrrolidone (PVP) iodine, octenidine, honey, and polyhexanide (polyhexanidine, polyhexamethylene biguanide, PHMB). Just as antibiotics, antiseptics are less effective against biofilm than planktonic cells.

Antibiotics are drugs that act selectively on bacteria to reversibly inhibit their growth (bacteriostatic) or irreversibly kill them (bactericidal). Due to the selectivity, they are less harmful to the host compared to bacteria. Topical administration of antibiotics is an area of controversies. Due to the possibility of inducing antibiotic resistance, it is generally advised against using topical antibiotics to treat chronic wound infections (D. J. Leaper et al., 2012). Widespread use of topical mupirocin and fusidic acid in some settings has already resulted in resistance that limits their potential efficacy (Williamson et al., 2017). In addition to selecting for resistance, topical antibiotics can be responsible for delayed hypersensitivity reactions, a response mediated by type 1 helper lymphocytes that leads to macrophage activation, and superinfections (Lipsky & Hoey, 2009; Maker et al., 2019). This cautious reluctance towards topical antibiotics may be at least partially due to the lack of appropriate dosage forms or DDSs that would allow precise control over drug release. Wound dressings impregnated with antimicrobials provide indispensable aid in controlling wound bioburden, however, the release of those antimicrobials is often uncontrolled and result in rapid increase in local concentrations, favoring local toxicity but also systemic absorption and related side effects. At the same time, drug levels dropping below therapeutic window could effectively induce resistance. Still, it is proposed that skillful use of topical antibiotics with more sophisticated delivery platforms should not be disregarded. This faith is illustrated by the growing number of scientific publications regarding topical antibiotics in novel wound dressings (X. Liu et al., 2021). Implementation of personalized topical therapeutics, antibiotics included, combined with molecular diagnostics has been shown to result in statistically and clinically significant improvements in wound healing (Dowd et al., 2011).

Progress in the development of novel nanotechnology-based wound dressings shows great promise in solving the abovementioned problems. The technology provides flexibility in creating fibrous wound dressings able to deliver different drugs directly to the site of action at defined rate for extended periods of time. Localized, clinically relevant drug concentrations in the wound can improve therapeutic efficacy, reduce toxicity and enhance patient compliance (Rambhia & Ma, 2015). Thus, antimicrobial drug-loaded nano- and microfibrous dressings are an interesting direction in the development of topical DDSs for treating wound infections.

2.5. Electrospinning

Electrospinning is a technique for fabricating polymeric nano- and microfibers using electrostatically driven jet of polymer solution or polymer melt. Typical needle-based setup is composed of four main constituents: 1) a polymer solution/ melt in a syringe equipped with a suitable needle/nozzle/spinneret, 2) syringe pump, 3) high-voltage power supply, and 4) grounded metal collector (Figure 1A). A drop of polymer solution or melt is pushed out of the capillary nozzle by

the pump under the action of high voltage, causing the droplet to become charged. As the electrostatic repulsion counteracts the surface tension, the droplet is stretched until at a critical point it forms the Taylor cone (Figure 1B) and a jet of polymer solution or melt is discharged toward a ground collector. The jet flows away in a nearly straight line but will bend into a complex path as it is stretched and thinned by the electrical forces. If molecular cohesion or chain entanglement in the droplet is sufficiently high, the jet continues to stretch until fine fibers are formed and collected on the grounded metal surface (Reneker & Yarin, 2008).

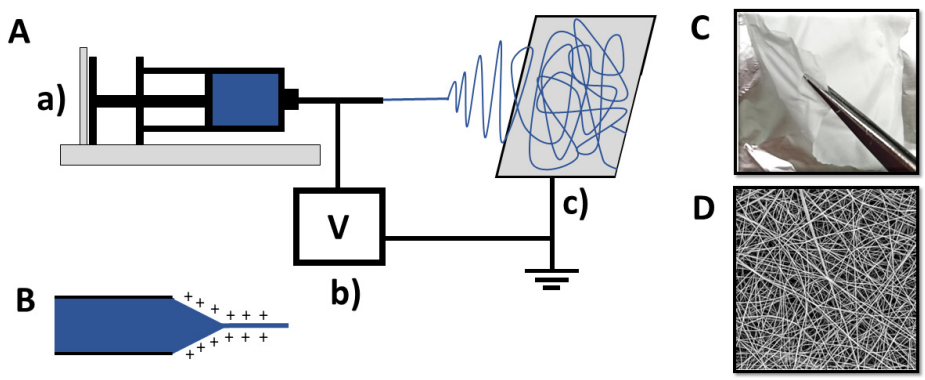

Figure 1. A. Schematic representation of an electrospinning setup comprised of a polymer solution in a syringe attached to a syringe pump (a), high voltage power supply (b) and grounded metal collector plate (c). B. Taylor cone formed of an electrospinning solution at the tip of the needle. C. Picture of an electrospun fiber matrix. D. Scanning electron microscopy micrograph of an electrospun fiber matrix.

The method is rather inexpensive and flexible, allowing the application of wide array of different polymers and other ingredients, resulting in a versatile selection of fibrous materials. In addition to the described setup, various modifications, mostly performed on the spinneret or collector, have resulted in novel electrospinning techniques. For example, core-shell structured nanofibers can be prepared using a coaxial needle instead of the common spinneret (Z. Sun et al., 2003; Yarin, 2011). Other techniques, including self-assembly and phase separation may be used for the production of such fibrous polymeric structures (Hartgerink et al., 2001), however, electrospinning shows the most promise for scale-up and mass production for commercial use. The yield of electrospinning could be increased by using either multi-needle or needleless free surface systems (Forward & Rutledge, 2012; Laidmäe et al., 2016; Molnar & Nagy, 2016; Yarin & Zussman, 2004). Also, solution blow spinning method has been developed that allows mass production of fibers without the need of high voltage (Vasireddi et al., 2019). In addition to large-scale production, a handheld

electrospinning device operating on batteries has been developed (Singh et al., 2018).

2.6. Factors affecting electrospinning

Although the electrospinning process seems simple, there is a wide variety of parameters that can be changed, and all these parameters modify the structural as well as mechanical properties of the obtained fibers or fiber mats (Teo et al., 2011). All these parameters need to be controlled and optimized to obtain a matrix with desired properties.

Factors that affect the electrospinning process can be divided into three main categories: electrospinning parameters, solution properties and environmental conditions. Electrospinning parameters include the applied voltage, solution flow rate, needle diameter and needle-to-collector distance. The solution properties comprise the nature of the solvent(s) and the polymer(s) together with their concentrations, solution viscosity and conductivity. The most important environmental factors that need to be monitored and controlled are relative humidity (RH) and temperature.

At a critical value of applied voltage, a droplet of polymer solution will deform into a Taylor cone and fibers will form. The following increase in voltage will decrease the diameter of fibers as the stretching of the polymer jet is correlated with the charge repulsion (Sill & von Recum, 2008). Further increase of voltage beyond a critical value will lead to the formation of beads and thicker fibers (A. Haider et al., 2018). Beaded structures could also be the result of excessive polymer solution feeding rate. Increasing the flow rate beyond the optimal value can also cause ribbon-like structures and other spinning defects, and increase fiber diameter and pore size due to low stretching and incomplete drying of the polymer jet (Megelski et al., 2002). If the flow rate is too slow, cone jets could alternate with receded jets, where the polymer solution emerges directly out of a needle without first forming a droplet or a Taylor cone. This instability results in nanofibers with a wide diameter distribution (Zargham et al., 2012). The needle-to-collector distance needs also to be maintained optimal, so the fibers have enough time to stretch and the solvent to evaporate as the jet travels through the air. Too short distance is likely to cause fibers to be defective and thick (Baumgarten, 1971; T. Wang & Kumar, 2006).

As the polymer concentration increases in the electrospinning solution, the viscosity of the solution also increases. The concentration needs to be sufficiently high to allow polymer chain entanglement for fiber formation (S. Haider et al., 2013). Inadequate chain entanglement can lead to beaded nanofibers or electrospray. Too high viscosity, on the other hand, causes problems with the solution flow through the needle and needle blockage (S. Haider et al., 2013; Pillay et al., 2013). In the appropriate concentration range, fiber diameter increases together with the concentration (Z. Li & Wang, 2013). Free charges need to be present in the solution to allow generation of electrostatic force by

the applied electric field. Increasing solution conductivity by adding electrolytes can thus improve electrospinning process. Still, increasing conductivity over a critical point can negatively affect the Taylor cone formation due to decreased tangential electric field (A. Haider et al., 2018).

The selection of appropriate polymer(s) and solvent(s) for electrospinning need to be carefully considered. First, the polymer is chosen, keeping in mind the functionalities and characteristics that the end-product needs to have and its final application. Second, a compatible solvent or a solvent mix is selected. The solvent needs to completely dissolve the polymer and, in most cases, any other substance that is added to the mix. Also, the solvent must have a relatively low boiling point, indicating good volatility, to facilitate the evaporation of the solvent during electrospinning. Too fast evaporation rate, on the other hand, can cause problems with needle clogging. Combining different solvents can help to overcome the shortcomings of a single solvent. Binary solvent systems composed of solvents and non-solvents can be used for the production of porous fibers (Lanno et al., 2020; Sill & von Recum, 2008).

Ambient conditions can greatly affect fiber properties. Both RH and temperature can affect solvent evaporation rate and thus the fiber solidification process. Higher RH reduces the evaporation rate, whereas higher temperature has the opposing effect. Faster solvent evaporation leaves less time for polymer jet elongation, resulting in thicker fibers (Pelipenko et al., 2013). On the other hand, delay in the solidification caused by too high humidity can lead to the formation of beads and poor drying (Szewczyk & Stachewicz, 2020). Increasing temperature can also reduce solution viscosity. High RH has been used to fabricate porous fibers as water vapor condenses as droplets on the fiber (Bae et al., 2013; Ramos et al., 2021).

2.7. Electrospun wound dressings

Electrospinning is a well-documented method for preparing fibrous non-woven wound dressings (Huang et al., 2003). The ideal wound dressing would accelerate the healing, prevent infection and restore the structures and functions of the skin (Abrigo et al., 2014). Electrospun matrices (Figure 1) meet these criteria as they have a unique collection of highly desirable and useful properties for wound care applications. Small fiber diameter, high porosity and specific surface area of these matrices are the main characteristics that distinguish these systems from other modern wound dressings, like hydrocolloids, hydrogels etc. These architectural features allow effective gaseous exchange, promote hemostasis and help to absorb wound exudate (Drobnik et al., 2017). The latter ensures appropriate moisture balance in the wound environment which is required for the action of growth factors, cytokines, and cell migration, all necessary for successful wound healing. (D. J. Leaper et al., 2012; Winter, 1962) At the same time, pores between the fibers can be small enough to protect the wound from contamination (Fahimirad et al., 2021). Although the exact composition of the

ECM depends on the tissue, fibrous-forming proteins, especially collagen fibers with a diameter ranging from 1 to 20 micrometers, are its main components (Theocharis et al., 2016; Ushiki, 2002). Owing to the morphological resemblance, electrospun matrices can mimic the ECM and provide an excellent environment for wound healing, facilitating cell migration and proliferation (Harding et al., 2002; Murugan & Ramakrishna, 2006). Electrospun matrices can reduce pain, inflammation and scarring (L. Sun et al., 2018). Another crucial aspect highlighting the benefits of electrospinning technique to produce wound dressings is the relative ease of allowing the incorporation of different pharmaceutically active ingredients (APIs). Hence, electrospun wound dressing can at the same time be a DDS. Although electrospun wound dressings are mostly intended for the local treatment of skin wounds, the treatment of wounds/infections at other locations like those in oral cavity, can benefit from the same advantages of fibrous DDSs as skin wounds.

2.8. Electrospun drug delivery systems

Electrospun matrices can be used as delivery vehicles for many different types of drugs, at the same time allowing high flexibility in the rate and site of drug delivery. Anticancer agents, antibiotics, anti-inflammatory drugs, antihistamines, cardiovascular and gastrointestinal drugs, contraceptives and palliative care medications have all been incorporated into electrospun matrices (Shahriar et al., 2019). Some examples of antibiotics in electrospun DDSs include tetracycline hydrochloride (Liao et al., 2015), vancomycin (Dhand et al., 2017), streptomycin sulfate (Unnithan et al., 2014), enrofloxacin (He et al., 2015), cefazolin sodium (Fazli & Shariatinia, 2017), nitrofurazone (Zhao et al., 2015), fusidic acid (Said et al., 2011), polymyxin B (X. Zhang et al., 2015), mupirocin (Chen et al., 2017) etc. Electrospun matrices have been proposed for oral, sublingual/buccal, ocular, nasal, vaginal, rectal, topical and transdermal routes (Anup et al., 2021). They can be designed both for immediate or prolonged drug release, or more complex profiles, like biphasic release and stimulus-controlled release (Kajdič et al., 2019)

Drug release from electrospun DDS can be complex as it often involves several simultaneously occurring processes. Two main steps can be described: (1) release of the drug out from the fiber into the void volume of the matrix and (2) release of the drug out from the void volume of the matrix into bulk solution via diffusion (Munj et al., 2017). Processes that result in drug molecules being released from the fiber include desorption of the drug from the fiber surface, polymer chains relaxation, diffusion within polymer, polymer dissolution/ degradation and swelling. Desorption, polymer relaxation and diffusion are dominating if the matrix geometry stays unchanged in dissolution medium. If the matrix starts to dissolve, degrade or swell in the time-frame of drug release, it will change diffusion pathway and facilitate drug release (G. Yang et al., 2018). Degradation can occur by either surface or bulk erosion. The first

happens if the polymer degrades faster than the dissolution medium can enter the matrix, opposite is true for the latter. Polymer swelling can have opposite effects, whether it creates additional pores into the fiber structure due to water absorption and thus aids drug diffusion, or reduces interfiber porosity and increases diffusion resistance (Ko et al., 2019; Munj et al., 2017).

The primary factors that shape the properties of electrospun DDS and its drug release profile could be categorized as follows: the loading method, meaning how the drug is incorporated into the matrix; the material properties, including the nature of both the drug and the polymer; and architectural features of the matrix, comprising the fiber dimensions, both fiber and matrix porosity, fiber matrix thickness, and layered structures.

2.8.1. Loading methods

Methods to incorporate drugs into electrospun matrices are summarized in Figure 2. The most common and simple way to incorporate a drug into an electrospun matrix is to blend it with a polymer solution prior electrospinning. In order to protect the drug or modify its release, it is also possible to encapsulate the drug before mixing with the electrospinning solution or encapsulate the drug into the fiber core by coaxial electrospinning or emulsion electrospinning. The drug could also be loaded after electrospinning by surface immobilization.

Blend electrospinning is suitable for creating both immediate and prolonged release DDSs. The resulting release profile is largely dependent on the properties and compatibilities of the carrier polymer(s), solvent(s) and incorporated drug(s), but also the drug load (Zeng et al., 2005). This one-step approach is advantageous for its simplicity, although more complex strategies may be needed for modifying the release. For instance, zero-order release is not easily achieved with blend electrospinning as there is often a problem with initial burst release, creating a biphasic release profile of burst release followed by sustained release (Wu et al., 2020). Biphasic release is beneficial if effective drug concentrations need to be achieved quickly and, at the same time, maintained over a longer time-period without the need for frequent administration of the drug (Kuang et al., 2018).

If the burst effect needs to be minimized, the drug could be encapsulated inside the fiber core or into nanoparticles or liposomes. The latter creates two barriers, the nanoparticle and the nanofiber, hence the release can be slower compared to either system alone (Y. Wang et al., 2011). Feeding two, or sometimes even more, different polymer solutions through concentric nozzles is the basis of coaxial electrospinning for creating core and shell structures, where the drug is typically loaded into the core and the shell acts as a physical barrier between the core and the environment. Alternatively, emulsion electrospinning is carried out by the emulsification of two phases using an emulsifier and feeding it through a conventional nozzle (Nikmaram et al., 2017). As the inner phase coalesces during electrospinning, core and shell fibers are created. If

coalescence does not occur, the inner phase could be preserved as droplets inside the fiber. This complicates the formulation and production, but at the same time gives additional room and possibilities for the design. Encapsulating the drug could also serve other purposes besides prolonging the release, like stabilizing and protecting the drug.

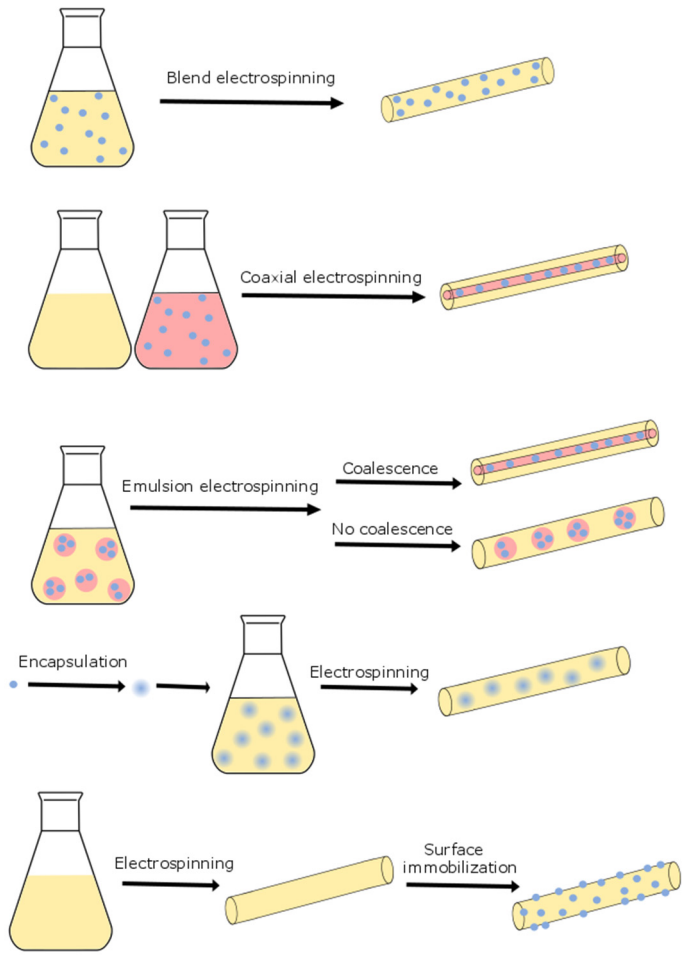

Figure 2. Drug loading methods into electrospun fiber matrices: blend electrospinning; coaxial electrospinning; emulsion electrospinning; encapsulation into nanoparticles prior electrospinning; and post-immobilization. Reprinted by permission from Springer Nature (Preem & Kogermann, 2018).

A drug could also be incorporated into the matrix after electrospinning. This could be done by simple immersion of the matrix in a drug solution, relying on non-specific adsorption process (Zdarta et al., 2019) or electrostatic interactions (Vonasek et al., 2017), or covalent binding. Covalent binding can be done directly, if suitable functional groups are present, or mediated by a crosslinker. Whereas adsorption leads to weak attachment of the drug onto the fibers, resulting in burst release (J. Wang & Windbergs, 2018), covalent bond is a strong chemical bond and drug release is only possible if the bond is degraded. Thus, covalent binding can significantly prolong drug release (Allafchian et al., 2020). The main advantage of these methods is that the drug and the electrospinning solution are handled separately, so the stability of the drug does not limit the choice of electrospinning solvent. This is especially important if biomolecules are loaded. On the other hand, the immobilization processes are laborious, and the matrix needs to preserve its structural integrity in the solvents that are used for post-processing.

In addition to the loading method, the amount of drug in the fibers is important consideration. Higher drug loading leads to more significant burst release and shorter period of release due to larger amounts of surface-associated drug and high surface area of the fibers (Cui et al., 2006; Natu et al., 2010). Although sustaining the release is easier with lower drug load, the concentrations thus achieved may be clinically ineffective. Thus, a compromise between drug load and release needs to be found.

2.8.2. Material properties

Although not all polymer solutions are electrospinnable, there exists a great variety of different polymers, including natural and synthetic, biodegradable and non-biodegradable, hydrophilic and hydrophobic, and combinations of them, that have been successfully employed as carriers for electrospun DDSs. The choice of a polymer is a key factor in the design of an electrospun DDS as it largely shapes its final properties, including drug release profile.

Natural polymers generally have good biocompatibility and cellular affinity, although they lack in mechanical properties and stability in physiological environment (Vineis & Varesano, 2018). The latter makes it difficult to design prolonged release formulations using natural polymers, whereas crosslinking can be helpful but brings concerns of toxicity (Campiglio et al., 2019). There are also problems with batch-to-batch variability. Some examples of natural polymers used for electrospinning include gelatin, chitosan, alginate, silk fibroin, and hyaluronic acid (Mele, 2016). Synthetic polymers, on the other hand, are usually more affordable, stable and have better mechanical properties, but do not provide bioactive cues for promoting cell attachment and proliferation, necessary for some biomedical applications, and may lack in hydrophilicity (Keshvardoostchokami et al., 2020). Some commonly used synthetic polymers for electrospinning include hydrophobic polyesters, like polycaprolactone (PCL), polyglycolic acid (PGA), poly(lactic-co-glycolic acid) (PLGA),

polylactic acid (PLA), and hydrophilic poly(ethylene oxide) (PEO), PVP and polyvinyl alcohol (PVA) (Keshvardoostchokami et al., 2020). The shortcomings of a single polymer, be it a natural or a synthetic one, is commonly balanced by blending it with another polymer. By combining different polymers, it is possible to improve electrospinnability and tune matrix properties and drug release as preferred. For example, chitosan is often blended with PEO (Ignatova et al., 2013) and PCL with gelatin or other hydrophilic polymers (Dulnik et al., 2016; Shi et al., 2018).

Polymer behaviour in water, more precisely its wetting, swelling, dissolution and degradation, largely affect the drug release profile. Hydrophilic water-soluble polymers are useful for immediate release DDSs. The dissolution rate and the apparent solubility of the drug are enhanced due to a high specific surface area and porosity of the matrix which creates a large contact area, allowing rapid wetting, disintegration and dissolution of the drug (Paaver et al., 2015). Manipulating with the wettability of the fibers, hence the rate at which the dissolution medium can penetrate the matrix, can alter the drug release. Addition of surfactants or complex-forming agents can increase dissolution rate, whereas hydrophobic matrices are more appropriate for prolonged release (Fathi-Azarbayjani & Chan, 2010; K. Wang et al., 2018). For example, super-hydrophobic matrices where release rate is directly dependent on the apparent contact area have been designed for long-term drug release (Yohe et al., 2012). Crosslinking can also effectively change dissolution/disintegration of the matrix, giving it more stability in aqueous medium and prolonging the drug release (Nada et al., 2016).

Electrospun DDSs are usually developed for a specific drug, meaning that a different drug in otherwise same formulation can behave in a completely different manner. Drug solubility and wetting properties are central to its release, together with the proper choice of the solvent and polymer to create a homogenous electrospinning solution. If the components are not compatible, e.g. the drug and the polymer have different polarities, the drug is most likely deposited on the fiber surface where it can readily contact dissolution medium (Zeng et al., 2005). As electrospun DDSs have a high specific surface area and the drug particles are very small, this results in rapid drug release. It is generally easier to prolong the release of hydrophobic drug molecules as they are compatible with hydrophobic polymers capable of sustaining the release, whereas hydrophilic polymers that are more compatible with hydrophilic drug molecules are usually not.

Solid state properties of the drug and polymer can change in the course of electrospinning and can significantly influence matrix properties. Polymer crystallinity affects its water uptake, mechanical properties and drug release. In general, higher crystallinity impedes the penetration of aqueous medium and drug diffusion takes preferentially place through amorphous regions of semi-crystalline polymer chains (Jeong et al., 2003). Both polymer-polymer and drug-polymer interactions can affect polymer crystallinity, but also the choice of the solvent (Chou & Woodrow, 2017; Hartman et al., 2010; Kamath et al.,

2020). Electrospinning tends to reduce drug crystallinity, often into an amorphous form (Verreck et al., 2003). Although an amorphous form of the drug has higher dissolution rate and apparent solubility, in case of electrospun DDSs, this effect to the overall release profile is not so straightforward. As drug recrystallization usually takes place on the fiber surface and amorphous form is more likely to be deposited inside the fibers, crystalline drug can dissolve more rapidly due to large contact area with the dissolution medium (Wei, 2012). Drug recrystallization is more likely if hydrophilic drug and hydrophobic polymer are combined (Zeng et al., 2005), although the polarity of the solvent of the electrospinning solution can greatly influence drug crystal formation too (Seif et al., 2015). Also, hydrophilic drug particles on the fiber surface can reduce the contact angle of the matrix, resulting in faster drug release (Zupančič et al., 2018).

2.8.3. Architectural features of the matrix

Electrospinning enables to tailor both morphology and intrinsic structure of a single nanofiber, but also the architecture of the matrix in whole, for example, its porosity, thickness, layering etc. All these features can have an impact on the drug release properties.

Modified release electrospun DDSs have been classified based on their internal structure as follows: matrix-type fibers, including monolithic and blended fibers; core-shell fibers, including reservoir-type fibers and multi-matrix fibers; and other systems, like janus structures, sandwich-type meshes and fibers with controlled bead diameter (Figure 3) (Kajdič et al., 2019).

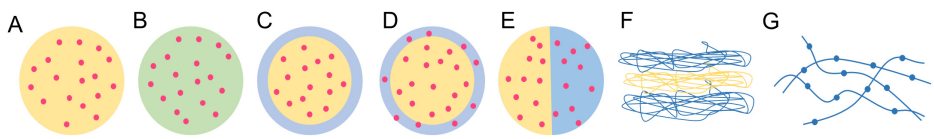

Figure 3. Classification of electrospun fibers based on their internal structure. The drug is depicted as pink dots in the cross-section of fibers, polymer matrix with yellow, green or blue color. Matrix type fibers include monolithic (A) and blended fibers (B); core-shell fibers include reservoir-type fibers (C) and multi-matrix fibers (D); other systems have also been developed, like janus structures (E), sandwich-type meshes (F) and fibers with controlled bead diameter (G).

Monolithic matrix-type fibers have a single carrier polymer mixed with a drug, whereas blended fibers have multiple carrier polymers. Reservoir-type core-shell fibers have drug(s) only in the core and multi-matrix fibers can have drug(s) in both core and shell. Janus structures have two side-by-side compartments, enabling simultaneous loading of multiple drugs into different compartments of the fibers. Unlike with core-shell structures, both compartments are in

contact with the environment (J. Yang et al., 2020). Sandwich-type meshes have multiple layers created by sequential electrospinning of different solutions. These layers may be composed of the same or different polymers whereas the drug is added only to the inner polymer layer (Jang et al., 2015) or multiple drugs can be loaded into different layers if they need to be released at different times (Okuda et al., 2010). Beads on fibers act as drug reservoirs and manipulating with the bead size enables to modify release kinetics (T. Li et al., 2017).

Fiber diameter and porosity affect drug release. In general, smaller fiber diameters mean higher surface area that usually leads to faster drug release. On the other hand, larger porous fibers can release the drug more quickly compared to smoother smaller fibers (Herrero-Herrero et al., 2018; Thakkar & Misra, 2017). Surface pores on fibers enhance drug release as they facilitate diffusion (Nguyen et al., 2012). Fiber diameter distribution could be manipulated to create DDSs with desired release profile (Petlin et al., 2017). Matrix porosity is also important as diffusion of release medium is impeded by its complex non-woven multilayered structure (Munj et al., 2017). More porous matrix means more space between fibers and less barriers for diffusion. Matrix thickness can affect drug release as it provides additional resistance for diffusion. If increasing matrix thickness prolongs the time it takes for the release medium to penetrate the matrix, then the thicker the matrix, the slower the release. Still, matrix thickness is not universally significant factor if wetting process and solution diffusion are not rate-limiting steps in drug release (Munj et al., 2017; Zupančič et al., 2018).

2.9. Characterization of electrospun wound dressings

A multitude of features shape the final properties of electrospun DDS, thus meticulous characterization is needed to understand the behavior and ensure functionality and quality of the pharmaceutical product. Some commonly applied tests are universal for all electrospun DDSs, some are more specifically based on the precise application of the product. For example, wound dressings need to have specific properties to be safe and effective, all of which need to be investigated during the design and development process. Electrospun wound dressings are novel DDSs, thus novel characterization methods are also needed besides those adopted from other dosage forms.

Regulatory aspects and required specifications depend on the classification of the wound dressing. Wound dressings can be classified either as medical devices or drug products. The United States Food and Drug Administration (FDA) recommends classifying wound dressings with drugs as Class II medical devices with special controls, requiring 510(k) premarket notification (Food and Drug Administration, 2016b). European Medicines Agency (EMA) categorizes wound dressings that incorporate an antimicrobial agent where the purpose of such an agent is to provide ancillary action on the wound as combination

devices covered by Rule 13. At the same time, if the primary function of the dressing relies on pharmacological, metabolic or immunological effect, the dressing is a medicinal product rather than a device (Medical Device Coordination Group, 2021).

The following section summarizes the most important features of electrospun wound dressings together with common characterization methods applied.

2.9.1. Morphology

Morphology is a primary feature of electrospun DDS as several unique characteristics arise directly from fiber diameter, porosity and arrangement. Optical microscopy is a simple and cheap technique, although its limiting resolution is typically about 200 nm. Thus, visualizing smaller nanostructures is not possible, but the technique is valuable for preliminary characterization. Scanning electron microscopy (SEM) and transmission electron microscopy (TEM) are widely used for more elaborate imaging of micro- and nanofibrous matrices. The latter can be especially beneficial for coaxial fibers to visualize the inner structure of a fiber. Atomic force microscopy gives additional information about surface topography at nanometric scale. Mercury porosimetry can provide information about sample porosity, pore size distribution and pore shape. A significant limitation is that the measurements are carried out under high pressure to force mercury into the pores and this can mechanically deform fibrous structures giving misleading data. Thus, the results must be interpreted with care. Specific surface area is better determined with Brunauer-Emmett-Teller (BET) method (Širc et al., 2012).

2.9.2. Solid state properties

Both drug molecules and carrier polymers in electrospinning solution will transform into solid state in the course of electrospinning. Thus, it is essential part of pharmaceutical product development and quality control to identify their solid state forms and stability. X-ray diffraction (XRD) can help to identify polymorphism or the amorphous form. Each crystalline material produces a unique pattern of sharp reflections, whereas amorphous halo appears if no periodic atomic arrangements exist. It is also possible to calculate the degree of crystallinity from XRD data (Doumeng et al., 2021). This helps to characterize possible changes in semi-crystalline polymers as polymer crystallinity can affect mechanical properties, drug release and interactions with living cells. Fourier transform infrared (FTIR) and Raman spectroscopy are complementary vibrational spectroscopy methods that provide additional information about solid state characteristics and help to elucidate possible intermolecular interactions between matrix components (Islam et al., 2019). As bond vibrations are indirectly affected by molecular arrangement, vibrational spectroscopy can be used for detecting polymorphism and the amorphous form (Bunaciu et al., 2015). Differential scanning calorimetry (DSC), as a thermal analysis method, provides

further information about sample solid state form, crystallinity and interactions between the ingredients. No melting endotherm suggests the presence of an amorphous form and shifts in melting endotherms potential interactions between the components (Munson, 2009).

2.9.3. Drug content, distribution, release and permeability

High performance liquid chromatography (HPLC) and ultraviolet-visible (UV-Vis) spectroscopy enable to quantify drug content in the matrices after sample preparation and evaluate possible drug degradation during the electrospinning process and storage. Collecting samples from various regions of the electrospun matrix helps to roughly analyze the uniformity of drug distribution within the matrix. Raman microscopic imaging provides more detailed insight about distribution of both carrier polymer(s) and API(s) in the fibers (L. Preem et al., 2017; Smith et al., 2017).

Drug release profile is one of the key parameters for a DDS and to determine that, modified dissolution test in reduced volume of dissolution medium is usually used. The drug content in samples drawn at set timepoints is analyzed by HPLC or UV-Vis spectroscopy. To analyze the drugs' ability to permeate through skin *in vitro* or *ex vivo*, Franz diffusion cell device equipped with either an artificial membrane or excised human or animal skin is used (Supe & Takudage, 2021).

2.9.4. Physical properties

Wound dressings should possess several qualities to ensure their performance, e.g., absorbency and fluid handling, gas transmission, adherence and suitable mechanical properties. The main international standard for the laboratory testing of these characteristics is BS EN 13726.

Wound dressings should be able to absorb wound exudate at least to some extent and according to that capability they may be used on different wound types. Thus, swellability and water absorptiveness are measured by a simple test of immersing the matrix in water or other fluid resembling wound exudate. From the mass increase, swelling index can be calculated (Nazemi et al., 2014). In addition, after drying the matrices, loss of mass can be calculated to give an understanding about the matrix structural stability in liquid environment. Matrix surface hydrophilicity/hydrophobicity is determined by contact angle measurements. In addition to giving information on how the matrix interacts with water, hydrophilicity/hydrophobicity can also predict how the matrix interacts with both eukaryotic and prokaryotic cells (Corsaro et al., 2021).

In addition to the adequate ability to absorb wound exudate, wound dressing should also enable good water vapor transmission and oxygen permeability as these are needed for normal wound healing. Standard testing methods exist for these measurements and special automated instruments have been developed for

user convenience (American Society for Testing Materials (ASTM), 2010, 2013).

Mechanical properties, like tensile strength, Youngs' modulus etc, can be assessed with texture analyzer. Strength and deformability of electrospun wound dressing are essential as the handling and user comfort, but also matrix interactions with cells depend on these parameters (Y. Zhang et al., 2005). Texture analyzer helps also to investigate bioadhesiveness of the dressing, for example, using *ex vivo* pig skin (Tamm et al., 2016).

2.9.5. Microbiological properties

2.9.5.1. Antimicrobial properties

To gain an understanding about antibacterial activity of electrospun DDS loaded with antimicrobials or antibiotics, several studies are possible to be carried out. One of the simplest methods is disc diffusion test on agar plates but antibacterial activity can also be assessed in liquid cultures to evaluate minimal inhibitory (MIC) and bactericidal (MBC) concentrations. Antibacterial activity testing should be carried out on both gram-positive and gram-negative bacterial species, preferably wound pathogens (clinical isolates). Anaerobic bacteria should also be included, although this necessitates special conditions for testing. In addition to these commonly used methods, it is important to investigate whether the dressing can help to manage biofilm. Also, the kinetics of antibacterial action is important as wound dressings should destroy pathogens quickly but at the same time continue this action over a longer period to control bacterial growth until the dressing is changed. Thus, novel testing methods are needed.

2.9.5.2. Microbiological quality

Microbiological quality is another important issue. As wound dressings are used on open skin wounds, sterile dressings are preferred. Microbiological quality can be ensured by either utilizing aseptic manufacturing or different sterilization/ disinfection methods. The production should be carried out in conditions that minimize possible contamination to enhance sterilization efficacy and reduce endotoxin levels, but sterilization may also be necessary, followed by sterility testing. Terminal sterilization after product packaging is recommended over other options as this can provide a sterility assurance level that is possible to calculate, validate and control (European Medicines Agency, 2016).

Different sterilization methods are described in pharmacopoeias, e.g. heat sterilization (dry heat or steam), ionizing radiation (gamma rays, a beam of electrons, or X-rays), gas sterilization (including alkylating and oxidizing agents, e.g. ethylene oxide) and membrane filtration. In addition to the accepted sterilization methods, several disinfection methods are in use to eliminate pathogenic microorganisms with the exception of bacterial spores, e.g. ultraviolet (UV) irradiation or treatments with ethanol solutions (Carolina Fracalossi

Rediguieri et al., 2016). Implementation of these methods on electrospun matrices can be challenging and much care needs to be put on choosing the optimal treatment method. For example, matrix materials need to be regarded. Biodegradable polymers with low melting points are often used for electrospinning (Cipitria et al., 2011). Thus, thermal sterilization methods are usually not applicable. Soaking in ethanol solutions must be disregarded if the matrix polymers are soluble in ethanol or if the matrix is drug-loaded. Gas sterilization is also problematic in case of electrospun matrices as these matrices are known for high surface area and porosity and can adsorb high amount of sterilant gases on their surface or in their structure, thus raising concerns for potential toxicity. For example, ethylene oxide is highly toxic and thus problematic agent for the sterilization of such matrices. Extensive purging steps following sterilization for 48 h at 50 °C, as recommended, could reduce the problem, but might still be inefficient or impractical in case of fiber formulations and lead to plastic deformation if polymers with low melting point are used (Odelius et al., 2008).

2.9.6. Safety

International Standard ISO-10993: Biological Evaluation of Medical Devices lists the requisites to call a dressing biocompatible. Wound dressings intended to be used on compromised skin for 24 h to 30 days need to be tested for cytotoxicity, sensitization and irritation. FDA recommends additional tests for acute systemic toxicity, material-mediated pyrogenicity and subacute/subchronic toxicity (Food and Drug Administration, 2016a).

Safety of electrospun wound dressings can be first assessed *in vitro* using appropriate cell cultures, usually skin fibroblasts or keratinocytes. The viability and morphology of cells incubated together with the matrix (direct method) or with the liquid obtained from incubating the matrix in growth medium (indirect method) are evaluated to see any harmful effects on the cells. Trypan blue and MTT (3-(4,5-dimethylthiazol-2-yl)-2,5-diphenyltetrazolium bromide) or MTS (3-(4,5-dimethylthiazol-2-yl)-5-(3-carboxymethoxyphenyl)-2-(4-sulfophenyl)-2H-tetrazolium)) tests are commonly applied for viability testing. Additionally, culturing cells on the dressing and monitoring their growth and proliferation can help to assess their biocompatibility. *In vitro* and *ex vivo* tests using animal or human skin are followed by animal models before the dressing can be finally introduced to clinical trials and patients for wound healing application.

2.10. Electrospun DDSs on the market

Although electrospun matrices have found their place on the market in other fields, e.g. for air filtration, and despite intensive ongoing research focusing on electrospun matrices as potential wound dressings and DDSs, the real transition from the academy to the pharmaceutical production and commercialization is yet to come (Omer et al., 2021). It is thought that the global market of electro-

spun fibers has the greatest growth potential in the medical and pharmaceutical fields (Mordor Intelligence, 2020), but currently only few examples of electrospun wound dressings or DDSs exist on the market, e.g., SurgiCLOT® fibrin sealant patch used for the delivery of human fibrinogen and thrombin for bone bleeding (Azimi et al., 2020), ReDura™ and NeoDura™ for the dural defect repair (Z. Liu et al., 2020), and Rivelin® patch designed for the unidirectional delivery of a pharmaceutical drug to a mucosal surface (Ruzicka et al., 2018). The scale-up technologies are rapidly developed and commercialization is expected to become easier (Omer et al., 2021). Still, the effect of scale-up on the multitude of functionality-related characteristics of an electrospun DDSs needs careful evaluation which slows the transition to clinical practice.

3. SUMMARY OF THE LITERATURE

It can be concluded that non-healing wounds represent a major challenge for the healthcare, whereas biofilm and microbial unbalance are crucial factors contributing to this problem. As current therapies lack in efficacy and may produce insufficient antimicrobial drug levels at the wound site, which can induce resistance and persistence, novel approaches are needed. Advanced wound dressings that have the capability to deliver antimicrobial drugs to the site of action at controlled rate for extended period, establishing localized, clinically relevant drug concentrations, can potentially improve the therapeutic outcomes. Electrospun polymeric nano- and microfiber matrices fill these requirements and, in addition, have several structural properties that make them promising wound dressing materials. Electrospinning is a very versatile method, allowing to use different materials, process parameters and drug-loading methods, which all affect the final properties of an electrospun DDS. Still, much is unknown about different aspects of the design on the performance and quality of these matrices.

One of the most important attributes of a DDS is its drug release profile and understanding the key factors that affect it can contribute to the rational design of suitable DDSs. Clarification of the role of matrix structural properties, solid state of the drug, drug-polymer and polymer-polymer interactions on drug release from electrospun matrices is needed. This is especially important in case of hydrophilic drug molecules, as sustaining the release of these drugs is more complex compared to hydrophobic drugs. Also, little is known of the impact of incorporation of multiple drugs to an electrospun matrix and how this affects and changes the release of each individual drug.

Meticulous characterization can help to understand the behavior and ensure the functionality and quality of the DDSs. A multitude of established methods used for the characterization of other dosage forms can be implemented, but the unique nature of electrospun drug-loaded matrices and the specific clinical problem that is aimed to be solved may warrant for more specific methods. As electrospinning is still a novel method for the production of DDSs and wound dressings, there is a lack of these more specific analytical methods. The problem is especially acute for evaluating drug release in biorelevant conditions that would resemble *in vivo* wound environment, so more relevant conclusions could be drawn in relation to their action and, in a bigger perspective, potential effects on real patients could be better predicted and understood. Also, established antibacterial activity testing methods may need modifications to better understand the kinetics of antibacterial action of differently designed DDSs. Moreover, available methods for investigating the formation and eradication of biofilms are more than limited despite the well-recognized role of biofilm in impeding wound healing.

Another important issue is concerned with the microbiological quality of electrospun DDS intended to be used on wounds. The knowledge about the

applicability of different sterilization techniques and possible effects of these treatments on the properties of electrospun DDSs is scarce and much needed.

All these insights would help to promote the performance and quality of these unique pharmaceutical products, help to rationalize their design and aid the transition to clinical practice.

4. AIMS OF THE STUDY

The goal of this research was to develop antibacterial drug-loaded electrospun matrices intended for the local treatment of wound infections and to comprehensively characterize these DDSs to gain understanding of the essential factors contributing to their performance and quality.

More specifically, the objectives were to:

- formulate and prepare antibacterial drug-loaded electrospun matrices using different carrier polymers and antibiotics (I, II)
- characterize the physicochemical, structural and mechanical properties of the matrices (I, II, III)
- evaluate possible interactions between different matrix components at the molecular level and matrix interactions with aqueous environment (I, II)
- develop and compare different analytical methods to analyze drug release behavior from the matrices (I-IV)
- evaluate the antibacterial activity of the matrices by applying established methods and developing novel methods (I, II, IV)
- assess safety of the matrices on *in vitro* cell cultures (I, II)
- compare the effects and efficacy of different sterilization/disinfection methods on various properties of the matrices (III)

5. EXPERIMENTAL

Complete description of materials and methods is provided in original publications (I–IV).

5.1. Materials

5.1.1 Active pharmaceutical ingredients

Antibacterial drugs chloramphenicol (CAM) (I, III, IV), metronidazole (MTZ) (II) and ciprofloxacin (CIP) hydrochloride hydrate (II) were used for the preparation of electrospun matrices (Figure 4). CAM and MTZ were purchased from Sigma-Aldrich (USA), CIP from Alfa Aesar (Germany).

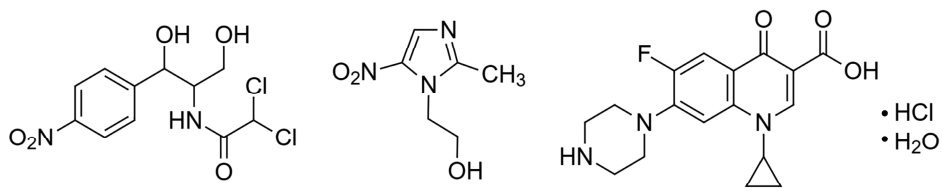

A. Chloramphenicol B. Metronidazole C. Ciprofloxacin hydrochloride hydrate

Figure 4. Chemical structures of chloramphenicol (A), metronidazole (B), and ciprofloxacin hydrochloride hydrate (C).

5.1.2. Polymers and solvents

Carrier polymers polycaprolactone (PCL) (Mn 80 000) and poly(ethylene oxide) (PEO) (Mw ≈ 900 000) (Figure 5), and solvents methanol (MET, gradient grade) and chloroform (CF, puriss p.a.) were purchased from Sigma-Aldrich. Solvents acetic acid (AA, 100%) and formic acid (FA, 98–100%) were from J. T. Baker, Germany.

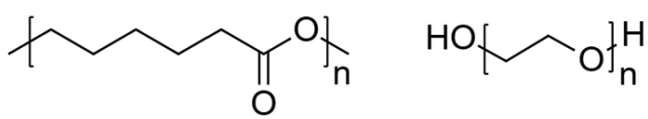

A. Polycaprolactone B. Poly(ethylene oxide)

Figure 5. Chemical structures of polycaprolactone (A), and poly(ethylene oxide) (B).

5.2. Preparation of electrospun matrices

Blend electrospinning method was used for the preparation of electrospun matrices. First, electrospinning solutions were prepared by dissolving the polymers in suitable solvent mixtures (Table 1). The solutions were allowed to mix by the aid of magnetic stirrer to allow all the components to dissolve. CAM was added to the solution at the same time as the polymer(s), whereas MTZ, CIP or both were added an hour before electrospinning.

Table 1. Electrospun fiber matrices and their compositions. Polymer concentrations in electrospinning solutions and theoretical drug concentrations in solid electrospun fibers are provided.

Fiber matrix	Polymers (% in solution)	Drug load (m/m% of fibers)	Solvents
PCL (I, III, IV)	12.5% (m/V) PCL	-	CF:MET (3:1 V/V)
PCL/CAM (I, III, IV)	12.5% (m/V) PCL	4% CAM	CF:MET (3:1 V/V)
PCL/PEO (I, III, IV)	10% (m/V) PCL 2% (m/V) PEO	-	CF:MET (3:1 V/V)
PCL/PEO/CAM ((I, III, IV)	10% (m/V) PCL 2% (m/V) PEO	4% CAM	CF:MET (3:1 V/V)
PCL (II)	15% (m/m) PCL	-	AA:FA (3:1 m/m)
PCL/MTZ (II)	15% (m/m) PCL	5% MTZ	AA:FA (3:1 m/m)
PCL/CIP (II)	15% (m/m) PCL	5% CIP•HCl•H_2O	AA:FA (3:1 m/m)
PCL/MTZ/CIP (II)	15% (m/m) PCL	2.5% MTZ 2.5% CIP•HCl•H_2O	AA:FA (3:1 m/m)

Key: AA – acetic acid; CAM – chloramphenicol; CF – chloroform; CIP – ciprofloxacin; FA – formic acid; MET – methanol; MTZ – metronidazole; PCL – polycaprolactone; PEO – poly(ethylene oxide).

CAM-loaded fiber matrices and their respective blanks were produced using NanoNC electrospinning robot (South Korea) and fiber matrices loaded with MTZ, CIP or both were produced using vertical electrospinning technology with a Fluidnatek LE-100 apparatus (Bioinicia, Spain). In all cases, monoaxial nozzle was used. Electrospinning parameters can be seen in Table 2. Aluminum foil-covered static collector plate (I) or rotating drum collector (II, III, IV) was used for collecting fibers. In the latter case, (III, IV) a roller (diameter 9 cm × width 20 cm) with the speed of 20 rpm (rotations per minute) together with the horizontally moving spinneret (distance 14 cm, speed 25 mm/min), or (II) a roller (diameter 9.55 cm) with the speed on 150 rpm together with the horizontally moving spinneret (distance 3 cm, speed 6.0 mm/min) were used.

Table 2. Electrospinning parameters used to produce different fiber matrices.

Fiber matrix	Solution feed rate (mL/h)	Applied voltage (kV)	Distance to collector (cm)
PCL (I, III, IV)	1	9	14
PCL/CAM (I, III, IV)	1	9	14
PCL/PEO (I, III, IV)	2.5	12	17
PCL/PEO/CAM ((I, III, IV)	2.5	12	17
PCL (II)	1	16-17 Collector charge -5 kV	15
PCL/MTZ (II)	1	16-17 Collector charge -5 Kv	15
PCL/CIP (II)	1	16-17 Collector charge -5 kV	15
PCL/MTZ/CIP (II)	1	16-17 Collector charge -5 kV	15

Key: CAM – chloramphenicol; CIP – ciprofloxacin; MTZ – metronidazole; PCL – polycaprolactone; PEO – poly(ethylene oxide).

In case of MTZ and/or CIP-loaded matrices, the process was run for different times to produce nanofiber mats of different thicknesses (Table 3). The thickness of the cross-sections of the matrices was determined by stereomicroscopy (Olympus SZX12, Japan).

Table 3. Summary of characteristics of MTZ and/or CIP-loaded nanofiber mats.

Type of nanofiber mat	Sample	Time of electrospinning (h)	Thickness (µm)
PCL nanofiber mat	PCL	6	
PCL/MTZ nanofiber mat	PCL/MTZ-1h	1	53 ± 9
	PCL/MTZ -2h	2	89 ± 29
	PCL/MTZ -4h	4	139 ± 18
	PCL/MTZ -6h	6	195 ± 21
	PCL/MTZ -8h	8	297 ± 36
PCL/CIP nanofiber mat	PCL/CIP-1h	1	57 ± 27
	PCL/CIP -2h	2	123 ± 20
	PCL/CIP -4h	4	199 ± 31
	PCL/CIP -6h	6	243 ± 43
PCL/MTZ/CIP nanofiber mat	PCL/MTZ/CIP	6	241 ± 37

Key: CIP – ciprofloxacin; MTZ – metronidazole; PCL – polycaprolactone.

Fiber matrices were stored in the airtight plastic bags at ambient conditions (temperature of 19–23 °C and relative humidity of 18–37%) until further analyses.

5.3. Characterization of electrospun matrices

5.3.1. Morphology (I–III)

5.3.1.1. Scanning electron microscopy (I–III)

The morphology and diameter of electrospun fibers was observed under SEM Zeiss EVO 15 MA, (Germany) (I, III); or Supra 35 VP, Carl Zeiss, (Oberkochen, Germany) (II). Randomly selected areas of the fiber mats were mounted on aluminum stubs and left uncoated (II) or magnetron-sputter coated with a 3 nm gold (I) or platinum (III) layer prior to microscopy.

5.3.1.2. Mercury intrusion porosimetry (MIP) (I)

The pore size distribution and density of electrospun fiber mats were determined by MIP using the POREMASTER-60-17 porosimeter (Quantachrome Instruments, USA). An MIP analysis was used to measure pores with diameters in the range 0.032–10 μm. The porosity of the fiber mats, describing the percentage of void volume of the sample, was calculated from the Equation 1:

$$Porosity(\%) = \left(1 - \frac{\rho_f}{\rho_m}\right) \cdot 100\% \quad (1)$$

where ρ_f is the density of fiber mat and ρ_m is the bulk density of corresponding materials, more precisely PCL 1.145 g/cm^3, PEO 1.21 g/cm^3 and CAM 1.547 g/cm^3.

5.3.1.3. Brunauer-Emmett-Teller (BET) analyses (I)

Krypton adsorption isotherms were measured on degassed (>58 h, 25 °C, vacuum) samples using an ASAP 2020 Accelerated Surface Area and Porosimetry System (Micromeritics, USA) at 77.4 K. The specific surface areas (S_{BET}) were calculated from sorption data according to BET equation (Brunauer et al., 1938).

5.3.2. Mechanical properties (III)

The mechanical properties of electrospun matrices were measured with a puncture test using CT3 Texture Analyzer (Brookfield, USA) equipped with a 10 kg load cell. 2 × 2 cm pieces of fiber matrices were used for analysis and their thicknesses were measured with Precision-Micrometer 533.501 (Scala messzeuge, Germany) with the resolution of 0.1 μm at 4 different points. The samples were secured between a film support fixture (TA-FSF) and punctured with a stainless-steel cylinder probe (TA-42, diameter 3 mm): trigger load 5 g, and test speed of 1.00 mm/s. The target distance 18 mm was chosen so all samples were punctured during the measurement. The applied force (N) and distance of the probe (mm) were recorded as the probe deformed the sample and

hardness (N), deformation at hardness (mm) and hardness work done (mJ) were calculated.

5.3.3. Drug content and distribution (I, III, IV)

The drug loading and its distribution in CAM-loaded matrices were determined using high-performance liquid chromatography (HPLC) analyses (I, III, IV). HPLC analyses were performed using Shimadzu Prominence LC20 with photo-diode array detector SPD-M20A (wavelength at 275 nm) and according to the official European Pharmacopoeia method for a related substance CAM sodium succinate. HPLC was equipped with a column Phenomenex Luna C18(2), 250 × 4.6 mm, 5 µm, and the mobile phase used was 20 g/L solution of phosphoric acid R, MET R, and water R (5:40:55 V/V/V). The flow rate was 1.0 mL/min, and injection volume was 20 µL. The CAM-loaded matrices were cut into 1 and 3 cm^2 pieces, weighed and dissolved in dichloromethane and MET (3:1 V/V). Pieces were taken from both center and edges of the matrix to see if differences occurred in drug distribution.

In addition to HPLC analysis, Raman scattering microspectroscopy (RSM) mapping was used to visualize the CAM distribution within the fiber samples (I). RSM was performed using Reinshaw InVia micro-Raman spectrometer (Reinshaw, England) with CCD Camera (1040 × 256) and 785 nm diode laser excitation. Exposure time of 150 s and 50× objective was used for the measurements. Raman mapping data were collected on approximately 92 (height) 119 (width) µm area of the fibers in the spectral range of 700 to 1800 cm^{-1} with 1 cm^{-1} resolution. The maps were collected with 1.2 µm step size in both direction and consisted of 5000−10000 points. Bright-field images of the samples were taken before each Raman mapping.

5.3.4. Solid state characterization (I–III)

5.3.4.1 X-Ray Diffraction (XRD) (I, II)

The XRD patterns of the starting materials, physical mixtures and electrospun fibers were obtained with X-ray diffractometer (D8 Advance, Bruker AXS GmbH, Germany). The XRD experiments were carried out in a symmetrical reflection mode (Bragg–Brentano geometry) with CuKα radiation (1.54 Å). The scattered intensities were measured with the LynxEye one-dimensional detector including 165 channels. The angular range was from 5° to 40° 2-*theta* with the step size of 0.0198° 2-*theta*.

The degree of crystallinity (X_c) was calculated with Bruker AXS software Topas 4-1 (Equation 2):

$$X_c = \frac{I_c}{I_c + I_a} \cdot 100\% \quad (2)$$

where I_c is the diffracted intensity of the crystalline phase and I_a is the diffracted intensity of amorphous phase.

5.3.4.2 Attenuated Total Reflection Fourier Transform Infrared (ATR-FTIR) Spectroscopy (I, II, III)

ATR-FTIR spectroscopy was performed on pure substances, physical mixtures, and electrospun matrices using an IR Prestige-21 spectrophotometer (Shimadzu Corp., Kyoto, Japan) and Specac Golden Gate Single Reflection ATR crystal (Specac Ltd., Orpington, UK). The spectra were collected with a resolution of 4 cm^{-1} between 600 and 4000 cm^{-1}, each spectrum was the average of 60 scans. All spectra were normalized.

5.3.4.3 Differential Scanning Calorimetry (DSC) (I–III)

Two different DSC equipments were used for thermal analysis: Mettler Toledo (USA) (I) and PerkinElmer DSC4000 (USA) (I, II, III). Thermal analysis was carried out with all electrospun fiber matrices with and without drug(s), and all the respective physical mixtures and powders of the raw material.

CAM-loaded fibers and their related samples were analyzed under 50 mL/min dry nitrogen purge in crimped aluminum pans without pinholes at a heating/ cooling rate of 10 °C/min from 0 to 180 °C and 180 to 0 °C. All DSC curves were normalized to a sample mass.

Fibers loaded with MTZ, CIP, and both of the drugs, and their related samples were analyzed under 19.8 mL/min dry nitrogen flow in crimped aluminum pans with a pin-hole in the middle of the lid. The DSC program was: hold for 3 min at 0 °C; heat from 0 to 190 °C at 10 °C/ min; hold for 1 min at 190 °C; cool from 190 to 0 °C at 10 °C/min.

Indium was used as a reference material. All DSC curves were normalized to a sample mass.

5.3.5. Contact angle (I, II)

The contact angles between the electrospun fiber matrices and deionized water (I) or 50 mM phosphate buffer (pH 7.4) (II) were measured with CAM 200 (Attension/Biolin Scientific Oy, Finland) (I) or Kruss DSA100 Goniometer (Germany) contact angle analyzer. A drop of liquid was applied on the surface of the fibers. In case of CAM-loaded samples and respective blanks, the fibers were deposited as a thin layer on a gold surface. Each sample was measured at least in triplicate.

5.3.6. Buffer uptake/swelling and loss of mass (I–III)

Buffer uptake or swelling was measured with a gravimetric method. CAM-loaded fibers and their respective blanks were cut into pieces with a surface area of 4 cm^2, weighed (m_d), and immersed in a glass vials containing 10 mL of

deionized water (I) or 20 mL of 50 mM phosphate buffer (pH 7.4) (III) at 37 ºC for 24 h. All other fibers were cut into round pieces with a surface area of 2.6 cm^2, weighed (m_d), and immersed in a glass vials containing 20 mL of 50 mM phosphate buffer (pH 7.4) and shaken at 150 rpm at room temperature (22 ± 3 ºC) for predetermined timepoints (II). After that, the samples were dabbed with a filter paper or paper towel to remove free surface liquid and weighed (m_w) to determine the buffer uptake/swelling index according to Equation 3:

$$\text{Swelling index (buffer uptake) (\%)} = \frac{m_w - m_d}{m_d} \times 100 \quad (3)$$

For comparison, the fiber matrices were also immersed in 10 mL 1% (m/m) Tween 80 solution (II). The samples were removed from the media after 5 min, dabbed with a paper towel, weighed and the uptake of 1% Tween 80 solution was also calculated using Equation (2).

To estimate biodegradation of differently sterilized CAM-loaded samples and their respective blanks (III), the samples were placed back to phosphate buffered saline (PBS) for another six days at 37 °C. The samples were then rinsed in deionized water, air-dried, and re-weighed for calculating the weight loss as reported previously (Nazemi et al., 2014).

5.3.7. Drug release (I–IV)

5.3.7.1. Drug release into buffer solution (I–IV)

The *in vitro* drug release of CAM from drug-loaded electrospun fiber matrices was carried out using 1 cm^2 samples (n = 3). These were weighed, placed into 10 mL of PBS (pH 7.4) at 37 °C in 50 mL plastic tubes. The tubes were put into dissolution apparatus vessel (dissolution system 2100, Distek Inc., NJ, USA) containing water and maintained at 37 °C. The tubes were rotated by the paddles at the speed of 100 rpm. Aliquots of 2 mL were removed and replaced with the same amount of PBS at set time-points. The aliquots were analyzed using UV-spectroscopy (Shimadzu UV-1800). Wavelength of maximum absorption (λ = 278 nm) was chosen for drug release analysis. (I, III, IV)

The *in vitro* drug release of MTZ and/or CIP from electrospun fiber matrices was carried out using 2.6 cm^2 sized samples (n=3). These were weighed, placed into glass vials prefilled with 10 to 20 mL of PBS (pH 7.4). The samples were shaken at 150 rpm at room temperature or 37 ºC to see the effect of temperature on drug release. To see the effect of surface area on drug release, also 5.2 cm^2 MTZ-loaded samples (PCL/MTZ-8h) were analyzed. At predetermined times, 0.5 mL of the solution was withdrawn and replaced with fresh buffer. The extracted samples were diluted with the buffer, filtered through a 0.2 µm filter, and analyzed using ultra performance liquid chromatography (Acquity Ultra Performance Liquid Chromatography (UPLC), Waters Corp., USA). The UPLC

method was developed to separate and quantify MTZ and CIP. Acquity UPLC CSH C18 1.7 µm 2.1 × 50 mm (Waters Corp., USA) column equipped with pre-column was used. Gradient elution was used for chromatographic separation with mobile phases A (25 mM phosphate buffer (pH 3.0) and 10% methanol) and B (acetonitrile and water 98:2). The gradient profile was: 0–1 min 0% B, 3 min 20% B, 3.2–3.6 min 50% B, and 4.4–5.0 min 0% B. The flow-rate was set at 0.5 mL/min, UV detection at 271 nm, the column temperature was maintained at 50 °C, and the injection volume was 5 µL. The area under the peak was used for calculating the drug concentration in the samples. (II)

5.3.7.2. Drug release into agar hydrogel measured by HPLC (IV)

The amount of drug released into agar plates was investigated by sampling different zones of the agar (illustrated with a figure in section 6.7.1). Pieces of PCL/CAM and PCL/PEO/CAM fiber matrix discs with a diameter of 1 cm were weighed, put onto pre-warmed lysogeny broth (LB) agar plates, kept at 37 ºC, and removed at set time-points. Zones of the agar were cut out, the agar sample was put into ethanol (96%) and sonicated for 15 min. This extraction process was repeated twice, and the obtained ethanol solutions were combined. The vials with ethanol solutions were left under a fume hood without caps, for the ethanol to evaporate. The residues left in the vials were dissolved in 1.5 mL of ethanol (96%) and the amount of CAM analyzed with HPLC as described previously. In the present study, the limit of detection for CAM was 1 µg/mL. Triplicate measurements were performed. The extraction efficacy was tested separately confirming that two times extraction resulted in 100% efficacy (see publication III Table A1).

5.3.7.3. Bioreporter Disc Diffusion Assay (IV)

For bacterial bioreporter disc diffusion assay agar plates with defined 3-(N-morpholino)propanesulfonic acid (MOPS) minimal medium (Neidhardt et al., 1974) supplemented with 0.4% (m/V) glucose as the carbon source and 1.5% (m/V) agar were prepared in sterile conditions by measuring 20 mL of warm agar medium per plate, and plates were dried for 30 min under laminar flow hood. Bioreporter strain dimethyl sulfoxide (DMSO) stock was thawed, diluted 20× into sterile PBS (cell number ~3×10^7 colony-forming units (CFU)/ml) and 75 µL was plated on each plate. A sterile cotton bud dipped into PBS was used to spread the cells evenly. Plates were left to incubate at 37 ºC for 10 h. After incubation, the weighted fiber matrices (PCL/PEO/CAM and PCL/CAM) were added to each plate. Individual plates were first scanned with the Amersham Typhoon scanner (GE Healthcare Europe GmbH, Freiburg, Germany) to measure fluorescence of GFP and mScarlet-I (pixel size 100 µm; green fluorescence: 488 nm laser, 525BP20 filter, photomultiplier tube (PMT) voltage 352V; red fluorescence: 532 nm laser, 570BP20 filter, PMT voltage 621V) after adding the

matrices and re-scanned every hour for 6 h. Scan time for each plate was approximately 6 min. The plates were incubated at 37 ºC between the scans.

5.3.7.4. Ultraviolet Imaging for monitoring drug release into hydrogel (IV)

Complementary to the traditional HPLC method, an Actipix D200 Large Area Imager (Paraytec Ltd., York, England) controlled by Actipix D200 acquisition software ver. 3.1.7.4 was used to image the release of CAM from PCL and PCL/PEO fiber matrices. These experiments were performed in a heating cabinet from Edmund Bühler TH30 (Bodelshausen, Germany) set to 37 ºC. Imaging was performed at four alternating wavelengths: 525 nm, 280 nm, 255 nm, and 214 nm. Images for each wavelength were recorded at a frequency of 0.125 s^{-1} for the release experiments as well as the standard curve. The imaging area (28 × 28 mm^2; pixel size 13.8 μm^2) encompassed three quartz cells (Pion Inc., UK; 62 mm × 4 mm × 7 mm (L × H × W)), allowing three measurements to be performed simultaneously. The fibers were cut to fit the inner dimensions of the quartz cells (7.0 mm in width and 4.0 mm in height). The fibers were positioned perpendicular to the imaging direction in contact with the agarose gel. The fibers were backed by silicone plugs to ensure good contact with the gel and correct alignment. Parafilm was used to seal the quartz cells preventing evaporation of water from the gels. The release of CAM from the fibers was imaged for 3 h at 37 ºC. Each imaging experiment allowed measurements of two CAM-containing fibers and one blank fiber (control). The positioning of the fibers in the imaging system (top, middle or bottom row) was randomized. Details for the preparation of standard curve for quantification by UV imaging are given in original publication IV.

5.3.8. Antibacterial activity (I, II, IV)

5.3.8.1. Microbial strains (I, II, IV)

Different strains of Gram-negative facultative anaerobe *Escherichia coli* were used in the studies: *E. coli* MG1655 (Blattner et al., 1997), uropathogenic *E. coli* CFT073 (Mobley et al., 1990) (kindly provided by Prof Harry Mobley) and *E. coli* DSM 1103 (clinical isolate, purchased from Leibniz Institute DSMZ-German Collection Microorganisms and Cell Culture). *E. coli* MG1655 strain was used for bioreporter construction. Cloning was performed in *E. coli* strain DH5α (Sambrook & D, 2001), using pSC101 plasmid with two fluorescent reporter genes *GFPmut2* and *mScarlet-I* (for all details, see publication IV).

All other bacteria used in assessing the antibacterial activity were purchased from the Leibniz Institute DSMZ-German Collection Microorganisms and Cell Cultures: Gram-positive facultative anaerobe *Streptococcus mutans* DSM 20523 (isolated from carious dentine), Gram-negative microaerophilic *Aggregatibacter actinomycetemcomitans* DSM 11123 (isolated from subgingival dental plaque), anaerobic Gram-negative *Fusobacterium nucleatum spp polymorphum* DSM

20482 (isolated from inflamed gingiva), *Porphyromonas gingivalis* DSM 20709 (isolated from human gingival sulcus) and *Staphylococcus aureus* DSM 2569.

5.3.8.2. Disc Diffusion Assay (I, II)

To test the antibacterial activity of CAM-loaded fibers, overnight liquid cultures of *E. coli* MG1655 and CFT073 were grown from DMSO stocks and the cell number was adjusted with fresh LB to ~3×10^7 colony-forming units (CFU)/ml. 100 µL of these dilutions were spread onto the surface of LB agar plates. Discs with a diameter of 6 mm cut from fiber matrices were applied to these plates. Positive controls were prepared by immersing 6 mm filter paper discs with 20 µL of CAM solution (1 mg/mL), so each disc contained 20 µg of the drug. Untreated filter paper was used as a negative control. The concentration of CAM in positive control was similar to that in drug-loaded fibers. The plates were incubated at 37 °C for 24 h. The inhibition zones free of bacterial growth were determined. Tests were run in triplicate.

To test the antibacterial activity of fibers loaded with MTZ, CIP or both, overnight liquid cultures of *E. coli* MG1655 and CFT073 were grown from DMSO stocks and the cell number was adjusted with fresh LB to ~4×10^7 CFU/ml. 100 µL of these dilutions were spread onto the surface of Viande-Levure agar plates (for aerobic conditions, no cysteine was added to the medium). All other bacteria (*S. mutans*, *A. actinomycetemcomitans, F. nucleatum* and *P. gingivalis*) were plated directly from glycerol stocks onto Columbia blood agar plate with 5% defibrinated sheep blood. Several colonies of each of these strains were transferred and spread onto fresh plates, each plate being covered uniformly with the bacteria. All fiber matrices cut into discs of 6 mm diameter were placed onto the plates together with controls. Positive controls were prepared by immersing 6 mm UV-sterilized filter paper discs with the solutions of the respective antibacterial drugs. Each positive control disc contained the same amount of drug as the corresponding drug-loaded fiber matrix. Untreated UV-sterilized filter paper was used as a negative control. *E. coli* plates were incubated in both aerobic and anaerobic conditions at 37 °C for 24 h. All other bacteria were incubated only in anaerobic conditions at 37 °C for 1–5 days until visible colonies appeared. Inhibition zones that were free of bacterial growth were determined, test being run in triplicate.

Preparation of DMSO and glycerol stocks are described in original publications I and II, respectively.

5.3.8.3. Modified Disc Diffusion Assay (IV)

The antibacterial activity of released CAM on agar plates was investigated at different time-points mimicking the drug diffusion tests into agarose hydrogel during UV imaging studies. Overnight culture (20 h) of *S. aureus* DSM 2569 was grown from DMSO stock (100 µL to 3 mL of LB). The culture was diluted to optical density 0.05 in LB and 100 µL was plated onto pre-warmed LB agar

plates (1.5% (m/V)). PCL/CAM and PCL/PEO/CAM fiber discs, and a positive CAM filter paper control were applied onto each plate. At specific time-points, the discs were removed and the LB plates were incubated at 37 ºC for 24 h prior to the measurement of inhibition zones.

5.3.8.4. Prolonged Disc Diffusion Assay (II)

The effect of fiber matrix thickness on antibacterial activity was measured by prolonged disc diffusion assay. In brief, PCL/MTZ fiber matrices of different thicknesses were placed on Columbia blood agar plates with 5% defibrinated sheep blood inoculated with *F. nucleatum* and incubated at 37 °C in anoxic conditions for 24 h after which the inhibition zones free of growth were determined. The fiber matrices were transferred onto a freshly inoculated plate and incubated in the same conditions. This was repeated at 48 h. After 72 h, the final inhibition zones were determined, so that antibacterial activity was assessed over 3 days. Positive controls were prepared as described above (5.3.8.1) and treated in the same way as fiber samples, test being run in triplicate.

5.3.8.5. Biofilm Assay (I)

Biofilm formation protocol was established based on the work of Brackman et al. (Brackman et al., 2011). Overnight liquid culture of *E. coli* CFT073 in LB was grown from DMSO stocks. The culture was diluted to about 5×10^7 CFU/ml with Dulbecco's Modified Eagle medium (DMEM) supplemented with 10% heat-inactivated Fetal Bovine Serum. One mL of the bacterial dispersion was added to 1 cm^2 samples in 24 well-plates. The well-plates were incubated at 37 °C for 24, 48, or 72 h. After that the samples were rinsed twice with PBS and put into 10 mL of fresh PBS in 50 mL plastic tube. For disrupting the biofilm alternating vortexing (Vortex-Genie 2, Scientific Industries) and sonication (Bandelin Sonorex digital 10 P, operating at 20% of maximum power) was performed in 30 s cycles. Each cycle was repeated 6 times, as this was seen to provide best compromise between biofilm disruption and bacterial viability. The CFUs were determined by making 10-times dilutions of the dispersion, plating these as 5 μL drops on LB agar plates and counting the CFUs at optimal dilutions after 18 h of incubation.

5.3.9. Cytotoxicity testing (I, II)

The CellTiter-Glo Luminescent Cell Viability Assay (Promega) was used as described by the manufacturers to investigate the cytotoxic effects of the fluid extracts of the CAM-loaded and respective blank fibers on murine fibroblastic NIH 3T3 cells. The cells were cultured in Dulbecco's Modified Eagle Medium (DMEM) supplemented with 10% heat-inactivated Fetal Bovine Serum and 1% penicillin-streptomycin. Cells were maintained at 37 °C in 5% CO2 incubator. The fluid extracts were prepared by immersing the drug-loaded and blank fibers in the same growth medium and kept in the incubator for 24 h. The cells were

cultivated on the 96 well-plates to near confluency and then the medium was replaced with the extracts (12.5, 25, 50, 100, or 200 μg/mL) or fresh medium and incubated for 24 h. Both treated and untreated cells were then transferred to opaque-walled 96-well plate in fresh culture medium (100 μL per well), alongside with control wells containing medium without cells to obtain a value for background luminescence. The plate was equilibrated at room temperature for 30 min. After that, 100 μL of CellTiter-Glo Reagent was added to each well and mixed for 2 min on an orbital shaker to induce cell lysis. The plate was further incubated at room temperature for 10 min and then luminescence recorded with VarioskanFlash 4.00.53 luminometer to quantify cell viability by the amount of adenosine triphosphate (ATP) present, which correlates to the presence of metabolically active cells. Each test was run in duplicate.

Safety and biocompatibility of fibers loaded with MTZ, CIP, and both, were evaluated on baby hamster kidney (BHK-21) fibroblasts using viability assays. Fibroblasts were grown in the Glasgow Minimal Essential Medium (GMEM) supplemented with 7.5% fetal bovine serum, 2% Tryptose Phosphate Broth (TPB, Difco), 20 mM HEPES, 100 μg/mL penicillin, and 100 μg/mL streptomycin. Cells were maintained at 37 °C in 5% CO2 incubator. Viability was measured by direct and indirect methods according to the ISO guideline (109993-5). In both cases, cells were grown to near confluence in 24 well-plates. By the direct method, 1 cm^2 fiber samples were placed into the well-plate together with cells and incubated for 24 h. By the indirect method, fluid extracts were prepared from the fiber matrices by incubating them in growth media for 24 h (fiber concentration 1.25 mg/mL). Media over the fibroblasts were replaced with the extracts, and incubation was continued for 24 h. Safety was assessed qualitatively by microscopy and quantitatively by trypan blue exclusion (automated cell counter, Invitrogen, Thermo Fischer, USA), counting dead and live cells from which the viability (%) was calculated. Cells treated with Triton X-100 (final concentration 0.1%) were used as the dead cell control, whereas cells exposed only to the unchanged growth medium were used as healthy untreated controls. The experiments were carried out in triplicate.

5.4. Sterilization and characterization of electrospun matrices (III)

Different sterilization and disinfection methods were used for the treatment of electrospun CAM-loaded and respective blank fiber matrices. After sterilization (except gamma sterilization), the fibers were placed with sterile forceps into sterile 50 mL Falcon tubes for storage until further analysis.

5.4.1. Sterilization/disinfection methods (III)

5.4.1.1. UV-sterilization

All electrospun matrices were removed from the foil and cut into appropriate pieces for later testing (1 × 1 cm or 2 × 2 cm) and exposed to UV-irradiation at 254 nm (UV-lamp: Heraeus model TNN 15/35, Germany) at the distance of 15 cm from the lamp for 15 min, 30 min or 1 h on both sides in ambient conditions. UV lamp power was 15 W. Differently treated and untreated matrices were characterized with other methods that have been described in previous sections.

5.4.1.2. Gamma-irradiation sterilization

All electrospun matrices that were later used for sterility testing were removed from the foil, cut into 1 × 1 cm pieces and transferred to 50 mL Falcon tubes for sterilization. Electrospun matrices that were used in other tests were left on foil and cut into appropriate pieces after sterilization. Gamma-sterilization was carried out by Scandinavian Clinics Estonia OÜ. Irradiation was performed using 60Co radiation source at the dose level of ~50 kGy.

5.4.1.3. Chlorine gas sterilization

Chlorine gas was generated *in situ* by mixing 10 mL of commercial chlorine-based bleach with 20 mL of acetic acid in sterilization chamber (250 mL beaker, covered with a rubber glove). The samples to be sterilized were removed from the foil and cut into appropriate pieces (1 × 1 or 2 × 2 cm) and placed into a weighing glass (without the cap) and immediately after mixing the bleach and acid, the weighing glass was put into the sterilization chamber. The generation of chlorine gas was detected visually as an appearance of yellowish gas and by the bleaching of wetted universal indicator paper (Lachema) attached above the liquid level, on the upper part of the sterilization chamber. The samples were kept in a sterilization chamber for 1 or 2 h.

5.4.1.4. Plasma sterilization

Plasma treatment was carried out with a capacitively coupled plasma reactor Femto-PC (Diener electronic GmbH, Germany) with the generator frequency 13.56 MHz and maximum power of 100 W. The power was kept at 30 W during the treatment which allowed to keep the reactor temperature below 30 °C. The treatment was performed at the pressure of 0.3 mbar with the argon working gas supplied to the reactor with the flow rate of 4 sccm. The floating potential during the plasma treatment was approximately 50 V and no additional bias voltage was applied. The samples were treated from both sides with the treatment time varying from 0.5 min to 2 min. Optical emission spectrum of plasma

with and without the electrospun matrices was acquired by UV–VIS spectrometer (OceanOptics 4000 USA).

5.4.2. Sterilization efficacy (III)

For sterility testing, two different culture media and incubation conditions were used, according to the European pharmacopoeia (9.0): (1) fluid thioglycolate medium (FTG) primarily suitable for the cultivation of anaerobic bacteria, but also allows the detection of aerobic bacteria; (2) soya-bean casein digest medium (also known as tryptic soy broth, TSB) for the detection of both aerobic bacteria and fungi. Both media were prepared according to the instructions provided by the manufacturer and dispensed into test tubes prior autoclaving. In both cases, the volume of dispensed aliquotes was 5 mL. The diameter of test tubes for FTG was 12 mm and for TSB 15 mm.

Autoclaving was carried out for 15 min at 121 °C. After the media had cooled to room temperature, both sterilized and unsterilized control fiber samples (1 × 1 cm) were inserted into marked test tubes under aseptic conditions (direct inoculation method). Each sample was tested in triplicate. Positive controls were obtained by inoculating FTG with anaerobic Gram-negative non-spore forming *F. nucleatum* (picking one colony from Columbia blood agar plate); and inoculating TSB with aerobic Gram-negative non-spore forming *E. coli* MG1655 (inoculum size about 8×10^8 CFUs). Untreated media were used as negative controls. FTG was incubated in anaerobic conditions at 30 °C and TSB in aerobic conditions at 20–25 °C for 14 days. If no evidence of microbial growth was found after the incubation period, the sample complied with the test for sterility. If evidence of microbial growth was found, the sample did not comply with the test for sterility. Also, for the test to be valid, no growth could occur in negative control, whereas for positive controls the growth had to occur. The results were recorded by making photographs of the tubes and analyzed visually.

5.5. Statistical analysis

The results are expressed as an arithmetic mean ± standard deviation of three replicates, unless otherwise stated. Students' t-test (I-IV) and one-way analysis of variance (ANOVA) with post-hoc Tukey test (II) or post-hoc t-test (I) were used for assessing statistical significance of differences ($p=0.05$). Holm's method was used for adjusting p-values for multiple comparisons (R 3.2.2 software). Data was analyzed and figures plotted using MS Excel 2013, 2016 and/or 2017, GraphPad Prism 7 ver. 7.04 or OriginPro 8.5 or 2017. The mean diameters of the fibers (n = 50–150) and inhibition zones in disc diffusion assay were calculated using ImageJ software (I–IV). Drug release profiles were compared by calculating difference (f1) and similarity (f2) factors. Time-points included to the analysis were from 0 to the last sampling point where cumulative amount of drug released did not exceed 85%. The profiles were con-

cluded different if f1 > 15 and f2 < 50 (II, III). The drug release data were fitted into mathematical models using the DDSolver, an add-in program for MS Excel. The Akaike Informative Criterion (AIC) and R^2 value were used to evaluate the applicability of the models (I). The CFU data from biofilm assay was log-transformed before statistical analysis (I).

6. RESULTS AND DISCUSSION

6.1. Morphological characterization of the matrices (I, II)

The morphology and structural properties of electrospun fiber matrices form the basis of their functionality and performance. Various parameters affect fiber diameter, diameter distribution, porosity and total surface area. Electrospinning can result in fibers in either micro- or nanometric scale according to the metric system. As seen from Table 4, all PCL blank and drug-loaded fibers were in nanometric range, whereas PCL/PEO blank and drug-loaded fibers were micro-fibers. The addition of a drug can affect the electrospinning solution viscosity, surface tension, conductivity etc., thus morphology of the fibers may also be affected. This was seen with increased PCL/PEO/CAM fiber matrix average fiber diameter and size distribution, whereas, although statistically not significant, addition of MTZ, CIP or both into the fiber matrices had an opposite effect. The latter can be related to the increased solution conductivity from 18.9 μS/cm to 2.75, 0.71 and 1.9 mS/cm, respectively.

Table 4. Average fiber diameters with standard deviations (SD)

Fiber matrix	Average fiber diameter ± SD (nm)
PCL (CF:MET)	496 ±306
PCL/CAM	496 ±339
PCL/PEO	2217 ±570
PCL/PEO/CAM	2863 ±1109
PCL (AA:FA)	565 ± 280
PCL/MTZ	325 ± 100
PCL/CIP	255± 75
PCL/MTZ/CIP	265 ± 40
PCL/MTZ/CIP	265 ± 40

Key: AA – acetic acid; FA – formic acid; CAM – chloramphenicol; CIP – ciprofloxacin; MET – methanol; MTZ – metronidazole; PCL – polycaprolactone; PEO – poly(ethylene oxide).

All fibers lacked beads or pores (Figure 6) and were otherwise smooth, only PCL fibers loaded with CIP or both CIP and MTZ had small visible crystals on the fiber surface. The presence of crystals on fiber surface can indicate phase separation and drug recrystallization during electrospinning process or storage. Drug recrystallization may take place if the chosen polymer(s), drug(s) and solvent(s) are not compatible, i.e., in case of combining ingredients with differing polarities. As both CIP and MTZ are hydrophilic drugs and PCL a hydrophobic polymer, drug recrystallization is very likely, whereas CAM, being also hydrophobic, is less likely to crystallize.

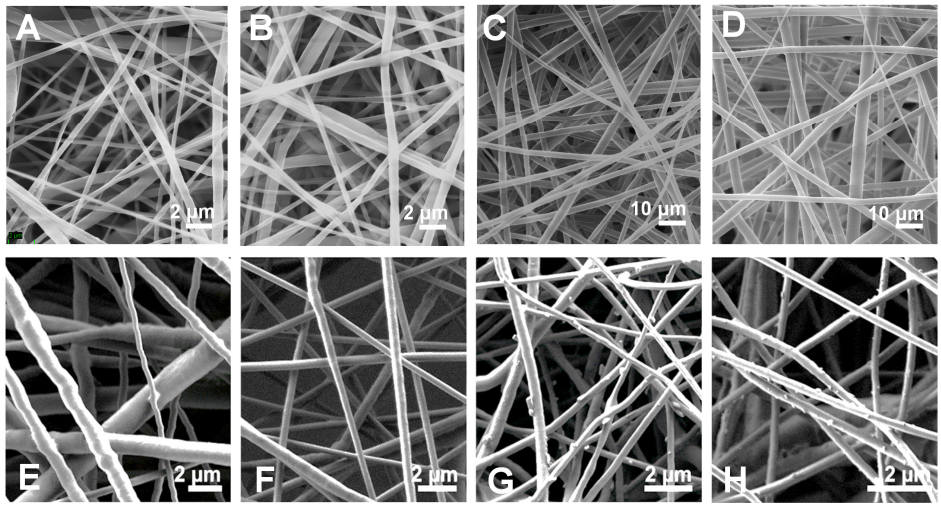

Figure 6. Scanning electron microscopy (SEM) micrographs of PCL blank fibers (solvents CF:MET 3:1 V/V) (A); PCL/CAM fibers (B); PCL/PEO blank fibers (C); PCL/PEO/CAM fibers (D); PCL blank fibers (solvents AA:FA 3:1 m/m) (E); PCL/MTZ fibers (F); PCL/CIP fibers (G); and PCL/CIP/MTZ fibers (H). Key: AA – acetic acid; CAM – chloramphenicol; CIP – ciprofloxacin; FA – formic acid; MET – methanol; MTZ – metronidazole; PCL – polycaprolactone; PEO – poly(ethylene oxide).

Although no pores were seen on the fibers, large interfiber space was observed on SEM images. Large internal porosity of the matrices was confirmed with both mercury intrusion porosimetry and more simple calculations based on matrix dimensions, weight and PCL density provided by the manufacturer (see Materials and Methods section 5.3.1.2). The prior method showed that all CAM-loaded fibers and their corresponding blanks had very similar porosity between ~87–89%. The porosities of other matrices were calculated with the latter method and presented slightly lower, although similar values between ~76–85%. These results comply with previously reported values of electrospun matrices' porosity ranging between 70–95% (Cortez Tornello et al., 2014).The thicknesses of PCL/MTZ, PCL/CIP and PCL/MTZ matrices were varied by varying the electrospinning time from 1 to 8 h, and no significant changes in porosity were observed with longer time of electrospinning (Table 5).

Mercury intrusion porosimetry also provided information about pore size distribution. In the case of electrospun fibers, pore size calculated from Washburn equation should be interpreted as fiber-to-fiber distance, rather than exact pore diameter. Figure 7 shows log differential intrusion volume vs pore diameter profile of PCL/CAM, PCL/PEO/CAM and their corresponding blank matrices. Average pore diameter was 2.4 ± 0.88 µm in PCL/CAM matrix (2.1 ± 0.04 µm in blank) and 6.3 ±1.26 µm in PCL/PEO/CAM matrix (5.9 ± 0.77 µm in blank), agreeing with the literature, that most prevalent pore diameter range for electrospun matrices is between 0.1–10 µm (Rutledge et al., 2009). There

appears to be a correlation between fiber diameter and pore size, as the larger the fibers, the larger the interfiber distance.

Table 5. Thickness, density and porosity values of PCL/MTZ, PCL/CIP and PCL/MTZ/CIP matrices with different electrospinning time.

Sample name with electrospinning time	Thickness (µm)	Density (mg/mm^3)	Porosity (%)
PCL-6h	287 ± 48	0.18 ± 0.04	85 ± 5
PCL/MTZ-1h	53 ± 9	0.23 ± 0.05	80 ± 6
PCL/MTZ-2h	89 ± 29	0.20 ± 0.07	82 ± 8
PCL/MTZ-4h	139 ± 18	0.23 ± 0.04	80 ± 5
PCL/MTZ-6h	195 ± 21	0.25 ± 0.03	78 ± 4
PCL/MTZ-8h	297 ± 36	0.28 ± 0.04	76 ± 5
PCL/CIP-1h	57 ± 27	0.20 ± 0.10	83 ± 12
PCL/CIP-2h	123 ± 20	0.18 ± 0.03	84 ± 4
PCL/CIP-4h	199 ± 31	0.17 ± 0.03	85 ± 4
PCL/CIP-6h	243 ± 43	0.21 ± 0.04	82 ± 5
PCL/MTZ/CIP-6h	241 ± 37	0.21 ± 0.04	82 ± 5

Key: CIP – ciprofloxacin; MTZ – metronidazole; PCL – polycaprolactone.

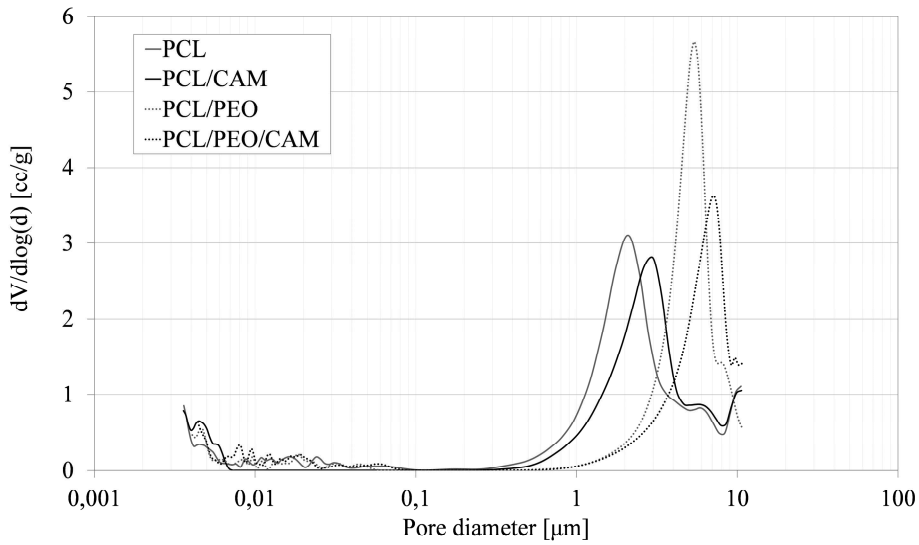

Figure 7. Mercury intrusion profile of electrospun fiber mats plotted as differential intrusion volume vs pore diameter. Key: CAM, chloramphenicol; PCL, polycaprolactone; PEO, poly(ethylene oxide).

In addition to mercury intrusion porosimetry, BET analysis of PCL/CAM, PCL/PEO/CAM and their respective blank matrices was carried out. The technique allows to detect the presence of pores up to 10 nm (Širc et al., 2012), thus giving an indication of the porosity of individual fibers, rather than the matrix. SEM images showed no visible porosity of individual fibers, and this was confirmed with very low values of BET surface areas.

6.2. Drug content and distribution (I)

Electrospinning process may result in drug inactivation or degradation, especially if biomolecules are loaded (Zamani et al., 2013). The amount of drug in final fiber matrix must thus be ascertained. HPLC results confirmed that CAM is stable during electrospinning as the measured amount of drug matched the loading concentration. Also, as the electrospun matrix needs to be cut into desired sized pieces for final application, the uniformity of the matrix must be ensured. Thus, RSM mapping was carried out, showing that CAM was uniformly distributed in the fibers, the distribution matching that of PCL (Figure 8). The prior was also confirmed in larger scale with HPLC by measuring drug content in samples cut from different locations of the matrix.

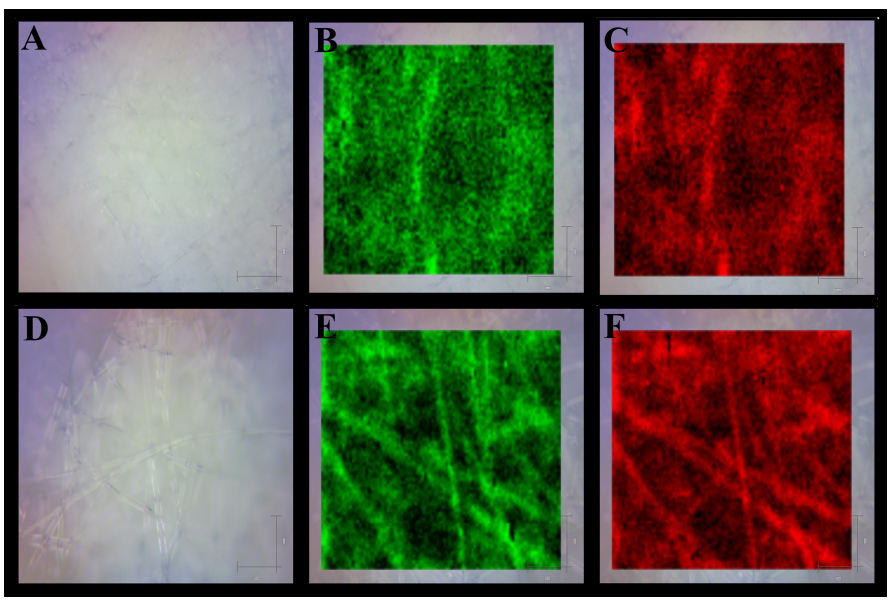

Figure 8. Bright-field microscopy (BFM) and Raman scattering microspectroscopy (RSM) images of CAM-loaded fiber matrices: PCL/CAM fibers BFM image (A); RSM images at CAM peak (1350 cm^{-1} vs 1380 cm^{-1}) (B) and at PCL peak (1724 cm^{-1} vs 1764 cm^{-1}) (C); and PCL/PEO/CAM fibers BFM image (D); RSM images at CAM peak (1349 cm^{-1} vs 1378 cm^{-1}) (E) and at PCL peak (1724 cm^{-1} vs 1760 cm^{-1}) (F). Key: CAM, chloramphenicol; PCL, polycaprolactone; PEO, poly(ethylene oxide).

Distribution of MTZ and CIP in the fibers was not studied, although it is expected that they are less homogenously distributed compared to CAM due to the crystallization. Still, if the drug crystals are distributed evenly, the drug content will not vary from sample to sample in larger scale.

6.3. Solid state characterization (I, II)

Electrospinning is recognized as a method that favors the formation of non-crystalline solid dispersions due to rapid solvent evaporation. Still, not every drug-polymer system allows amorphization and intrinsic properties of the drug together with drug-polymer interactions control which solid state form is established (Verreck et al., 2003).

XRD diffractograms (Figure 9) showed that crystalline CAM reflections present in physical mixtures were not visible in PCL/CAM nor PCL/PEO/CAM matrices. This indicates drug amorphization during electrospinning. On the other hand, in MTZ-loaded matrices characteristic reflections of the drug were seen as in physical mixtures, suggesting drug crystallization (Figure 10). As no drug crystals were visible on SEM images, the crystallization may have taken place inside the fibers. With CIP loaded matrices, only one reflection at ~6.3° 2-θ was detected, whereas no typical crystalline reflections of CIP HCl hydrate, the solid state form initially incorporated into the electrospinning solution, were found (Figure 10). Comparing the XRD results with the theoretical calculated CIP structures from Cambridge Structural Database indicated that CIP may have changed its solid state form to a free CIP base, new solvate or CIP formic acid salt.

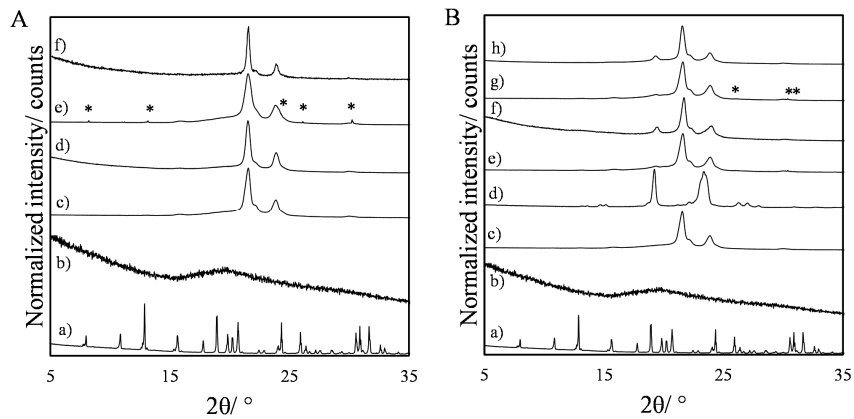

Figure 9. XRD diffractograms of A. (a) crystalline CAM powder, (b) amorphous CAM powder, (c) PCL powder, (d) PCL fibers, (e) PCL/CAM physical mixture, (f) PCL/CAM fibers; B. (a) crystalline CAM powder, (b) amorphous CAM powder, (c) PCL powder, (d) PEO powder, (e) PCL/PEO physical mixture, (f) PCL/PEO fibers, (g) PCL/PEO/CAM physical mixture, (h) PCL/PEO/CAM fibers. Key: CAM – chloramphenicol; PCL – polycaprolactone; PEO – poly(ethylene oxide); * – crystalline reflection of CAM.

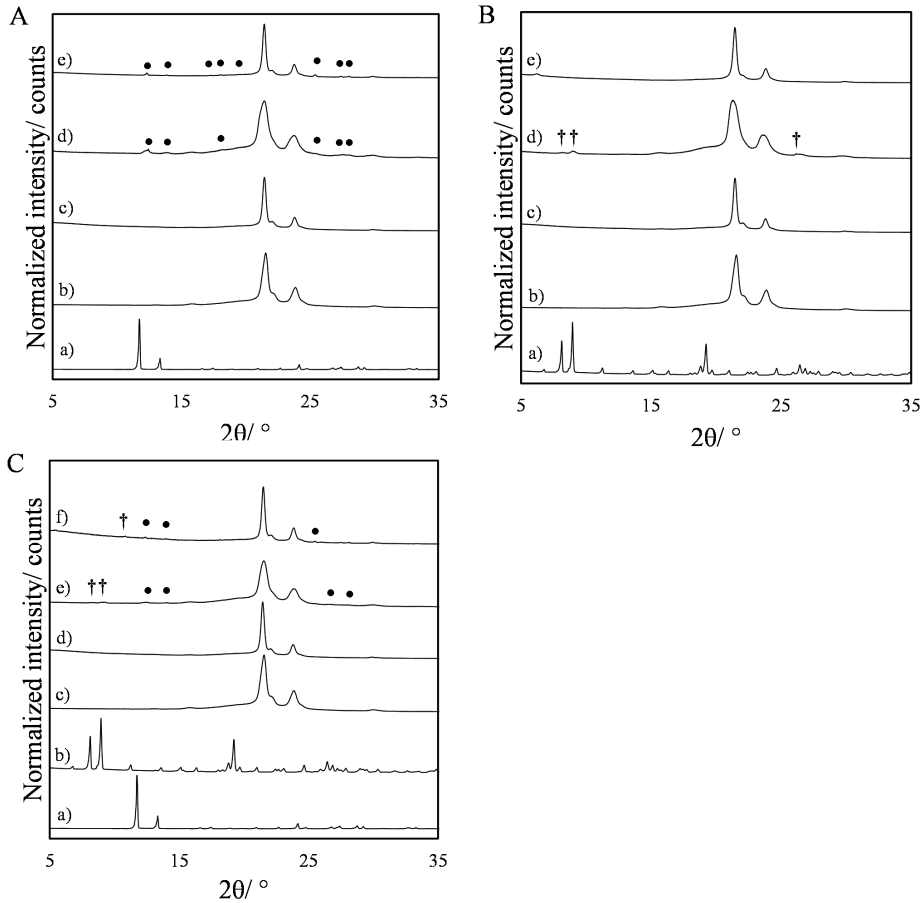

Figure 10. XRD diffractograms of A. (a) crystalline MTZ powder, (b) PCL powder, (c) PCL fibers, (d) PCL/MTZ physical mixture, (e) PCL/MTZ fibers; B. (a) crystalline CIP HCl hydrate powder, (b) PCL powder, (c) PCL fibers, (d) PCL/CIP HCl hydrate physical mixture, (e) PCL/CIP fibers; C. (a) crystalline MTZ powder, (b) crystalline CIP HCl hydrate powder, (c) PCL powder, (d) PCL fibers, (e) PCL/MTZ/CIP HCl hydrate physical mixture, (f) PCL/MTZ/CIP fibers. Key: CIP – ciprofloxacin; CIP HCl – ciprofloxacin hydrochloride; MTZ – metronidazole; PCL – polycaprolactone; • – crystalline reflection of MTZ; † - crystalline reflection of CIP hydrochloride hydrate.

XRD results were confirmed, and possible drug-polymer interactions further elaborated with ATR-FTIR. Table 6 summarizes the characteristic peaks of PCL, PEO, CAM, MTZ and CIP, according to the literature data.

Table 6. Selected characteristic infrared bands of PCL, PEO, CAM, MTZ and CIP.

	Assignments	Wavenumber (cm^{-1})
PCL	$'\nu_{as}(CH_2)$	2949 (amorphous) (Elzein et al., 2004; T. Yang et al., 2014)
	$\nu_s(CH_2)$	2865 (crystalline) (Elzein et al., 2004; T. Yang et al., 2014)
	ν(C=O)	1731(amorphous) (T. Yang et al., 2014), 1724 (crystalline) (Elzein et al., 2004; T. Yang et al., 2014)
	ν(C-O C-C)	1295 (crystalline) (X. Wang et al., 2013; T. Yang et al., 2014), 1157 (amorphous) (Elzein et al., 2004)
	ν_{as}(COC)	1245 (crystalline) (Elzein et al., 2004; T. Yang et al., 2014)
	ν(OC-O)	1192 (crystalline) (Elzein et al., 2004; T. Yang et al., 2014)
	ν_s(COC)	1170 (Elzein et al., 2004; X. Wang et al., 2013)
	ν(COC)	1107 (Abdelrazek et al., 2016)
	$\gamma_{in}(CH_2)$	731 (crystalline) (T. Yang et al., 2014)
	$\gamma_{out}(CH_2)$	710 (crystalline) (T. Yang et al., 2014)
PEO	$\nu_{as}(CH_2)$	2946 (Miyazawa et al., 1962)
	$\nu_s(CH_2)$	2886 (Miyazawa et al., 1962)
	$\omega(CH_2)$	1361 (Rocco et al., 2002), 1343 (Rocco et al., 2002)
	$\tau(CH_2)$	1281 (Davison, 1955), 1242 (Davison, 1955)
	ν(COC)	1145 (crystalline) (Rocco et al., 2002), 1095 (crystalline) (Rocco et al., 2002), 1059 (crystalline) (Rocco et al., 2002)
	$\rho(CH_2)$	963 (Oliveira et al., 2013), 843 (Oliveira et al., 2013)
CAM	ν(C=O)	1686 (Sajan et al., 2008)
	ring stretch	1563 (Sajan et al., 2008)
	$\nu_{as}(NO_2)$	1520 (Sajan et al., 2008)
	ν_{as}(C-Cl)	817 (Sajan et al., 2008)
	ring deformation	643 (Si et al., 2009)
MTZ	NO_2 scissoring	824 (Chamundeeswari et al., 2011)
	C—H out-of-plane bending	864 (Chamundeeswari et al., 2011)
	$C_{14}C_{17}$ stretching +	907 (Chamundeeswari et al., 2011)

	Assignments	Wavenumber (cm^{-1})
	C—N—C in plane bending	
	C—O stretching	1074 (Chamundeeswari et al., 2011)
	O—H in plane bending + $C_{12}H_2$ twisting	1265 (Chamundeeswari et al., 2011)
	C—C stretching ($C_{17}H_2$ scissoring)	1473 (Chamundeeswari et al., 2011)
	NO_2 asymmetric stretching	1535 (Chamundeeswari et al., 2011)
CIP	O—H bending	1272 (Sahoo et al., 2011)
	Vibration of CH_2 on the benzene ring	1474 (Tan et al., 2012)
	C—C ring stretching	1608 (Martínez-Alejo et al., 2014)
	Vibration of CH_2 on the benzene ring	1629 (Tan et al., 2012)

Key: CAM – chloramphenicol; CIP – ciprofloxacin; MTZ – metronidazole; PEO – poly(ethylene oxide); PCL – polycaprolactone.

Crystalline and amorphous CAM presented some differences in their spectra and similar changes were seen when physical mixtures were compared with electrospun fibers (Figure 11). For instance, a peak shift from 814 cm^{-1} to 808 cm^{-1} was observed for amorphous compared to crystalline CAM. Similar shift from 816 cm^{-1} to 810 cm^{-1} was seen with CAM-loaded fibers compared to respective physical mixtures. A sharp peak of crystalline CAM at 1682 cm^{-1} turned out broader and shifted to 1670 cm^{-1} for amorphous CAM. The peak appeared clearly in physical mixtures, whereas in electrospun fibers, it was not visible. Peaks at 1563 cm^{-1} and 649 cm^{-1} were also absent in the spectra of CAM-loaded fibers. These results confirm that CAM was indeed in an amorphous form in fibers.

Also, the changes in the spectra suggest interactions between CAM and PCL (Figure 11). As a peak at 1510 cm^{-1}, corresponding to NO_2 asymmetric stretch shifted to 1522 cm^{-1} and 1520 cm^{-1} in PCL/CAM and PCL/PEO/CAM fibers, respectively, changes in hydrogen bonding may have occurred. Hydrogen bonding and thus interactions are also possible for PCL and PEO. This may be a reason why a peak at 1107 cm^{-1} with a shoulder at 1094 cm^{-1} that was present in a physical mixture of PCL and PEO turned into a single peak with increased intensity in electrospun PCL/PEO fibers.

FTIR spectra of MTZ-loaded fibers (Figure 12A and B) presented several characteristic peaks of MTZ, similarly to physical mixtures: peak at 1535 cm^{-1}, corresponding to NO_2 asymmetric stretch and a shoulder at 1184 cm^{-1}, corresponding to wagging $C_{17}H_2$ together with twisting $C_{14}H_2$. This confirms XRD results that MTZ was indeed crystallized into the original form in the fibers. Still, possibly partial amorphization took place as the intensity of some MTZ peaks was changed and some peaks almost disappeared from the spectra of fibers compared to physical mixtures. Intermolecular interactions between PCL and MTZ could also be responsible of some changes, although the interactions most probably were not very strong, as no peak shifts of MTZ nor PCL were observed.

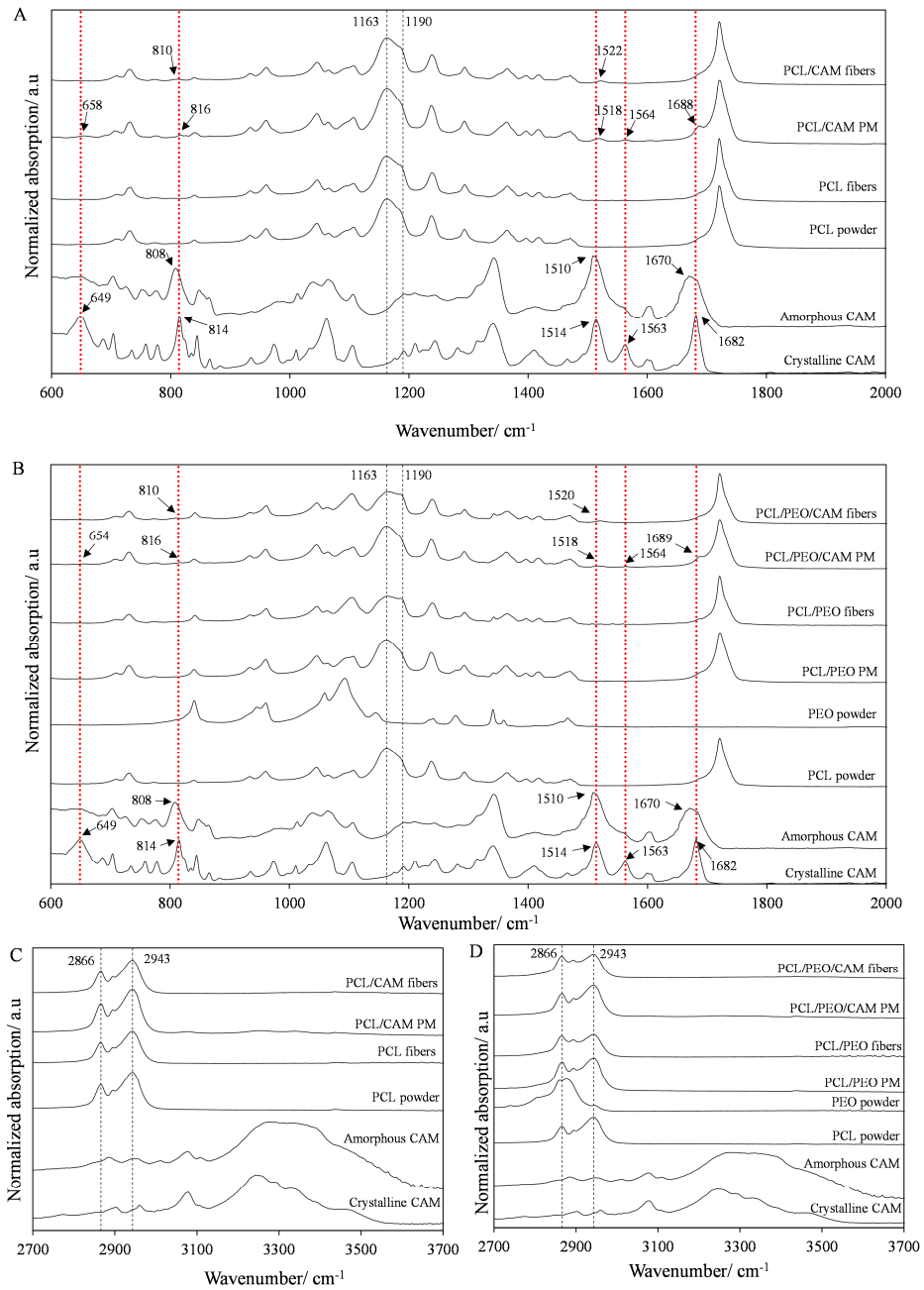

Figure 11. ATR-FTIR spectra of the electrospun fibers in comparison with the respective physical mixtures, crystalline and amorphous CAM, and carrier polymers PCL and PEO. Red dotted lines represent positions of CAM bands and black dashed lines represent positions of PCL bands. Key: CAM, chloramphenicol; PCL, polycaprolactone; PEO, poly(ethylene oxide).

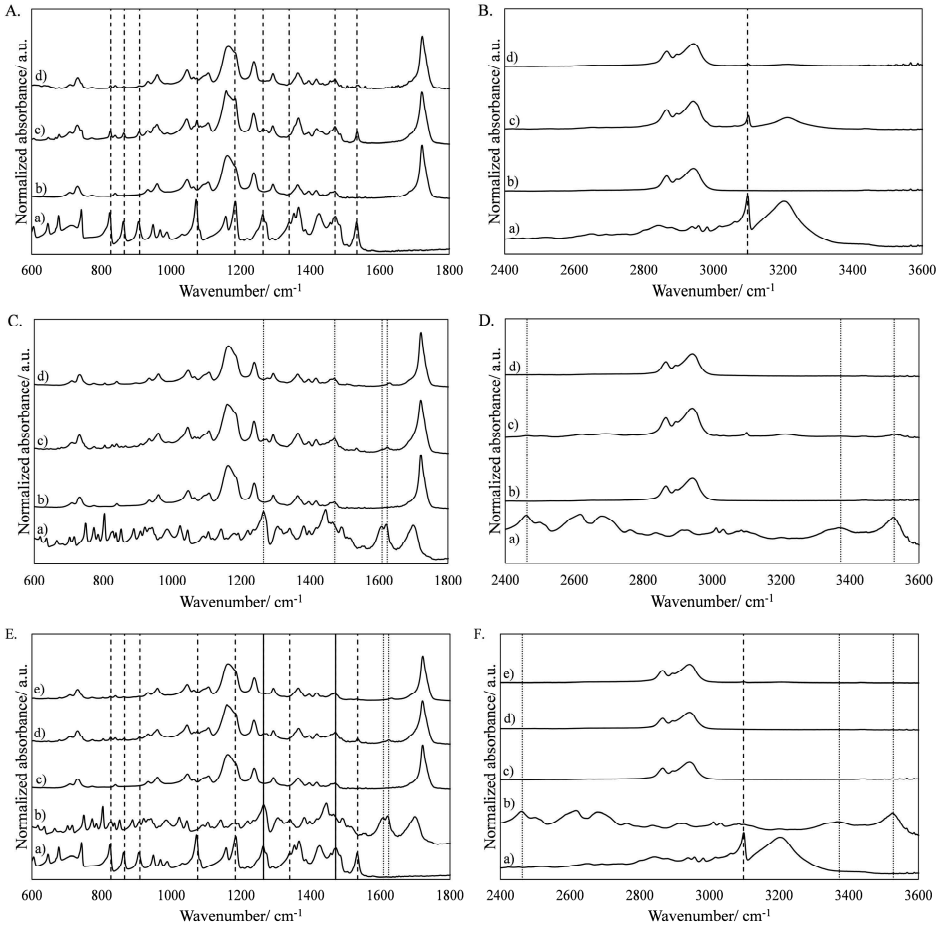

Figure 12. ATR-FTIR spectra of the electrospun fibers in comparison with the respective physical mixtures: A. and B. (a) MTZ powder, (b) PCL fibers, (c) PCL/MTZ physical mixture, (d) PCL/MTZ fibers; C. and D. (a) CIP HCl powder, (b) PCL fibers, (c) PCL/CIP HCl physical mixture, (d) PCL/CIP fibers; E. and F. (a) MTZ powder, (b) CIP HCl powder, (c) PCL fibers, (d) PCL/MTZ/CIP HCl physical mixture, (e) PCL/MTZ/CIP fibers. Key: CIP – ciprofloxacin; CIP HCl – ciprofloxacin hydrochloride; MTZ – metronidazole; PCL – polycaprolactone; dashed, dotted and solid lines mark the positions of MTZ, CIP HCl and overlapping peaks, respectively, in physical mixtures.

Several peaks of CIP-loaded fibers in the FTIR spectra (Figures 12C and D) had shifted to higher wavenumbers compared to the physical mixtures and CIP HCl hydrate powder: CIP peak at 1265 cm^{-1}, corresponding to the bending vibration of O-H (Demirci et al., 2014), moved to 1277 cm^{-1} in fibers; CIP peak at 1624 cm^{-1}, corresponding to vibration of CH_2 on the benzene ring (Tan et al., 2012) moved to 1630 cm^{-1} in fibers. Also, several characteristic CIP HCl peaks were not detected from the fibers, whereas new peaks appeared. This supports XRD data

that CIP solid state form has changed, although the new form still needs to be confirmed. Peak shifts and absence of peaks at 3500-3450 cm^{-1}, corresponding to OH stretching and intermolecular H-bonding (Martínez-Alejo et al., 2014), indicate that the hydrate form is lost and/or there may be interactions like hydrogen bonding between PCL and CIP. The solid state properties of MTZ and CIP in fiber matrices loaded with both drugs were similar to the ones loaded with either drug alone.

Crystallinity of the carrier polymer may also change during electrospinning. Both PCL and PEO are semi-crystalline polymers, meaning that crystallites with ordered structure exist together with amorphous regions. As the amorphous/ crystalline ratio changes, polymer properties can also change, which in bigger perspective affects the behavior of the DDS. For example, it has been shown that the degree of PCL crystallinity affects the drug release kinetics from diffusion controlled systems as the drug can only diffuse out through amorphous regions (Jeong et al., 2003). PCL has two characteristic crystalline reflections in the XRD diffractograms at 21.55 and 23.87° that correspond to the planes (110) and (200), respectively (Figures 9 and 10). Both were present in all physical mixtures as well as in fiber matrices, suggesting that the semi-crystallinity is preserved. The same was true for PEO. Although the polymers maintained their semi-crystalline nature, the degree of crystallinity may still have changed. The crystallinity of PCL can be assessed by comparing 110/200 intensity ratios from XRD diffractograms (J. L. Li et al., 2014). We saw that the crystallinity of PCL in our electrospun matrices was higher compared to the physical mixtures, although the method for producing physical mixtures must also be considered. As the manufacturer provided PCL as pellets, these were modified to produce powder that could be mixed with other ingredients. This process may have also reduced the polymer crystallinity, thus comparing the crystallinity of PCL in fibers and that in physical mixtures must be done with caution. There are reports in the literature that electrospinning reduces both PCL (Kuzelova Kostakova et al., 2017; X. Wang et al., 2013) and PEO (Xu et al., 2014) crystallinity. This contradiction with our results could be explained by higher crystallinity of PCL in pellets compared to our produced PCL powder form, supported by literature data (J. L. Li et al., 2014). Increased crystallinity was also observed with FTIR in PCL/CAM, PCL/PEO and PCL/PEO/CAM fibers compared to blank PCL fibers, as intensity of the peak at 2943 cm^{-1}, corresponding to an asymmetric CH_2 stretch in amorphous form, decreased, and the intensity ratio of crystalline vs amorphous peaks at 1724 cm^{-1} and 1731 cm^{-1}, respectively, increased (T. Yang et al., 2014). This suggests that adding drugs or other carrier polymers to the electrospinning solution affects the crystallinity of PCL in final electrospun fibers.

DSC analysis showed that both carrier polymers have lower melting points compared to the crystalline drug substances used in our studies: PCL 60.1 ºC, PEO 69.4 ºC, CAM 151.1 ºC, MTZ 163.2 ºC, CIP HCl hydrate 315.2 ºC. Thus, the lack of melting endotherm of the drug on the thermogram cannot be used to interpret the crystallinity of the drug if the drug is mixed with either of these

polymers (Kajdič et al., 2018). Other methods confirmed that amorphous CAM and at least partially crystalline MTZ and CIP were present in electrospun fibers. The thermograms, on the other hand, all lacked melting endotherms of the drug as expected due to the drug dissolution in the polymer melt before reaching its melting temperature. Similar results were seen with physical mixtures, confirming the hypothesis.

Solid state analysis suggested intermolecular interactions between PCL, PEO and CAM. A deeper understanding of these interactions was sought with MD simulations (see publication I). The simulations showed that the number of hydrogen bonds between PEO and water was almost double compared to PCL and water, although both polymers had the same number of oxygen atoms capable of forming hydrogen bonds (see publication I Figure 7A). This is expected as PEO is hydrophilic, whereas PCL is hydrophobic. For that reason, hydrophobic CAM is more likely to interact with PCL compared to PEO. The contact area of the polymer and the drug showed that PCL and CAM were practically always in contact, indicating strong interactions. In contrast, for PEO and CAM any contact was probably accidental, not related to real interactions. The dominant form of interactions in both PCL/CAM and PCL/PEO/CAM systems were nonpolar-nonpolar contacts, i.e., hydrophobic interactions. Polar-polar contacts that could be related to hydrogen bonding between the drug and a polymer made up only a very small fraction of total contacts. Thus, hydrogen bonding is clearly not the dominant mechanism of the interaction between PCL and CAM. Altogether, the simulations provided evidence that CAM has a clear attractive interaction with PCL that is predominantly due to hydrophobic (entropy driven) interactions, and that interaction between PEO and CAM is extremely weak.

6.4. Wettability of the matrices (I, II)

Contact angle value helps to describe the wettability of a surface, thus indicating materials' hydrophobicity/hydrophilicity. As both PCL and CAM are hydrophobic, it is not surprising that PCL/CAM fibers were also hydrophobic with contact angle values of 98°, whereas addition of a hydrophilic polymer PEO caused the contact angle value to drop to 45°. Thus, PCL/PEO/CAM fibers were hydrophilic. Interestingly, when hydrophilic drugs MTZ, CIP or both were incorporated into the PCL matrix, the contact angle value was not significantly affected, and the matrices preserved their hydrophobic nature. However, it was observed that on a certain location of PCL/MTZ/CIP fiber matrices the droplet quickly penetrated into the matrix, reducing the contact angle to 0° (Figure 13). Thus, the surface properties were not uniform for the whole matrix. This was also seen when PCL/MTZ/CIP matrix was immersed into the buffer: in 1 s, localized wetting occurred, whereas longer immersion resulted in complete wetting of the matrix (Figure 13C).

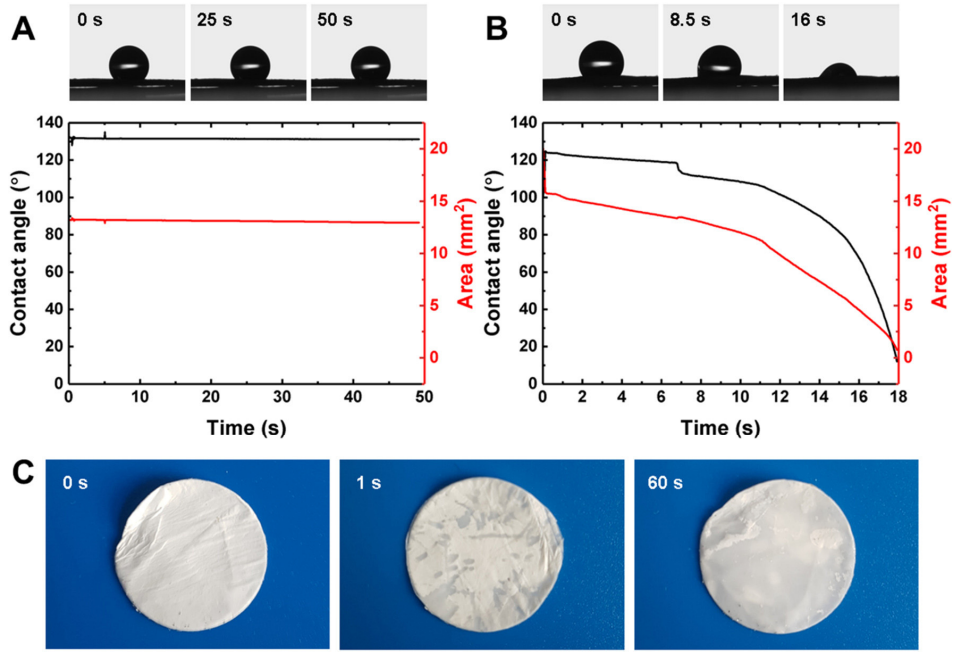

Figure 13. The change in contact angle and area of droplet on the image with time at two different locations on the surface of nanofiber matrices loaded with both drugs (MTZ 2.5% and CIP, 2.5%) (A and B). Representative images of the PCL/MTZ/CIP nanofiber matrix before and after immersion into the 50 mM phosphate buffer for 1 s and 60 s (C). Key: CIP – ciprofloxacin; MTZ – metronidazole; PCL – polycaprolactone.

6.5. Buffer uptake and swelling of the matrices (I, II)

Buffer uptake and swelling properties provide a finer understanding of the whole matrix' interactions with liquid medium. This is important to consider as it can affect the drug release properties and for wound dressings, the ability to absorb wound exudate is directly related to its' functionality. It is known that PCL does not swell (Sultanova et al., 2016) and this was also seen in our study as the degree of swelling values were negligible for blank PCL matrix (5.0% ± 3.82%). At the same time, PCL/PEO fibers showed a completely different profile, as the degree of swelling was close to 250% (248% ± 15%). This indicates that the addition of a hydrophilic polymer greatly increased water absorption. The addition of CAM molecules slightly increased water absorption (38% ± 10%) compared to the blank PCL matrix, probably due to creating structural changes in the matrix as the drug was released, enabling the water to diffuse in. At the same time, the addition of CAM to PCL/PEO matrix decreased the swelling nearly four times. Interestingly, the buffer uptake of PCL matrices loaded with hydrophilic drugs MTZ and/or CIP was much larger compared to

PCL/CAM matrices (Figure 14), even though the contact angle values were comparable.

Significant differences in the rate of buffer penetration were observed between PCL/MTZ, PCL/CIP and PCL/MTZ/CIP matrices. The buffer penetrated slowly into PCL/MTZ matrices, whereas the wetting was immediate for PCL/CIP and PCL/MTZ/CIP matrices (Figure 14). In addition, the buffer uptake values were significantly different ($p=0.05$) between these three electrospun matrices (Figure 14). The highest buffer uptake was observed with the PCL/CIP matrix (500%), followed by PCL/MTZ/CIP matrix (300%), and the lowest uptake being with the PCL/MTZ matrix (140%). These differences cannot be explained by average nanofiber diameter or density of fiber matrices, since these did not significantly differ among the samples (Tables 4 and 5, respectively). One factor that did differ was the location of the drug. A hydrophilic drug is usually incorporated within the hydrophobic carrier polymer close to the surface or may even be deposited only on the surface, resulting in an uneven distribution in nanofibers (Zeng et al., 2005). SEM images revealed no visible MTZ crystals, and thus these were positioned inside the nanofibers, whereas some of CIP was observed on the nanofiber surface as small nanocrystals (Figures 6G and H). MTZ incorporates well into PCL and >20% drug loading can be achieved (Xue et al., 2014). The crystallization of CIP on the surface of PCL nanofibers is in line with the reported data for levofloxacin, an antimicrobial agent from the same chemical group as CIP (Hall Barrientos et al., 2017). Differences in localization can be attributed to differences in the compatibility and interactions between these drugs, PCL and the solvents. As CIP crystallized on the nanofiber surface, it could draw the medium into the nanofiber matrix due to its hydrophilic (Olivera et al., 2011) and hygroscopic properties (Kakkar et al., 1997), thus being responsible for better buffer penetration compared to matrices where only MTZ was present inside the nanofibers.

Also, to gain an insight about the maximum buffer uptake capacity, the matrices were immersed in 1% (m/m) Tween 80 solution, resulting in an immediate uptake as the surfactant decreased the surface tension of the medium and improved the wetting properties of the matrices. The results indicated that complete wetting of PCL/MTZ matrix was not achieved in the time of the experiment as immersion in the surfactant solution increased the buffer uptake to 330%. At the same time, for PCL/CIP and PCL/MTZ/CIP matrices the buffer uptake did not differ when the surfactant was added.

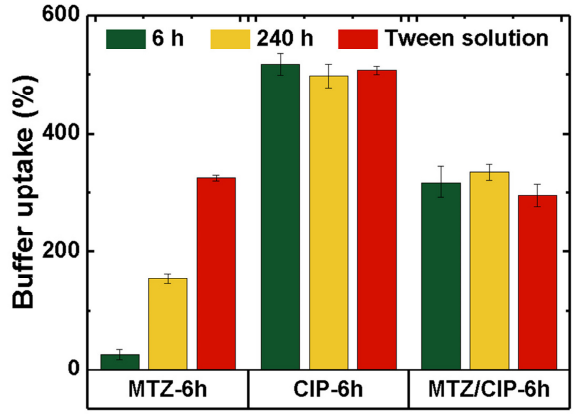

Figure 14. Histogram showing buffer uptake after 6 h and 240 h immersion of PCL/MTZ-6 h, PCL/CIP-6 h, and PCL/MTZ/CIP-6 h into 50 mM phosphate buffer and immersion into 1% Tween 80 solution after 5 min. Data are averages of three replicates and error bars denote standard deviation. Key: CIP – ciprofloxacin; MTZ – metronidazole; PCL – polycaprolactone. Details about samples descriptions are shown in Table 3.

6.6. Drug release and factors affecting it (I, II)

Sustaining the release of hydrophobic drug molecules is often achieved using simple strategies, like monoaxial electrospinning of a drug-polymer blend using slowly disintegrating carrier polymers. This, however, is mostly, although not universally, unsuccessful in case of small hydrophilic molecules (Karuppuswamy et al., 2015; Sultanova et al., 2016; Xue et al., 2014; Zupančič et al., 2016). It is important to find out critical parameters that are responsible for these differences and that would help to explain the mechanism of drug release. This knowledge can help to design and develop DDSs with desired release profiles, especially when simple strategies fail, or the release needs to be finely tuned.

6.6.1. Effect of carrier polymers on the drug release (I)

For PCL/CAM matrix, sustained release was achieved as after 78 h only ~60% of the drug was released (Figure 15A). Still, significant burst release occurred during the first hour, as ~19% of the drug was released. Addition of PEO into the fiber matrix enhanced the drug release from the matrix, as in 15 min ~92% of the drug was released and ~95% after 1 h (Figure 15B). As previously stated, PCL/CAM matrix was hydrophobic, whereas PCL/PEO/CAM matrix hydrophilic due to the different nature of carrier polymers. It has been proposed that increasing matrix hydrophobicity can prolong the drug release (Falde et al., 2015; Yohe et al., 2012), and conversely, increasing hydrophilicity accelerates the release. This illustrates the importance of choosing proper carrier polymer(s) to prepare DDSs with suitable and desired release kinetics.

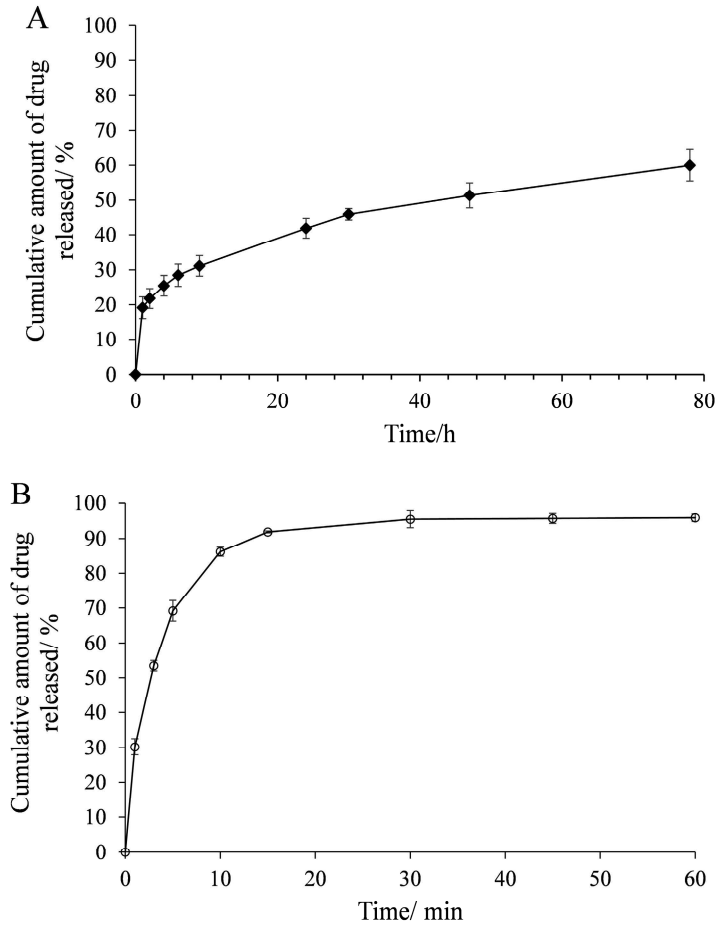

Figure 15. Drug release profiles of PCL/CAM fibers (A); and PCL/PEO/CAM fibers (B) in phosphate buffered saline (PBS) at 37 °C. Data are averages of three replicates and error bars denote standard deviation. Key: CAM, chloramphenicol; PCL, poly-caprolactone; PEO, poly(ethylene oxide).

To further elucidate the release mechanisms and reveal the impact of different carrier polymers on CAM release, the dissolution data were fitted into different mathematical models describing possible release kinetics: zero-order, first-order, Higuchi, Korsmeyer-Peppas, Hixson Crowell and Weibull. The model best describing the release from PCL/CAM fibers was Korsmeyer-Peppas (Akaike Information Criterion (AIC) = 26.9, coefficient of determination (R^2) =0.9964). The value of release exponent n was below 0.45, suggesting Fickian diffusion as the release mechanism (Dash et al., 2010). This agrees with the literature which states that the diffusion-controlled release is the only option for non-swellable and very slowly degrading PCL systems (Sultanova et al., 2016). For PCL/PEO/CAM the best fit was Weibull model (AIC = 23.7, R^2 =0.9981). The value of exponent b has been shown to be an indicator of the mechanism of transport of the drug through the polymer matrix (Papadopoulou et al., 2006). The b value in PCL/PEO/CAM matrices was 0.74, suggesting that the system was homogeneous (Kosmidis et al., 2003a, 2003b) and very little, if any, phase separation between the two polymers and the drug occurs during electro-spinning, as suggested by RSM results. The results support that the fast release from PCL/PEO/CAM matrix was not due to incompatibility of drug and the polymers but rather enhanced diffusion of the release medium into the matrix due to better wetting properties.

6.6.2. Effect of fiber matrix thickness on the drug release (II)

Figure 16 shows the drug release profiles of PCL/MTZ, PCL/CIP and PCL/ MTZ/CIP fiber matrices electrospun for different times, resulting in matrices with varying thicknesses. Matrix thickness was an important parameter affecting the drug release of MTZ from PCL/MTZ fiber matrices as increased thickness prolonged the drug release (Figure 16A). Over 90% of MTZ was released from the thinnest PCL/MTZ-1 h matrix (53 ± 9 μm) in the first 4 h, whereas the thickest PCL/MTZ-8 h matrix (297 ± 36 μm) released 44% of the drug on the first day, followed by a linear pattern of drug release over the following 19 days.

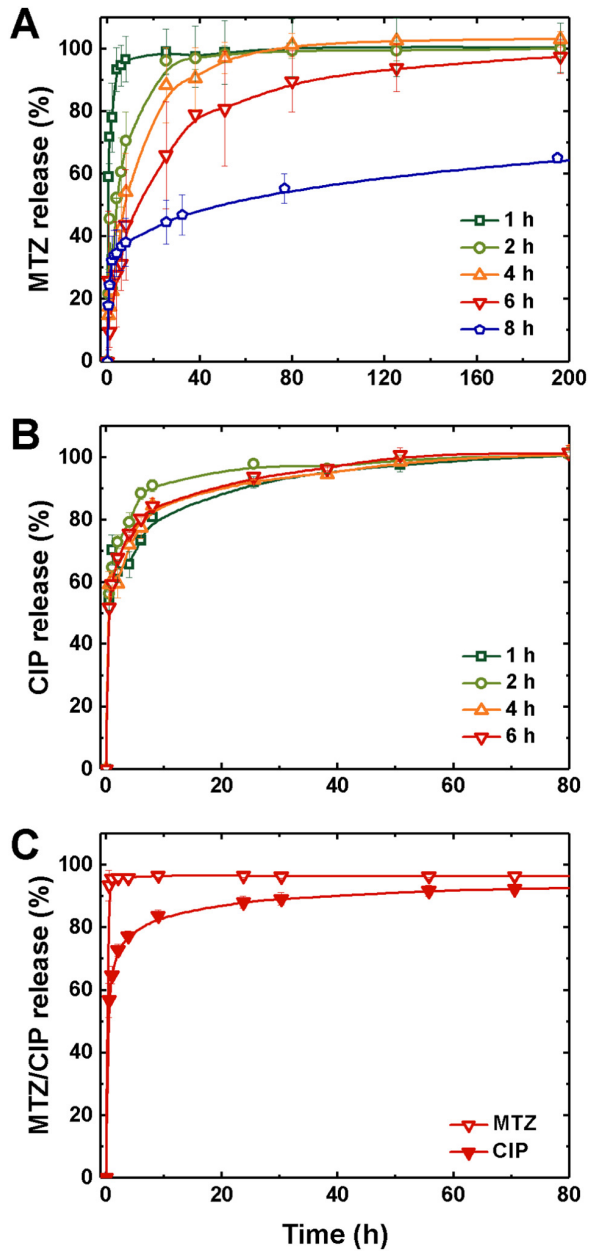

Figure 16. Release of drugs from (A) PCL/MTZ, (B) PCL/CIP, and (C) PCL/MTZ/CIP nanofiber matrices of different thickness. The thickness of PCL/MTZ nanofiber matrix varied from 53 ± 9 μm (sample PCL/MTZ-1 h) to 297 ± 36 μm (sample PCL/MTZ-8 h) and PCL/CIP nanofiber matrix from 57 ± 27 μm (sample PCL/CIP-1 h) to 243 ± 43 μm (sample PCL/CIP-6 h). The PCL/MTZ/CIP-6 h nanofiber matrix was 241 ± 37 μm thick. Data are averages of at least three replicates and error bars denote standard deviation. Key: CIP – ciprofloxacin; MTZ – metronidazole; PCL – polycaprolactone.

On the contrary, the nanofiber matrix thickness had no effect on CIP release. Approximately 80% of CIP was released in the first 10 h and the remaining 20% over the following 50 h, irrespective of matrix thickness (Figure 16B). PCL/MTZ/CIP-6 h matrix released CIP in a similar manner to CIP-loaded nanofibers, whereas MTZ was released immediately (Figure 16C) and faster compared to similarly thick PCL/MTZ matrix. The similarity between the samples was also statistically analyzed by calculating the difference (f1) and similarity factors (f2) (Table 7). The difference between samples was confirmed in case of the release profiles of PCL/MTZ matrices and the similarity was proven in case of PCL/CIP matrices.

Table 7. The difference (f_1) and similarity (f_2) factors between release profiles of investigated nanofiber matrices.

Tested samples	f_1	f_2	Similarity
PCL/MTZ-6h vs PCL/MTZ-1h	312.5	13.9	No, $f_1 \geq 15$ and $f_2 \leq 50$
PCL/MTZ-6h vs PCL/MTZ-2h	79.6	30.7	No, $f_1 \geq 15$ and $f_2 \leq 50$
PCL/MTZ-6h vs PCL/MTZ-4h	40.2	44.8	No, $f_1 \geq 15$ and $f_2 \leq 50$
PCL/MTZ-6h vs PCL/MTZ/CIP-6h	/	/	Cannot be calculated due to immediate release
PCL/CIP-6h vs PCL/CIP-1h	7.7	60.2	Yes, $f_1 \leq 15$ and $f_2 \geq 50$
PCL/CIP-6h vs PCL/CIP-2h	7.1	64.3	Yes, $f_1 \leq 15$ and $f_2 \geq 50$
PCL/CIP-6h vs PCL/CIP-4h	4.8	67.8	Yes, $f_1 \leq 15$ and $f_2 \geq 50$
PCL/CIP-6h vs PCL/MTZ/CIP-6h	5	70.2	Yes, $f_1 \leq 15$ and $f_2 \geq 50$
PCL/MTZ-8h: 2.63 cm^2:5.26 cm^2	4.2	74.2	Yes, $f_1 \leq 15$ and $f_2 \geq 50$
PCL/MTZ-8h: 25 ºC: 37 ºC	29.2	44.6	No, $f_1 \geq 15$ and $f_2 \leq 50$

Key: CIP – ciprofloxacin; MTZ – metronidazole; PCL – polycaprolactone.

6.6.3. Effect of solid state on the drug release (I, II)

Solubility is one of the most crucial factors that influences the rate and extent of drug release and different solid state forms can exhibit significant differences in the apparent solubility. As amorphous form lacks highly ordered three-dimensional crystal structure, it possesses higher free energy and has higher apparent solubility. Thus, the preparation and stabilization of an amorphous form has been recognized as a valid strategy for improving the drug release rate (Bhujbal et al., 2021). In case of electrospun matrices, the situation is more complex. Solid state analysis confirmed that CAM was in an amorphous form in both PCL/CAM and PCL/PEO/CAM fiber matrices (Figures 9 and 11), although the release rate was significantly different (Figure 15). Moreover, slow release from PCL/CAM matrices was possible despite CAM being in an amorphous form.

On the other hand, both MTZ and CIP had recrystallized at least partially in the matrices (Figures 10 and 12), but MTZ was released immediately from PCL/MTZ/CIP matrix, whereas CIP exhibited prolonged release (Figure 16). Also, remarkable differences were observed in MTZ release from PCL/MTZ and PCL/MTZ/CIP matrices and not in CIP release from PCL/CIP and PCL/MTZ/CIP matrices, whereas the solid state forms of the drugs were the same in matrices loaded with one drug or both drugs. Thus, solid state form of the drug cannot solely be responsible for different release profiles. Still, the effect can be indirect. An amorphous form of the drug is usually deposited inside the fibers, whereas recrystallization takes place on or near the fiber surface. Due to the large surface area of the fiber matrices and small size of the drug crystals, release medium has better access to the crystallized drug compared to the amorphous drug inside the fibers. Thus, in case of electrospun DDSs, amorphization can actually prolong the drug release. Also, hydrophilic drug crystals on the fiber surface can facilitate buffer uptake, which in turn can enhance drug release.

6.6.4. Effect of buffer uptake on the drug release (II)

As both drug release and buffer uptake were slower for PCL/MTZ matrix compared to PCL/CIP and PCL/MTZ/CIP matrices, we wanted to understand if these two properties are related. Buffer uptake curves are compared with drug release curves in Figure 17. The buffer penetrated both PCL/MTZ-2h and PCL/MTZ-6h matrices slowly, correlating well with drug release data (Figure 17A and B). It has been shown that slow penetration of buffer into the nanofiber matrix is due to the air entrapped in the pores between the fibers which decreases the contact area with release medium (Lembach et al., 2010), makes up a barrier for buffer uptake and prolongs the drug release (Falde et al., 2015; Yohe et al., 2012).

On the other hand, for both PCL/CIP matrices (Figure 17C and D) and PCL/MTZ/CIP matrix (Figure 17E), the buffer uptake was immediate. This was probably related to the localization of recrystallized CIP on the fiber surface which due to its hydrophilic and hygroscopic nature helped to draw in the buffer. CIP release from these matrices was not immediate, whereas MTZ release was. This implies that buffer penetration into the matrix is a rate-limiting factor for MTZ release, but not for CIP. The reason for the different release times of MTZ and CIP is most likely related to the different physicochemical properties of the drug molecules, e.g. aqueous solubility (MTZ ~10 mg/mL, CIP <100 μg/mL) (Olivera et al., 2011; Camila F. Rediguieri et al., 2011), ionization and pKa (MTZ 2.62, CIP 6.8 and 8.73–8.76) (Olivera et al., 2011; Camila F. Rediguieri et al., 2011), melting temperature (MTZ ~160 °C, CIP ~300 °C), and molecular weight (MTZ 171.2 g/mol, CIP 367.8 g/mol)), all of which influence their interactions with the release medium as well as the polymer.

For some systems suitable drug release kinetics can be tailored by altering the matrix thickness, as was seen in the present study for PCL/MTZ matrix. The

thicker the matrix, the slower buffer penetration was observed. Similarly, CAM release was most probably affected by the rate of buffer penetration into the fiber matrix, only in that case the differences were due to different hydrophilicity/hydrophobicity of the carrier polymers, resulting in different wettability of the fiber matrices.

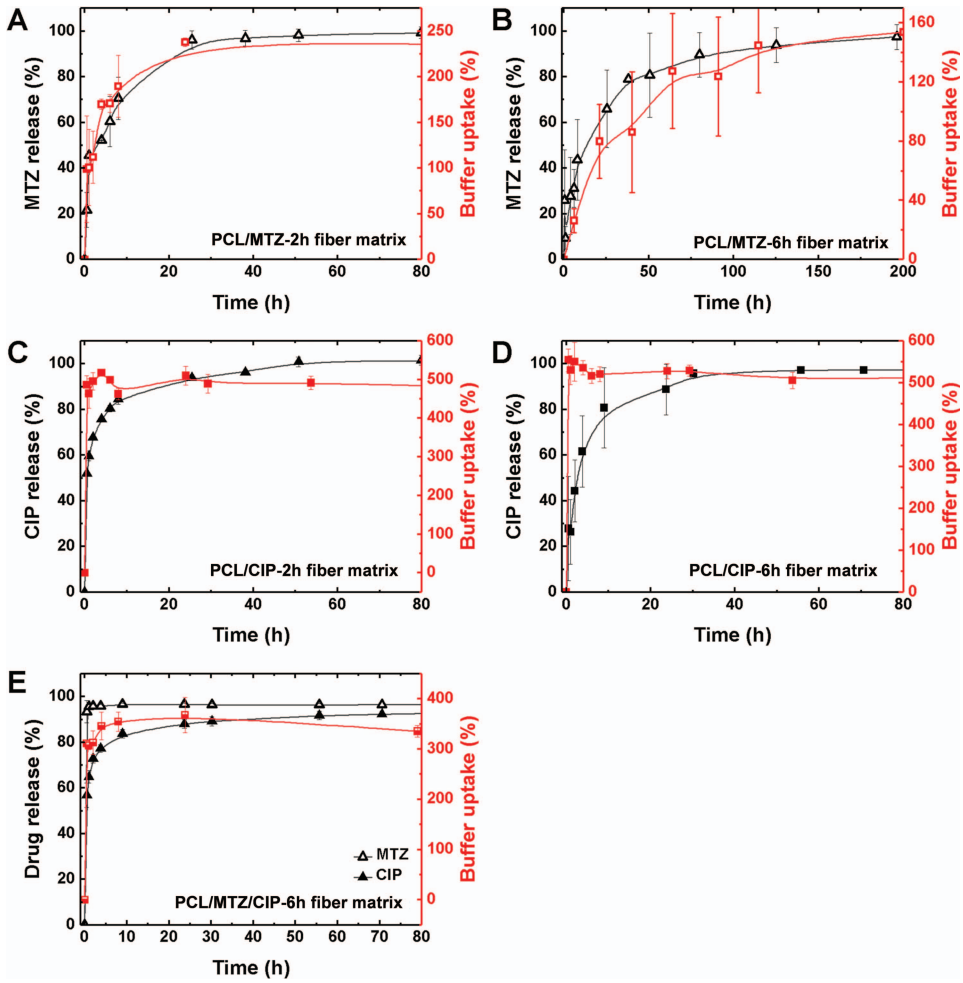

Figure 17. Drug release from and buffer uptake into (A) PCL/MTZ-2 h, (B) PCL/MTZ-6 h, (C) PCL/CIP-2 h, (D) PCL/CIP-6 h, and (E) PCL/MTZ/CIP-6 h nanofiber matrices. Data are averages of three replicates and error bars denote standard deviation. Key: CIP – ciprofloxacin; MTZ – metronidazole; PCL – polycaprolactone.

6.6.5. Effect of release medium temperature and surface area of the matrix on the drug release (II)

The additional experiment revealed that the surface area of PCL/MTZ fiber matrices did not influence the MTZ release profile (Figure 18A and Table 7). By contrast, the temperature of the release medium was a critical parameter (Figure 18B, f1 = 29.2, f2 = 44.6). Burst release was greater at higher temperatures, whereas slow drug release was detected during the next few days independent of the medium temperature. After 20 days, the fiber matrices incubated at 37 °C released all the incorporated drug and the matrix incubated at 22 °C released only 80% of the total drug content (Figure 18B).

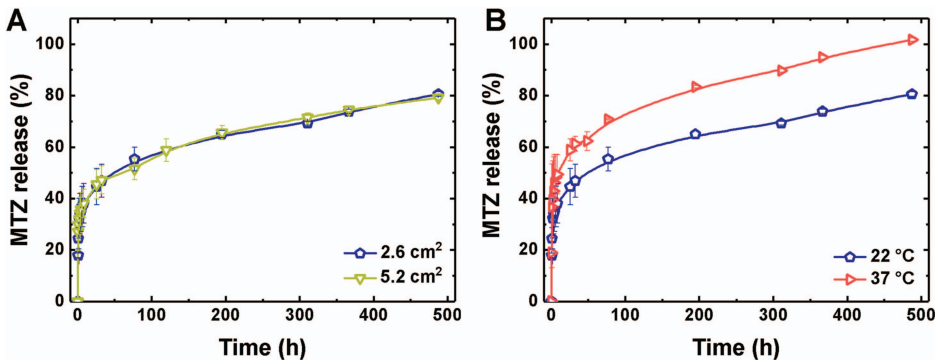

Figure 18. The effect of (A) different surface areas (2.6 vs. 5.2 cm^2), and (B) temperature of release medium (22 vs. 37 °C) on the MTZ release from PCL/MTZ-8 h nanofiber matrices. Data are average of three replicates and error bars denote standard deviation. Key: MTZ – metronidazole; PCL – polycaprolactone.

6.7. Novel methods for monitoring drug release (IV)

Drug release from electrospun matrices is usually studied using some modification of pharmacopoeia methods for dissolution testing, although no standard method exists. The most important difference from the traditional methods is that the volume of release medium is much smaller to allow drug concentrations to be in detectable range using relatively small samples (Chou & Woodrow, 2017; Hu et al., 2015). These methods, however, have some limitations for analysing wound dressings as the testing conditions do not reflect the wound environment adequately. For example, the amount of available liquid in the wound is much smaller compared to the situation when the dressing is fully immersed into the buffer, usually resulting in sink conditions. Also, as a second step, the diffusion further into the wound and reaction with the surrounding tissue and environment is important (Weiser & Saltzman, 2014). This can cause difficulties for correlating and predicting biological activity from the dissolution

data. Other methods have been developed, for example, the release of terbinafine hydrochloride has been studied using a wound dressing-skin model where the electrospun drug loaded fibers were set on filter papers (Paskiabi et al., 2017) and tetracycline release has been measured in a dialysis bag mimicking the human skin-like conditions (Sadri et al., 2016). We proposed and compared novel drug release methods based on hydrogels rather than buffer solutions as release media, and using different detection methods. Hydrogels may represent a simplistic wound model onto which drug may be released followed by drug diffusion into the hydrogel matrix. As hydrogels have more similar hydrodynamic conditions to wound tissue compared to aqueous solutions, they provide more biorelevant testing option and enable to monitor both release and diffusion of the drug. Previously described PCL/CAM and PCL/PEO/CAM matrices were used for the testing.

6.7.1. Drug release into agar hydrogel measured by HPLC (IV)

The extent of CAM release from the matrices and diffusion into the agar hydrogel was quantified using HPLC upon extraction of CAM from the agar hydrogel. The experimental setup was similar to disc diffusion assay conditions as this is the main method for assassing antibacterial activity of electrospun matrices (Alippilakkotte et al., 2017; Ibrahim et al., 2015; Zhaoyang Sun et al., 2016). The agar on the plates was divided into five concentric circular zones (Figure 19A) and the CAM concentration in each zone was determined. The amount of drug released from electrospun matrices to the agar plates at different time-points at 37 ºC is summarized in Figure 19.

The drug diffusion patterns for PCL/CAM and PCL/PEO/CAM fiber matrices were qualitatively similar, although quantitatively less drug was released from PCL/CAM matrices within the same time period. It is clear that most of the drug is present in the 1 cm diameter section (zone 1) right below the fiber matrix at early time-points of the release experiment. As time passed, less drug was recovered in the inner circle (zone 1) and relatively more in zone 2 (the next circle around the matrix). Interestingly, after 120 min, the drug was not detectable in the 3rd and further zones in the matrices. Thus, CAM concentrations released from PCL/CAM and PCL/PEO/CAM differ mainly in zone 1 and to some extent in zone 2. After 24 h, CAM had reached the outer circle (see publication IV Table A1). The diffusion of CAM in agar is thus rather slow, which can make it difficult to detect differences in antibacterial activity in disc diffusion assay, even when the drug is released differently from the delivery vehicle, and therefore may lead to different antibacterial efficacy *in vivo* (Mekkawy et al., 2017)

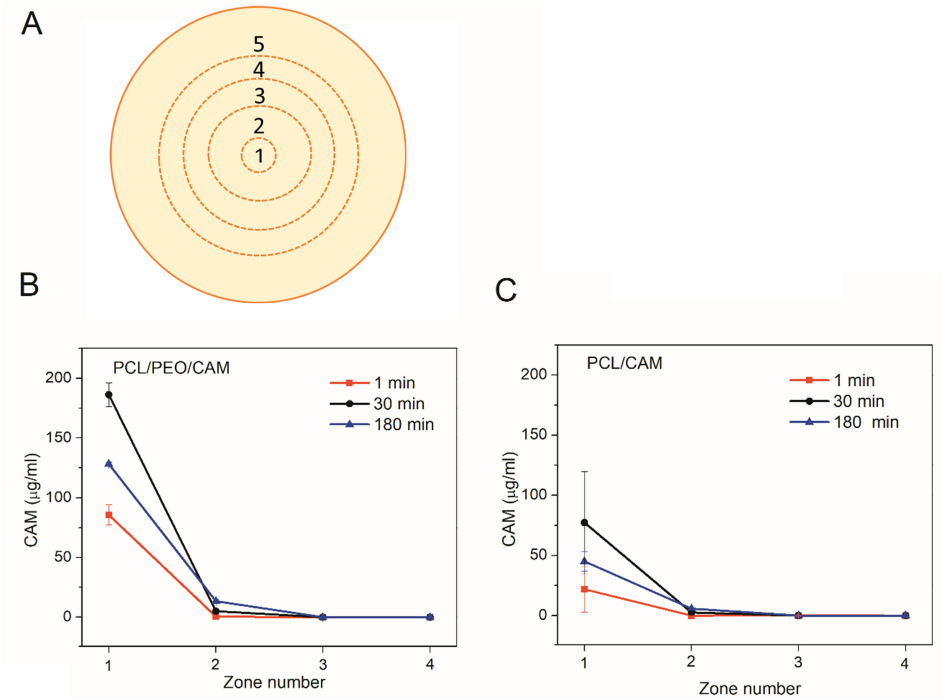

Figure 19. Schematic illustrating the division of the agar plate into zones (A). Zones 1-5 are numbered starting from the inner circle. Zone diameters: 1.0 cm, 3.0 cm, 4.4 cm, 5.8 cm, and 8.6 cm. Concentrations of released CAM (detection limit of 1µg/mL) from PCL/PEO/CAM (B) and PCL/CAM fiber matrices (C) into 1.5% (m/V) agar hydrogel at 37 ºC in different time-points (1 min, 30 min, 180 min) and into different zones (1–4). Data are averages of three replicates and error bars denote standard deviation. Key: CAM - chloramphenicol; PCL - polycaprolactone; PEO – poly(ethylene oxide).

6.7.2. Drug release into agar hydrogel detected with bioreporter strain (IV)

In addition to chemical and physical methods for determining antibiotic concentrations during the release, it is also possible to use bacterial bioassays (Melamed et al., 2012). Hence, simultaneously to the antibacterial effects, the drug release can be monitored. We genetically engineered reporter bacteria (*E. coli* MG1655) to produce dose-dependent quantifiable green and red fluorescent signals in the presence of antibacterial drug CAM. The CAM-bioreporter has green fluorescent protein (GFP) as a control protein for expression and a red mScarlet-I as a reporter protein. In the presence of CAM GFP signal (green) will be reduced due to protein synthesis inhibition, and mScarlet-I signal (red) will increase due to transcription continuation as a result of ribosomal stalling in the transcription attenuation system. Therefore, the CAM release and diffusion

can be illustrated in different time-points (selected time-points 60, 180, and 360 min) using fluorescence data (Figure 20).

It is clearly seen that bacterial growth is inhibited close to the fiber matrices (inhibition zones surrounding the matrices) where CAM concentrations are the highest. Fluorescent bacteria surrounding the inhibition zones reveal the distance from the matrices where the CAM levels can still be detected. Compared to the agar hydrogel diffusion tests (Figures 19), bacterial bioreporter study results on agar hydrogel did not reveal large differences between the PCL/CAM and PCL/PEO/CAM fiber matrices with the respect of released drug amounts and its effect on bacteria (Figure 20C), however, the largest difference in released amount of CAM in the prior test was observed in the zone directly under the fiber matrix, which could not be analyzed with this method. Growth inhibition was very slightly more pronounced in PCL/PEO/CAM fiber matrix (fast release) after 60 min of incubation; however, this difference was statistically insignificant and disappears in later time-points (180 min). In later time-points (6 h) red fluorescence detected from bacteria enabled determining the CAM concentrations even below MIC (in sub-MIC concentrations) (Figure 20D and E). After 6 h of incubation, the peak of the reporter protein signal is located further (approximately 0.75 cm) from the matrix in case of PCL/PEO/CAM fiber matrix (fast release) (Figure 20D) compared from PCL/CAM fiber matrix (slow release; located approximately 0.60 cm) (Figure 20E). This indicates that effective CAM concentration was achieved on larger area (at a further distance from the fiber matrix) with PCL/PEO/CAM fiber matrix, although the difference between the two fiber matrices was minor. Most likely, this is due to the fact that most of the differences between the two different electrospun fiber matrices can only be seen in early time-points which cannot be distinguished using fluorescent bacteria in these settings.

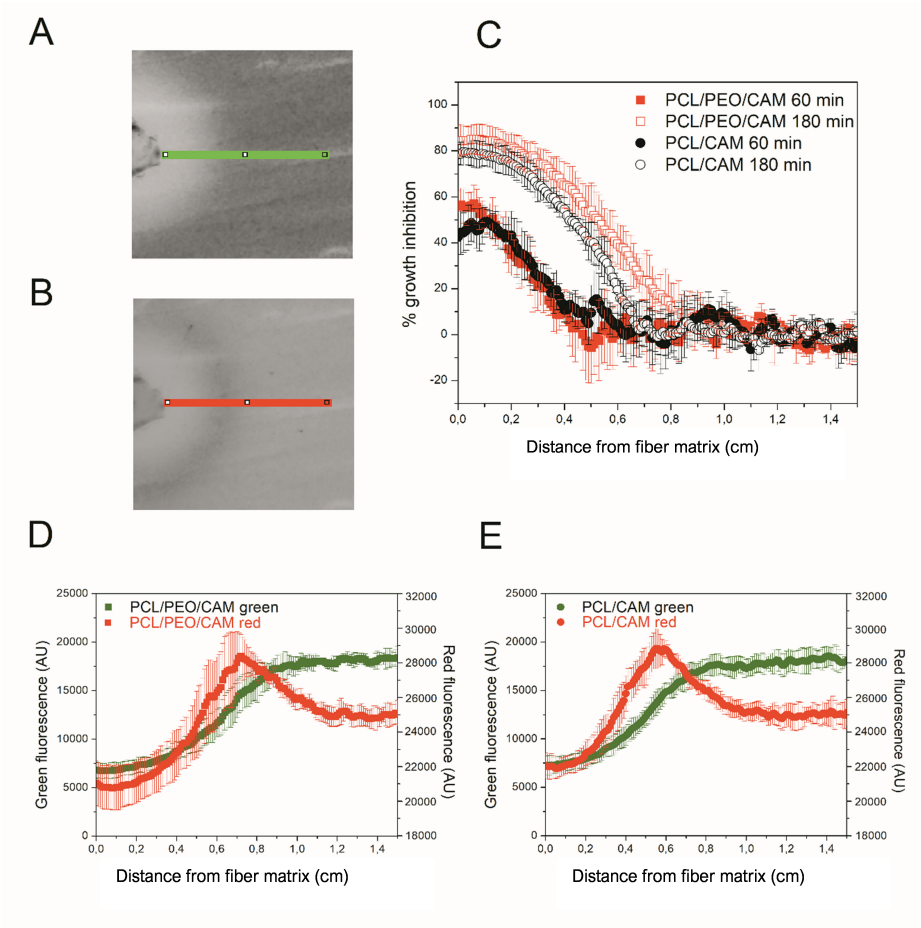

Figure 20. (A-B) Shows the analyzed region of interest (0.8 mm X 1.5 cm) of bio-reporter CAM-containing fiber disc diffusion assay from green fluorescence (A) and red fluorescence (B) scan images. Green fluorescence images in different time-points (60 min and 180 min) allow estimating bacterial growth inhibition due to CAM released from PCL/PEO/CAM and PCL/CAM fiber matrices (C). Combined green and red fluorescent figures at 6 h reveal the fluorescence levels which can be correlated with the released CAM from PCL/PEO/CAM (D) and PCL/CAM fiber matrices (E). Data are averages of three replicates and error bars denote standard deviation. Key: CAM, chloramphenicol; PCL, polycaprolactone; PEO, poly(ethylene oxide).

6.7.3. Drug release into agarose hydrogel using UV imaging (IV)

The assessment of CAM release by cutting of zones from agar plates followed by extraction and analysis of the drug is both a destructive and laborious sampling procedure. The fast release of CAM cannot be monitored using bio-reporter bacteria that require time for growth and detectable signal production. Therefore, UV imaging was investigated as a potentially less labor intensive and more robust (reproducible/repeatable) approach for monitoring CAM release from the electrospun fiber matrices. An additional benefit of the non-intrusive imaging method is the high spatial as well as temporal resolution offered. Due to a lack of transparency of the agar plates used in antibacterial activity tests, a hydrogel matrix based on agarose was applied instead. Moreover, the Actipix D200 Large Area Imager allowed imaging of three samples in parallel enabling comparison.

The UV imaging results reveal that PCL/CAM fibers provide slower drug release into the gel whereas PCL/PEO/CAM fibers release the drug faster (Figure 21). The differences were observed with respect to the total amount of released drug mainly at the early time-points. Only slight differences between the PCL/CAM and PCL/PEO/CAM fiber matrices with respect to their drug release behavior were detected in average drug release profiles, although these were not statistically significant and can be considered as more of a tendency.

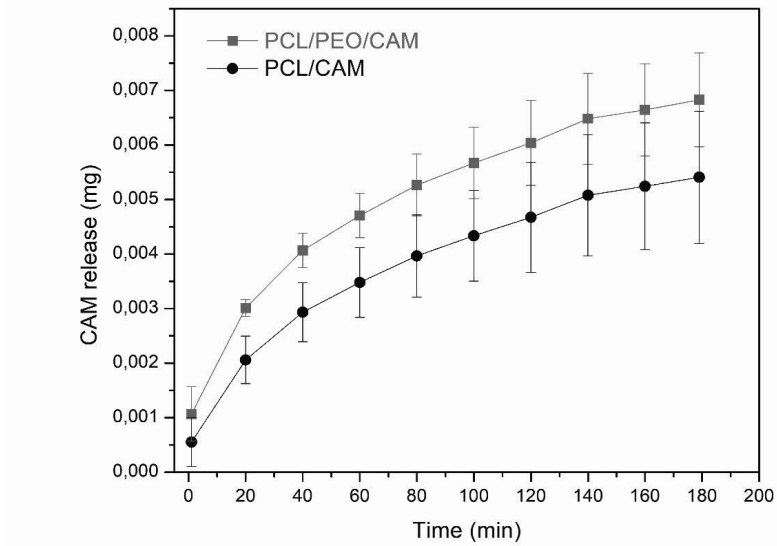

Figure 21. Amount of CAM released from PCL/PEO/CAM (■) and PCL/CAM (●) fiber matrices into 0.5% (m/V) agarose hydrogel at 37°C based on UV imaging experiment data. Data are averages of five replicates and error bars denote standard deviation. Key: CAM, chloramphenicol; PCL, polycaprolactone; PEO, poly(ethylene oxide).

6.7.4. Comparison between different drug release model systems (IV)

Irrespective of the *in vitro* release model system employed, the release of CAM was found to be faster from the PCL/PEO fiber matrices as compared to the PCL fiber matrices (Figure 22). However, the extent to which the release differed tended to vary between the model systems.

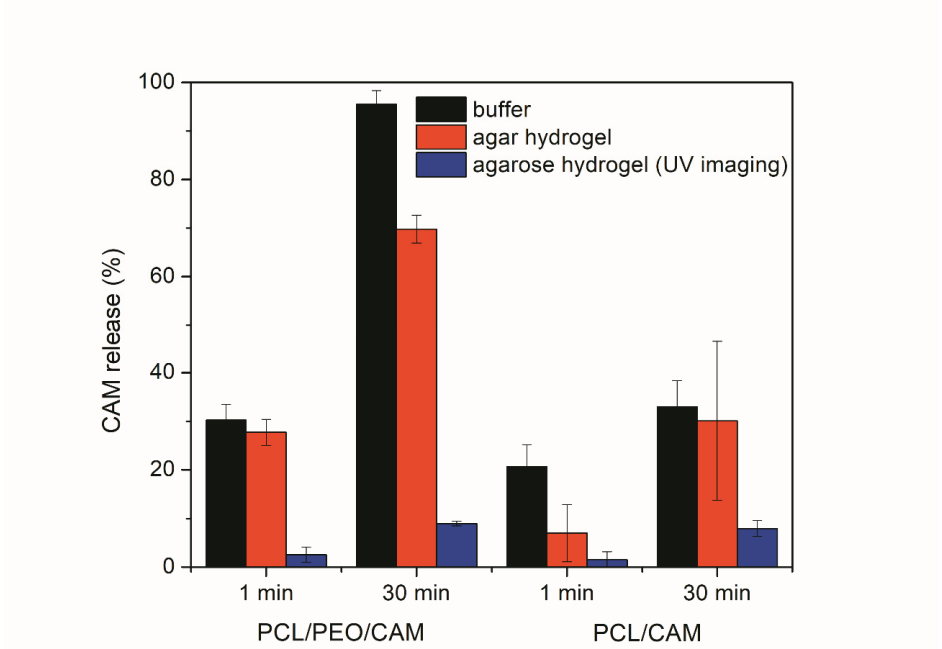

Figure 22. Amount of CAM released from PCL/PEO/CAM and PCL/CAM fiber matrices into phosphate buffered saline at pH 7.4 and 37°C and 1.5% (m/V) agar hydrogel at 37°C and 0.5% (m/V) agarose hydrogel at 37°C. Data are averages of at least three replicates and error bars denote standard deviation. Analyzes were performed using UV-VIS spectrophotometry (CAM concentration in a buffer solution), HPLC (CAM concentration extracted from hydrogel) and UV imaging (CAM concentration within hydrogel). Key: CAM – chloramphenicol; PCL – polycaprolactone; PEO – poly(ethylene oxide).

Drug release into buffer revealed that after 30 min the PCL/PEO/CAM fibers had released nearly all CAM into the buffer, whereas only a minor amount (approximately 30%) of drug was released from PCL/CAM fiber matrices (Figure 22 and for drug release curves, see publication IV Figure 1). When the CAM release into hydrogel was monitored by agar disc diffusion and extraction method, the amount of CAM released from PCL/PEO/CAM fiber matrix after 30 min was approximately 70% and the released CAM amount from PCL/CAM matrix was similarly approximately 30% (with huge variability between 17–48% for individual PCL/CAM fiber matrices). UV imaging, however, showed

that the differences with respect to the amount of drug released into the agarose hydrogel between PCL/CAM and PCL/PEO/CAM fiber matrices after 30 min were less pronounced as compared to the differences in CAM release into buffer (Figure 22). It was also seen that much less CAM was released and diffused to the region of analysis from both fiber matrices (approximately 9% and 8% for PCL/PEO/CAM and PCL/CAM fiber matrices, respectively) within the same time period. Most likely, less CAM is released from the fiber matrices into the hydrogel according to the UV imaging due to the different geometries of the setup. In the UV imaging setup, diffusion is limited to one direction perpendicular to the matrix, whereas diffusion in the agar setup may occur in three dimensions. The latter will favor a relatively larger release of CAM. We believe that the concentration may be more likely to build up at the interface in the UV imaging setup. As might be expected due to the similarity of the release matrices (hydrogel), the UV imaging drug release and diffusion profiles matched more with the drug release into agar hydrogel extraction (Figures 19–21) than release and dissolution into buffer (see publication IV Figure 1). The contact of the matrices with the hydrogels may be different between the agar and agarose hydrogels. It is not known whether the agar hydrogel may contain components interacting, and thereby facilitating the release of CAM. Similarly to UV imaging, less pronounced differences between the two different electrospun CAM-loaded fiber matrices were also observed with bacterial bioreporters (Figure 20C). It is due to the fact that the drug has to diffuse away from the matrix before it will be detected (UV imaging and bacterial bioreporters), whereas in the agar hydrogel extraction method, the area under the fiber mat will be included into the total released and detected drug amount.

The differences with respect to CAM release from the matrices observed using the *in vitro* release testing model systems are related to the different properties of the release media (volume, agitation, and viscosity), its capability to penetrate into the fiber matrix, the sample size of fiber matrices, effect of shaking, and geometry of the setup. It is believed that drug diffusion and wetting of the samples were the rate-limiting steps for the drug release from fiber matrix into agar and agarose hydrogels. The release into buffer solution, however, was more affected by the hydrodynamics of the buffer measurements as agitation may have led to increased erosion and/or disintegration of the PCL/PEO/CAM fiber matrices as compared to the PCL/CAM fiber matrices.

In terms of repeatability, the model systems and analytical methods were all comparable. It can be seen that larger variations in drug release between replicates were detected for PCL/CAM fiber matrices compared to PCL/PEO/CAM fiber matrices. This was seen with both drug release model systems (buffer vs. hydrogel) as well as different techniques (UV-VIS spectrophotometry, HPLC, UV imaging, and bacterial bioreporters). This might be explained by the different wettability of the PCL/CAM fiber matrices compared to PCL/PEO/CAM fiber matrices as discussed previously. The hydrophilicity of the PCL/PEO/CAM fiber matrices makes them wet more homogeneously, whereas for

PCL/CAM fiber matrices the sample-to-sample variations in wettability may also cause variability in the drug release behavior.

Compared to agar diffusion assay (extraction of CAM from hydrogel), the UV imaging was easier to conduct. Although for both these methods the size of sample, the release environment (hydrogel) and static conditions resembled the *in vitro* antibacterial activity testing conditions. Bacterial bioreporter study enabled to monitor CAM release into agar hydrogel during diffusion in later time-points where even sub-MIC concentration of CAM was determined based on the green and red fluorescence intensity. The method has the advantage of revealing the released antibacterial drug effect directly on bacteria.

Burst release effect is a favorable characteristic for electrospun matrices intended for the treatment of wound infections. The extent of the burst release is often associated with device geometry, surface characteristics of host material, heterogeneous distribution of drug within the polymer matrix, intrinsic dissolution rate of drug, and heterogeneity of matrices (Fu & Kao, 2010). From the drug release experiments, we see that the burst release is smaller with the hydrogels compared to the buffer solution (Figure 22). Larger differences in the burst release between the samples were observed with hydrophobic PCL/CAM fiber matrices (Figure 22). For the drug release to occur from the PCL fiber matrix, the medium needs to penetrate into the electrospun fiber matrix to cause the diffusion of the drug to the exterior. Initially, the diffusion is affected by the electrospun matrix composition and the fiber characteristics, as for PCL/PEO/CAM fiber matrices the release was also affected by swelling and dissolution of PEO. As a second step, the diffusion further into the wound and reaction with the surrounding tissue and environment is important (Weiser & Saltzman, 2014). The gels *in vitro* and the wound tissue *in vivo* can be envisioned to provide a diffusion barrier or matrix minimizing burst release effects. Local transport mechanisms determine the volume in which the drug is distributed; thus, understanding these mechanisms is essential for optimizing the effectiveness of local delivery (Weiser & Saltzman, 2014). The *in vitro* methods that enable to mimic the *in vivo* conditions most closely are likely to enable accurate predictions of the drug release and transport in the wound environment.

6.8. Antibacterial activity (I, II, IV)

6.8.1. Disc Diffusion Assay (I, II)

Disc diffusion assay is one of the most frequently used antimicrobial susceptibility testing methods and thus was chosen as the first approach to test the antimicrobial activity of the electrospun matrices. The antibacterial activity of CAM-loaded electrospun fibers was first studied on two strains of *E. coli*, non-pathogenic laboratory strain MG1655 and uropathogenic CFT073. Facultative anaerobe *E. coli* was chosen as it is commonly present in infected wounds (P. G. Bowler et al., 2001) and is also extensively studied and known model

microorganism. It is important to test the antibacterial activity on both non-pathogenic and pathogenic strains of bacteria, as different strains can have different antibiotic sensitivity (Beceiro et al., 2013). Matrices loaded with MTZ and/or CIP were also tested on *E. coli*, but also on anaerobes *F. nucleatum* and *P. gingivalis*, facultative anaerobe *S. mutans*, and microaerophilic *A. actinomycetemcomitans*. These bacteria are associated with periodontal infections, and as the growth of anaerobes is also facilitated in an inadequately perfused chronic wounds with low oxygen levels (Siddiqui & Bernstein, 2010), it is important to include these types of bacteria with different oxygen tolerance in the development of antibacterial activity testing methods. The cultivation and thus testing are more challenging compared to using microbes that survive and thrive in aerobic conditions. Thus, these bacteria can be viewed as anaerobic/microaerophilic model organisms for the development of suitable analytical techniques that are necessary for the assessment of DDSs intended for the treatment of skin or oral wound infections.

Clear inhibition zones on inoculated agar plate would indicate efficient antibacterial concentrations. It can be seen in Figures 23A and B that no such inhibition zones were observed around blank fibers nor negative control discs but appeared around both drug-loaded fibers and positive controls, indicating adequate antibacterial activity of CAM in fibers. The inhibition zone sizes were not statistically different between PCL/CAM fibers, PCL/PEO/CAM fibers and control discs. On the other hand, there appeared to be a difference between the two strains as the inhibition zones were slightly bigger in case of *E. coli* MG1655 compared to CFT073.

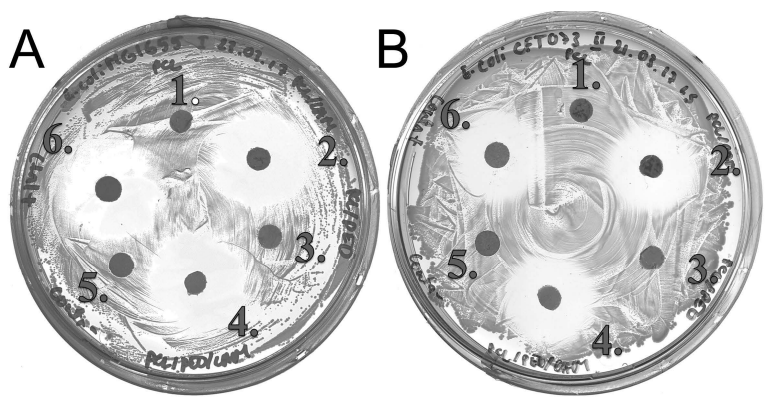

Figure 23. Antibacterial activity of electrospun matrices. Disc diffusion assay results with (A) *E. coli* MG1655 and (B) *E. coli* CFT073 strains: 1, PCL blank; 2, PCL/CAM; 3, PCL/PEO blank; 4, PCL/PEO/CAM electrospun matrices; 5, filter paper; 6, filter paper impregnated with CAM solution (20 μg).

MTZ-loaded PCL nanofiber matrices were effective against *F. nucleatum*, *P. gingivalis* and *A. actinomycetemcomitans* (Figure 24). PCL/CIP nanofiber matrices were effective against all tested bacteria in anaerobic conditions and also against *E. coli* in aerobic condition. CIP-loaded nanofiber matrices were more active against *A. actinomycetemcomitans* compared to the MTZ-loaded nanofiber matrices. On the other hand, *F. nucleatum* was more sensitive to MTZ than CIP. The antibacterial efficacy of PCL nanofiber matrices loaded with both drugs was better than the mats loaded with either drug alone, noted by a broader overall spectrum and/or larger inhibition zones. The efficacy of the treatment of periodontal diseases with combinations of different drugs has been proven and a synergistic effect has been shown for MTZ combinations with amoxicillin (Pavicic et al., 1991) and CIP (Slots, 2004). Another benefit of MTZ and CIP drug combination is that non-periodontopathogenic viridans streptococcal species with potential to inhibit several pathogenic species are resistant to this antibacterial combination and help recolonize the subgingival sites, hence favoring a healthy microbiome (Slots, 2004).

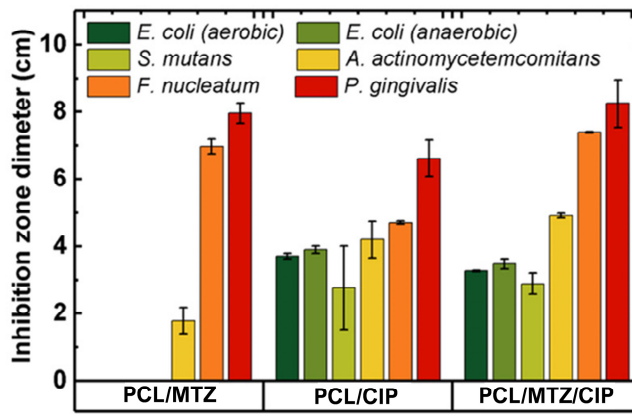

Figure 24. Antibacterial activity of electrospun matrices. Disc diffusion assay results with *E. coli* (DSM 1103) under aerobic and anaerobic conditions, and in anaerobic conditions with *F. nucleatum*, *A. actinomycetemcomitans*, *S. mutans* and *P. gingivalis* using PCL/MTZ, PCL/CIP and PCL/MTZ/CIP electrospun matrices. Data are averages of three replicates and error bars denote standard deviation.

The size of the inhibition zone around the disk depends on the diffusion rate of the antibiotic, the growth rate and MIC of the bacteria (Gefen et al., 2017). Hence, different antibiotic release profiles might result in differences in disc diffusion assay, but no such observations were made with PCL/CAM and PCL/PEO/CAM matrices. Similar results have been reported for curcumin-loaded antibacterial fibers with different release kinetics (Tsekova et al., 2017). This can be explained by relatively high drug-loading and initial burst release which

quickly brings the concentration of antibacterial drug above MIC. Also, as seen from drug release results, the diffusion of CAM in the agar hydrogel is quite slow and most of the drug is present near the fiber matrix disc in early time-points (Figure 19). Thus, if drug diffusion in the agar is slower compared to drug release, and drug concentrations are relatively high, no differences in the inhibition zone size can be detected.

Disc diffusion assay enabled to confirm if the released drugs and their concentrations were effective against tested microbes but could not differentiate between different drug release profiles of electrospun matrices. Neither could disc diffusion assay with bioreporter bacteria reveal these differences, although it suggested differences in the distances from the fiber matrices where effective CAM concentration were achieved. Another limitation of a traditional disc diffusion assay is that the method can only provide information about early release phase and does not indicate how long the concentrations stay sufficient in case of prolonged release dosage forms. Thus, we developed two modifications of the disc diffusion assay to address these problems.

6.8.2. Modified disc diffusion assay (IV)

Drug release studies showed that CAM release from PCL/CAM and PCL/PEO/CAM matrices were different, although the size of the difference varied depending on the testing method. As no differences in antibacterial activity could be observed in disc diffusion assay, we developed a modified assay, where the matrices were physically removed from the surface of the solid growth medium at specified time-points and the antibacterial effect of the released drug on model bacteria *S. aureus* DSM 2569 was determined by measuring the size of the inhibition zones after 24 h.

Faster CAM release from PCL/PEO/CAM matrices compared to the PCL/CAM matrices correlated with larger inhibition zones (Figure 25). Thus, this method was able to distinguish small differences in the antibacterial activity of differently designed electrospun fiber matrices. The differences were larger at earlier time-points as observed in drug release experiments into hydrogel. Control filter paper impregnated with CAM confirmed that the wetting of the sample is the major triggering factor for further drug release and diffusion.

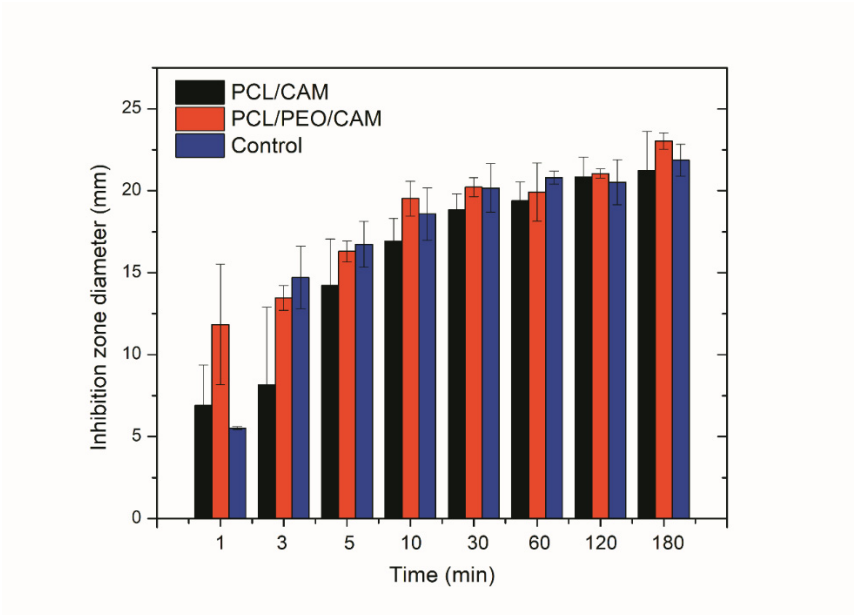

Figure 25. Inhibition zone diameters measured after 24 h on agar plates. X-axis indicate exposure time of discs (PCL/PEO/CAM or PCL/CAM fiber matrices) onto the hydrogel. *S. aureus* DSM 2569 was used for the study. Filter paper wetted with CAM solution and dried (same CAM concentration) served as a control. Data are averages of at least three replicates and error bars denote standard deviation. Key: CAM, chloramphenicol; PCL, polycaprolactone; PEO, poly(ethylene oxide).

6.8.3. Prolonged disc diffusion assay (II)

We wanted to test if prolonged release of an antibiotic from electrospun matrix results in prolonged antibacterial activity. Thus, we compared PCL/MTZ-1h and PCL/MTZ-8h nanofiber matrices in prolonged disc diffusion assay (Figure 26A) as the prior fiber matrix released over 90% of MTZ in the first 4 h into the buffer, whereas the latter released 44% of the drug on the first day, followed by a linear pattern of drug release over the following 19 days.

After 24 h incubation, the largest inhibition zones occurred due to the highest amount of drug released over that time in both cases (Figures 26B and C). There was no difference in the size of inhibition zones between PCL/MTZ-1 h and PCL/MTZ-8 h nanofiber matrices, similar to their respective filter paper controls, i.e. the resulting concentrations were rather high and the zone size reached a plateau. Clear differences were seen at day 2 when only a minor or no inhibition zone formed around the PCL/MTZ-1 h nanofiber matrices, whereas substantial zones occurred around PCL/MTZ-8 h nanofiber matrices. Interestingly, no inhibition zone formed around PCL/MTZ-8 h matrix on day 3. Although PCL/MTZ-8 h matrices had zero-order release after 24 h, and hence day 2 and day 3 plates should look similar, drug release on agar plate may not correlate

perfectly with that in buffer solution as seen with the experiments with CAM, emphasizing that drug release results from buffer solution cannot be directly transferred to other circumstances. Thus, the amount of drug that is released over 24–48 h is larger than over 48–72 h, and the latter is actually too small concentration to produce visible inhibition.

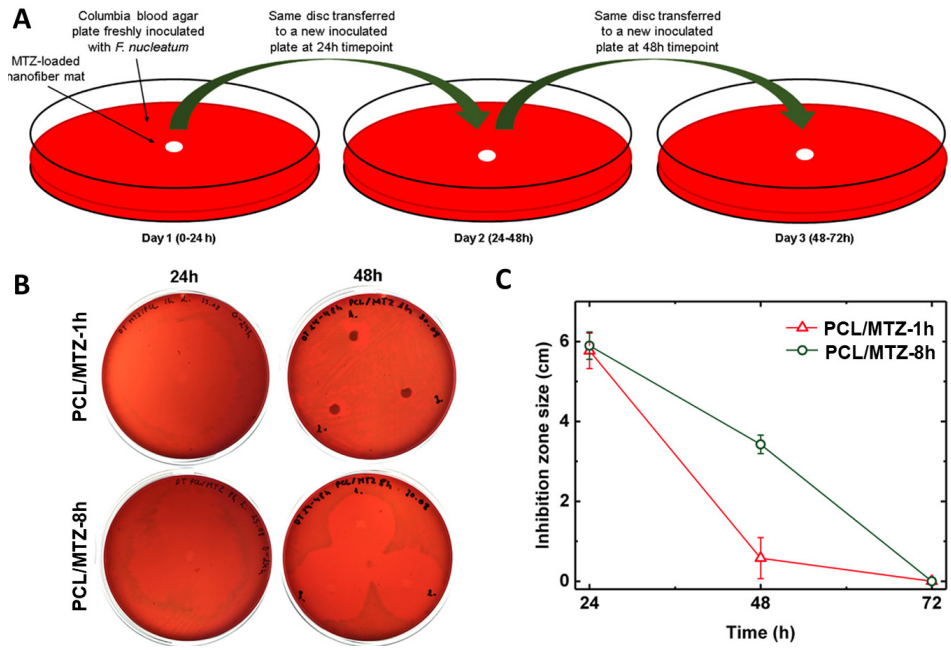

Figure 26. (A) Schematic representation of the study design of the prolonged disc diffusion assay with the MTZ-loaded PCL nanofiber matrices and *F. nucleatum* in anaerobic conditions; (B) images of prolonged disc diffusion assay plates for MTZ-loaded PCL nanofiber matricers of different thicknesses (PCL/MTZ-1 h and PCL/MTZ-8 h nanofiber matrices), where one disc was applied on the first time-point plate and all 3 replicates were added to one plate at following time-points; (C) diameter of inhibition zones of PCL/MTZ-1 h and PCL/MTZ-8 h nanofiber matrices in the prolonged disc diffusion assay. Data are averages of three replicates and error bars denote standard deviation.

Although no inhibition was seen on day 3 with the PCL/MTZ-8 h nanofiber matrices, this should not be interpreted as a lack of effect after 48 h. For the treatment of periodontitis, disc diffusion tests seem to mimic real conditions more closely than drug release tests in the buffer solution. Still, the disc diffusion testing conditions do not simulate the complexity and dynamics of real *in vivo* conditions precicely. Based on the obtained *in vitro* results it is expected that the matrices provide initially faster drug release, creating appropriate local antibiotic concentrations that would be complemented by their following

constant release. This would maintain appropriate drug concentrations for a prolonged time and improve antibacterial efficacy important for real clinical situations.

6.8.4. Biofilm assay (I)

Biofilms are complex communities of bacteria embedded within a matrix of extracellular polymeric substance attached to a surface of a substrate (Lam et al., 1980). Bacteria are traditionally studied in their nonadherent state, although bacterial cells in a biofilm are phenotypically and physiologically different from planktonic bacterial cells. One of the most important differences is that cells in a mature biofilm require much higher concentrations of antimicrobial drugs for killing compared to the planktonic cells (Stewart et al., 2001). As 60−100% of chronic wounds have been shown to contain biofilm (James et al., 2008; Oates et al., 2014) and delayed wound healing is increasingly associated with biofilm formation, (Schierle et al., 2009) it is important to seek possibilities to eradicate mature biofilm and prevent new biofilm formation. Furthermore, wound dressing material should not promote the growth of bacteria and preferentially it should also have antibiofilm properties.

A biofilm assay was developed and tested with both PCL and PCL/PEO blank and CAM-loaded matrices to assess the ability of bacteria to form biofilm on these electrospun fiber matrices. The biofilm was established by immersing the fiber matrices into an artificial wound exudate inoculated with a high number of bacteria. PCL blank matrix provides the best substrate for bacterial attachment as the number of CFU-s is up to 2 orders of magnitude higher than with PCL/PEO blank matrix (Figure 27). The surface of most polymers can be colonized leading to biofilm formation. Increased hydrophilicity has been shown to prevent the bacterial adhesion and consequently also biofilm initiation (Davidson & Lowe, 2004). The primary reversible attachment of bacteria to a surface has been shown to be highly dependent on the environmental conditions as well as the nature of the surface, with rugosity and hydrophobicity increasing adhesion (Beloin et al., 2008). Fiber surface chemistry and properties, such as wettability and surface charge, have been found to affect the ability of bacterial cells to attach and proliferate throughout the nanofiber matrices (Abrigo et al., 2015). As discussed before, PCL surface is much more hydrophobic than PCL/PEO surface, and preferentially bacteria adhere on this electrospun matrix. As expected, both drug-loaded fiber matrices showed reduction in biofilm formation in comparison to blank fiber matrices (Figure 27).

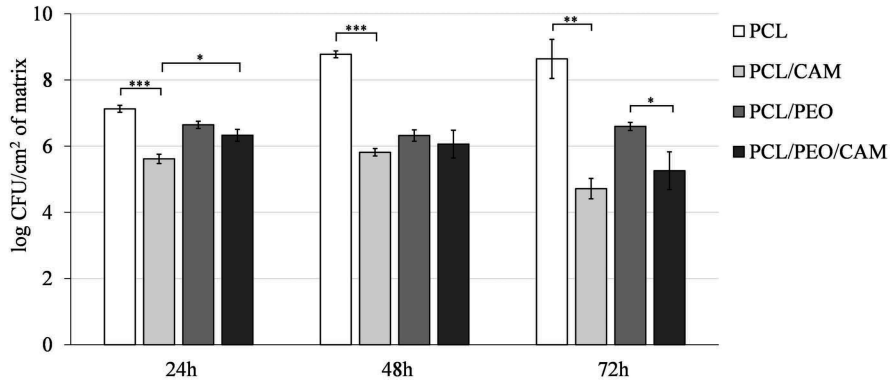

Figure 27. Number of colony-forming units (CFU) of *E. coli* CFT073 in biofilm formed on each matrix after 24, 48, and 72 h incubation at 37 °C. Data are averages of three replicates and error bars denote standard deviation. The data was log-transformed before statistical analysis and pairwise t-tests were carried out. The p-values were adjusted using Holm's method. *, $p < 0.05$; **, $p < 0.005$; ***, $p < 0.0002$. Key: CAM, chloramphenicol; PCL, polycaprolactone; PEO, poly(ethylene oxide).

Interestingly, in comparison to blank fiber matrices the drug-loaded matrices showed an opposite trend, as the average cell number was less with hydrophobic PCL/CAM fibers than with hydrophilic PCL/PEO/CAM fibers at all time-points, suggesting that biofilm formation was greatly influenced by the release rate of CAM from the matrix. It is likely that the incorporation of CAM changed the surface and swelling properties of fibrous matrices, or the nature of the substrate might have influenced the vulnerability of the bacteria to antibiotic treatment, which could also contribute to this effect. Still, it seems that prolonged release of antibacterial drug from the matrix generated a situation where antibiotic concentration in the growth medium is lower than that in the fibers, hence bacteria do not benefit from attaching to that surface. On the other hand, if antibiotic concentration in the fibers is lower than in the growth medium, bacteria can find shelter from harsh environmental conditions through adhering onto the dressing and forming a biofilm, thus potentially aggravating the clinical situation, and emphasizing the need for designing dressings that take these interactions into account.

The strongest effect on biofilm reduction can be seen at the 72-h time-point for both drug-loaded matrices (Figure 27). The amount of nutrients available in growth media decreases in time and this, together with the stress from the antibiotic, may be responsible for the observed effect. Altogether, our data indicate that the complex interplay between the nature of the drug, drug release kinetics and carrier polymer properties determine the effectiveness of antimicrobial therapy. Interactions between drug molecules and carrier polymers can have a detrimental effect on the antibacterial activity, as was shown by Hassounah *et al.* demonstrating that hydrogen bonding between PVP carrier and antitubercu-

losis drugs resulted in the loss of antibacterial activity (Hassounah et al., 2014). It seems that most beneficial release profile would be initial burst release to quickly reach effective antibacterial concentrations followed by more prolonged release to keep the concentrations sufficient for longer time and prevent biofilm formation on the dressing and in the wound. To have all desirable properties necessary for wound healing, antimicrobial multilayered wound dressings with different characteristics could have great potential to be used for successful wound therapy.

6.9. Safety of the matrices (I, II)

Safety of the fiber matrices was investigated using cell viability assays on fibroblasts according to the ISO guideline (109993-5). Indirect cell viability assay using liquid extracts of PCL/CAM and PCL/PEO/CAM fiber matrices showed good tolerability by the mammalian cells. There were no statistically significant differences between group means in viability as determined by one-way ANOVA ($F(20,27) = 1.302$, $p = 0.25$). Neither did PCL/MTZ, PCL/CIP nor PCL/CIP/MTZ fiber matrices affect cell viability compared to the untreated controls (cells incubated in plain growth medium) in assays performed by both direct (cells incubated together with fiber matrices) and indirect methods ($p<0.05$, see publication II Figure 7A). In addition, the cell morphology was not changed in the presence of these drug-loaded fiber matrices (see publication II Figure A4). Thus, the developed matrices were considered safe to fibroblastic cells, giving an indication that further studies, including *in vivo* tests on animal models, could be continued to reach the final goal of introducing the dressings to human patients.

6.10. Sterilization of the matrices (III)

Sterility is an important quality attribute of electrospun DDS-s intended to be used on open wounds as contamination of medical devices can lead to infection and severe complications prolonging or suspending healing (Darouiche & Darouiche, 2001). Sterilization and disinfection of electrospun DDSs can be challenging due to several restrictions on the process conditions and the amplitude of functionality-related characteristics that need to be maintained. We studied the efficacy and effects of four different perspective sterilization or disinfection methods (gamma irradiation, UV-irradiation, *in situ* generated chlorine gas and low-temperature argon plasma) on previously described PCL/CAM and PCL/PEO/CAM matrices.

6.10.1. Sterilization efficacy (III)

As sterility testing results are affected by the presence of antimicrobial drugs and European pharmacopoeia states that it is necessary to inactivate any

antimicrobial substances contained in the sample, only blank fiber matrices without CAM were included in these tests to reveal only the effect of sterilization and not to confound it with the antimicrobial activity of CAM. All controls produced expected results, thus tests were considered valid. The results confirmed that all untreated control samples were contaminated and resulted in microbial growth in both aerobic and anaerobic conditions (Table 8).

Table 8. Sterility or non-sterility of tested electrospun fiber matrices after different treatments. For each treatment a number of samples exhibiting microbial growth out of three replicates is presented. Note: no growth was observed in negative controls, growth was observed in positive controls.

Sample	Untreated	UV 15 min	UV 30 min	UV 60 min	Gamma radiation	Cl_2 1h	Cl_2 2h	Plasma 0.5 min	Plasma 1 min	Plasma 2 min
PCL in TSB	3/3	0/3	0/3	0/3	0/3	0/3	0/3	1/3	0/3	1/3
PCL in FTG	3/3	0/3	0/3	0/3	0/3	0/3	0/3	0/3	0/3	0/3
PCL/PEO in TSB	3/3	0/3	0/3	0/3	0/3	0/3	0/3	1/3	1/3	1/3
PCL/PEO in FTG	3/3	1/3	0/3	0/3	0/3	0/3	0/3	0/3	0/3	0/3

Key: FTG – fluid thioglycollate medium; PCL – polycaprolactone; PEO – poly(ethylene oxide); TSB – tryptic soy broth.

Both gamma irradiation (50 kGy) and chlorine gas treatments for 1 and 2 h were able to effectively sterilize the samples (Table 8). Although the prevailing gamma irradiation dose used for sterilization is 25 kGy, it has been reported that doses below 35 kGy were ineffective to completely eliminate microorganisms from PCL scaffolds (Augustine et al., 2015), and thus higher doses may be necessary. When nanofibrous matrices are concerned, gas sterilization has its disadvantages due to a high surface area and possibility of residual gas inclusion in the fiber matrices. This has been seen with ethylene oxide treatments (Horakova et al., 2018), although whether it would be a problem with chlorine gas still needs to be determined.

UV-radiation was also an effective method for decontaminating electrospun matrices, although the shortest treatment time of 15 min on both sides gave unreliable results as one sample in FTG medium still exhibited microbial growth (see publication III Figure 3). Longer exposure times were able to sterilize the samples (30 min per side and 1 h, respectively). The effective exposure time has been reported to vary between 2 min to 2 h, depending on the materials and the geometry of DDS (Dai et al., 2016; Guerra et al., 2018; Rainer et al., 2010).

Low-pressure argon plasma treatment was able to reduce the bioburden as seen from the reduced number of contaminated samples compared with untreated samples (Table 8) but was still ineffective sterilization method independent on the treatment times used in this study (30 s, 60 s and 120 s). There are conflicting results about the efficacy of argon plasma sterilization in the literature (Ghobeira et al., 2017; Holy et al., 2000; L. Yang et al., 2009) and

although it proved to be ineffective in our study, plasma technology should not be disregarded as using other process conditions/plasmas could help to effectively sterilize electrospun matrices. Also, an important factor not often discussed that affects the sterilization efficacy and complicates the comparison of the results from different studies is the presterilization bioburden. The manufacturing conditions must thus be designed to support minimal contamination during preparation and packaging to increase the sterilization efficacy and reduce endotoxin levels in the end product.

In further analyzes, the shortest effective sterilization time was used for UV and chlorine gas treatments (30 min per side and 1 h, respectively) and 1 min treatment with argon plasma.

6.10.2. Drug content (III)

Drug-loaded matrices need to preserve the integrity of the active ingredient after sterilization to ensure the therapeutic efficacy and reduce the amount of possibly toxic degradation products. Still, sterilization of drug-loaded products can result in the loss of active ingredient due to degradation and to understand the extent of this effect the drug content of untreated and differently treated matrices was analyzed with HPLC. The results revealed that sterilization process can indeed lower the amount of drug present in the matrices, but more interestingly, the extent of this loss is largely influenced by the polymeric composition of the matrix (Figure 28).

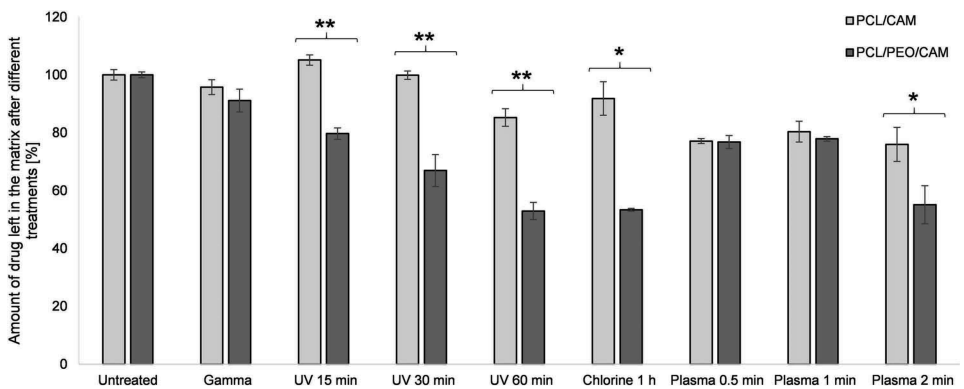

Figure 28. Chemical stability of CAM in untreated and differently treated electrospun fiber matrices: gamma irradiation, UV-treatment for 15, 30 and 60 min on both sides, *in situ* generated chlorine gas treatment for 1 h and argon plasma treatment for 0.5 min, 1 min and 2 min on both sides. Data are averages of three replicates and error bars denote standard deviation. Statistical significance of differences (depicted by asterisks) was analysed by applying two sample t-tests assuming equal or unequal variances depending on the results of the prior F-test ($p < 0.05$). * $p<0.05$; ** $p<0.001$. Key: CAM – chloramphenicol; PCL – polycaprolactone; PEO – poly(ethylene oxide).

In case of UV-sterilized, chlorine gas sterilized and 2 min plasma-sterilized PCL/CAM and PCL/PEO/CAM matrices, there were statistically significant differences in the remaining drug content. With all these methods, the CAM loss was significantly greater in PCL/PEO/CAM matrices. Statistically significant loss of drug was detected in case of PCL/CAM matrices treated with UV for 60 min on both sides and with all plasma treatments, probably due to photolytic degradation of CAM (Bakare-Odunola et al., 2009).

As for PCL/PEO/CAM matrices, all sterilization methods resulted in statistically significant loss of drug. The presence of water is known to hasten drug degradation through several proposed mechanisms (Szakonyi & Zelkó, 2012), and this could explain why drug loss was greater in hydrophilic PCL/PEO/CAM matrices. Also, structural differences between the matrices could contribute to this as larger pores between PCL/PEO/CAM fibers could fascilitate the penetration of gases, like chlorine in this study, into the matrix and thus have a better access to the drug deeper inside the matrix and cause more degradation. Gamma sterilization had the least detrimental effects on PCL/PEO/CAM matrices' drug content and from that point of view would be the most favorable sterilization method. Gamma sterilization has been shown to be suitable for sterilization of CAM-loaded pharmaceutical preparations due to low level of CAM radiolysis at irradiation dose of 25 kGy, moreover, the radiolysis products that are generated are safe for human health (Hong et al., 2002).

6.10.3. Solid state changes (III)

Different sterilization/disinfection treatments did not affect the solid state form of CAM (see publication III Figure 3). Slight changes appear in the peak position of ν_{as}(C-Cl) of CAM (Si et al., 2009) in the spectra of PCL/CAM matrices treated with plasma and chlorine gas (shift from 810 to 816 cm^{-1}) and UV-treatment for 30 min (shift to 814 cm^{-1}), which could indicate recrystallization. On the other hand, the position of ν(C=O) peak (Si et al., 2009) in spectrum remained at 1686 cm^{-1} after all treatments, suggesting that at least partially CAM was still present in an amorphous form in the matrices. Also, peaks related to the ring deformation (649 cm^{-1}) and stretch (1563 cm^{-1}) (Si et al., 2009) were not visible in spectra, further indicating amorphousness. No new peaks or loss of existing peaks were observed in the spectra of matrices after sterilization, neither related to the drug nor the polymers. Thus, it is unlikely that any chemical bonds were formed or broken during these procedures. Similarly, it has been reported that gamma irradiation using doses up to 45 kGy (Bosworth et al., 2012) and UV treatment for 3 h (Ghobeira et al., 2017) have not caused any chemical alteration of PCL, although cleavage of ester bonds in gamma irradiated PCL matrices have been observed (Augustine et al., 2015).

According to our FTIR results, PCL crystallinity was unaffected as no changes were observed in the ratio of crystalline and amorphous C=O stretch peak intensities (1724 vs 1731 cm^{-1}) or in the intensity of peak at 2943 cm^{-1} which is related to the amorphous form (T. Yang et al., 2014). DSC results (see publication III Figures S1 and S2) showed increased PCL melting temperatures in all four gamma-treated matrices, which can suggest increased crystallinity (Bosworth et al., 2012). Longer UV treatments have also been shown to increase PCL crystallinity (Guerra et al., 2018), but the exposure time in our study was probably too short to cause such changes. The crystallization temperatures of plasma treated matrices increased, which can be due to the nucleating effect of impurities or additives (Mucha et al., 2015). As this was seen equally with blank and drug-loaded matrices, drug degradation products alone cannot explain the phenomenon and most likely changes in polymer structure have also occurred.

6.10.4. Morphology and mechanical properties (III)

As morphology and structural properties of electrospun matrices are related to other properties, e.g. mechanical properties (Wong et al., 2008), cell attachment and proliferation (Badami et al., 2006; Lowery et al., 2010), but also drug release (Xie & Buschle-Diller, 2010), it is important to know if any changes have occurred as a result of sterilization/disinfection procedure. SEM micrographs revealed that the treatments did not cause any visible damage to the fiber structure (fusion or breaking of fibers etc., Figure 29) and diameter analysis confirmed that no statistically significant changes in fiber diameters were brought about (see publication III Table 4). Sterilization has been shown to affect the preferential orientation of PLA fibers after ethylene oxide treatment, although not after exposure to gamma or UV-radiation (Valente et al., 2016). Short-term UV treatment (Ghobeira et al., 2017) and gamma irradiation in the dose range of 15-65 kGy (Augustine et al., 2015; Bosworth et al., 2012) have been shown not to cause any changes in the morphology of PCL fibers, in agreement with our results.

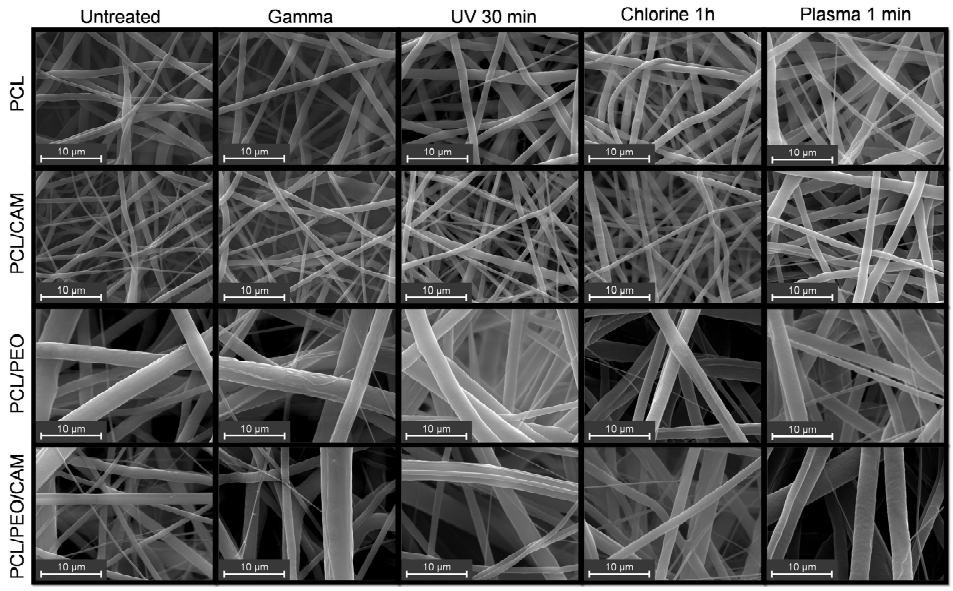

Figure 29. Scanning electron microscopy (SEM) images (x10000 magnification) of untreated and differently treated (gamma irradiation, UV-treatment for 30 min on both sides, *in situ* generated chlorine gas treatment for 1 h and argon plasma treatment for 1 min on both sides) PCL, PCL/CAM, PCL/PEO and PCL/PEO/CAM electrospun fiber matrices.

Although the treatments did not visually change the structures of electrospun fiber matrices, changes in mechanical properties were observed. Gamma-sterilized PCL and PCL/CAM matrices became both stronger and more elastic as the hardness of these matrices increased together with the deformation at hardness (Figure 30). The latter change was statistically significant only for PCL/CAM matrices. These changes can be attributed to crosslinking (Cottam et al., 2009) and/or increased crystallinity of the polymer, the latter also correlating with our solid state analysis results. Higher doses of gamma irradiation have, on the other hand, been shown to reduce tensile strength due to reduced crystallinity (Augustine et al., 2015).

Plasma treatment caused statistically significant increase in the deformation at hardness of PCL/CAM matrix, but not its hardness. Other treatments did not significantly affect the mechanical properties of these matrices (Figure 30).

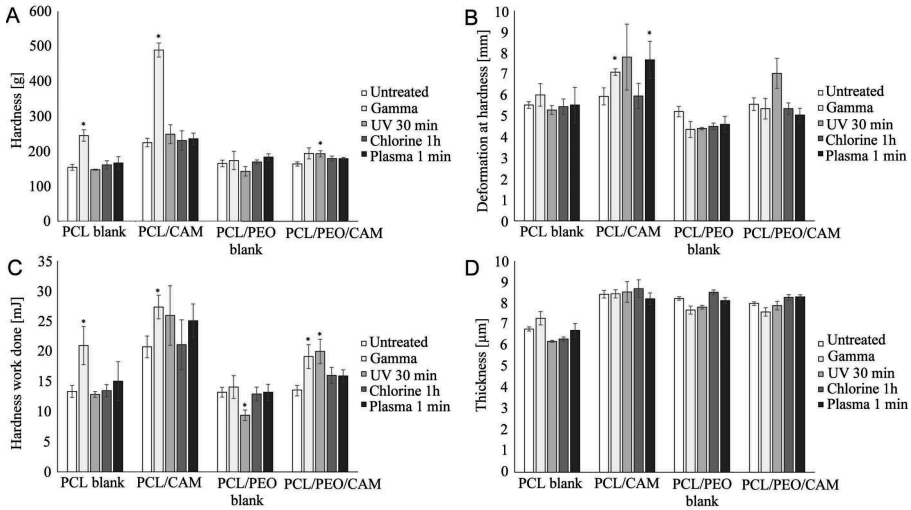

Figure 30. Mechanical properties and thickness of untreated and differently treated (gamma irradiation, UV-treatment for 30 min on both sides, *in situ* generated chlorine gas treatment for 1 h and argon plasma treatment for 1 min on both sides) PCL, PCL/CAM, PCL/PEO and PCL/PEO/CAM electrospun fiber matrices: hardness (A); deformation at hardness (B); hardness work done (C) and thickness (D). Data are averages of three replicates and error bars denote standard deviation. Statistical significance of differences (depicted by asterisks, $p<0.05$) was analysed by applying two sample t-tests assuming equal or unequal variances depending on the results of the prior F-test ($p < 0.05$). Holm's method was used for adjusting p-values. Key: CAM – chloramphenicol; PCL – polycaprolactone; PEO – poly(ethylene oxide).

For PCL/PEO and PCL/PEO/CAM matrices, UV-treatment had more pronounced effects on the mechanical properties. Interestingly, the hardness, deformation at hardness and hardness work done all decreased after 30 min treatment of PCL/PEO matrices (only the latter being statistically significant change) but increased if the same matrices were drug-loaded (deformation at hardness not statistically significant). This could indicate that the drug or its degradation products aided the UV-induced photocrosslinking, whereas if no drug is present, polymer(s) may have gone through some changes impairing their mechanical properties, i.e chain scissioning. It is known that PEO can undergo chemical and physical changes due to UV-irradiation and photoreactions are induced by structural defects, impurities or additives (Kaczmarek et al., 2001; Ochoa Machiste et al., 2005).

As seen, irradiation treatments had greater effect on the mechanical properties of electrospun matrices and depending both on the polymers and the drug, the resulting effects can be different. Hence, sterilization processes can both enhance and impair mechanical properties of electrospun matrices.

6.10.5. Swelling and loss of mass (III)

It is also important to consider how interactions with the aqueous environment mimicking physiological buffers could change in the course of sterilization/disinfection. This does not only affect how much exudate a wound dressing is able to absorb or how long it takes for the matrix to degrade *in vivo* or in the environment after use. But it can also affect the drug release profile, one of the most important parameters for a DDS.

As discussed before, remarkable differences occurred in the swelling behavior between PCL (PCL/CAM) and PCL/PEO (PCL/PEO/CAM) matrices and slight differences also occurred between CAM-loaded and blank PCL matrices (Figure 31A, see also section 6.6). PCL/PEO blank and drug-loaded matrices exhibited similar capacities to quickly absorb buffer, and this does not change with different sterilization/disinfection treatments. On the other hand, both plasma-treated PCL and PCL/CAM matrices exhibit tremendous increase in the swelling index, exceeding even the swelling index values on any of the PCL/PEO matrices. Other treatments did not result in statistically significant changes in swelling. Gamma treatment seemed to increase swelling, although huge variability between samples was seen and thus the difference was not statistically significant. It has been shown before that gamma irradiation could decrease the water contact angle of electrospun PCL matrices and increase wetting due to the formation of surface polar groups (Augustine et al., 2015). Also, differences in polymer crystallinity noted with solid state analysis can play their part.

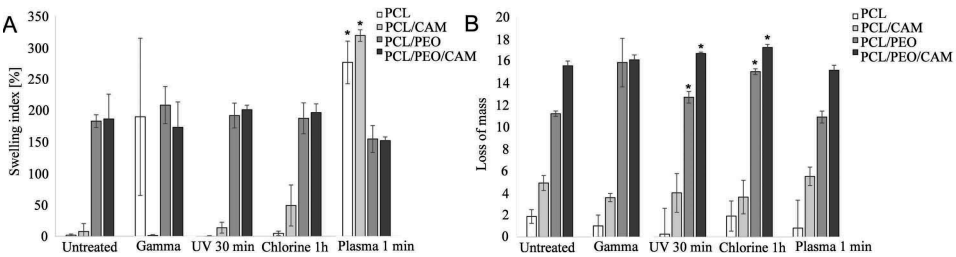

Figure 31. Swelling indices (A) and loss of mass (B) of untreated and differently treated (gamma irradiation, UV-treatment for 30 min on both sides, *in situ* generated chlorine gas treatment for 1 h and argon plasma treatment for 1 min on both sides) PCL, PCL/CAM, PCL/PEO and PCL/PEO/CAM electrospun fiber matrices. Data are averages of at least three replicates and error bars denote standard deviation. Statistical significance of differences (depicted by asterisks, $p<0.05$) was analysed by applying two sample t-tests assuming equal or unequal variances depending on the results of the prior F-test ($p < 0.05$). Holm's method was used for adjusting p-values. Key: CAM – chloramphenicol; PCL – polycaprolactone; PEO – poly(ethylene oxide).

After one week, minimal loss of mass was seen with PCL matrices (0.3–1.9%), independent of the treatment. Similar, although slightly higher was the loss of mass of drug-loaded PCL/CAM matrices (3.6–5.5%) (Figure 31B). This is expected, as with these matrices, drug release occurs in parallel with possible biodegradation and loss of mass depends on both. Similar trend was seen with PCL/PEO and PCL/PEO/CAM matrices, where the drug-loaded matrices exhibited higher loss of mass. Compared to the untreated matrices, small, although statistically significant increase in the loss of mass was seen with both blank and drug-loaded PCL/PEO matrices treated with UV light for 30 min per side ($11.2 \pm 0.2\%$ vs $12.7 \pm 0.5\%$ and $15.5 \pm 0.4\%$ vs $16.7 \pm 0.1\%$, respectively), and also those treated with chlorine gas ($11.2 \pm 0.2\%$ vs $15.0 \pm 0.3\%$ and $15.5 \pm 0.4\%$ vs $17.2 \pm 0.3\%$, respectively). It must be noted that PCL degradation is a long process, thus one week may have been too short time to fully appreciate the extent of possible effects on degradation rate. However, environmental considerations may be more important here compared to the functionality of the wound dressing which needs to be changed before the degradation becomes apparent.

6.10.6. Drug release (III)

No statistically significant differences were seen in the drug release behavior between untreated and chlorine treated PCL/CAM matrices (difference factor $f1 = 9.6$; similarity factor $f2 = 66.2$). On the other hand, after gamma treatment, the release was faster ($f1 = 16.0$; $f2 = 59.8$) and after UV-treatment, slightly slower ($f1 = 15.4$; $f2 = 58.2$). UV is a surface sterilization method thus any degradation of the drug during this process occurs probably on the fiber matrix surface. As burst release is mainly associated with the release of the drug near the fiber or fiber matrix surface, this could explain the reduced burst release, although the loss of drug during 30 min UV treatment in our study was not statistically significant. Still, the most dramatic change was seen after argon plasma treatment where prolonged release was lost and practically all the drug was released instantly (Figure 32A).

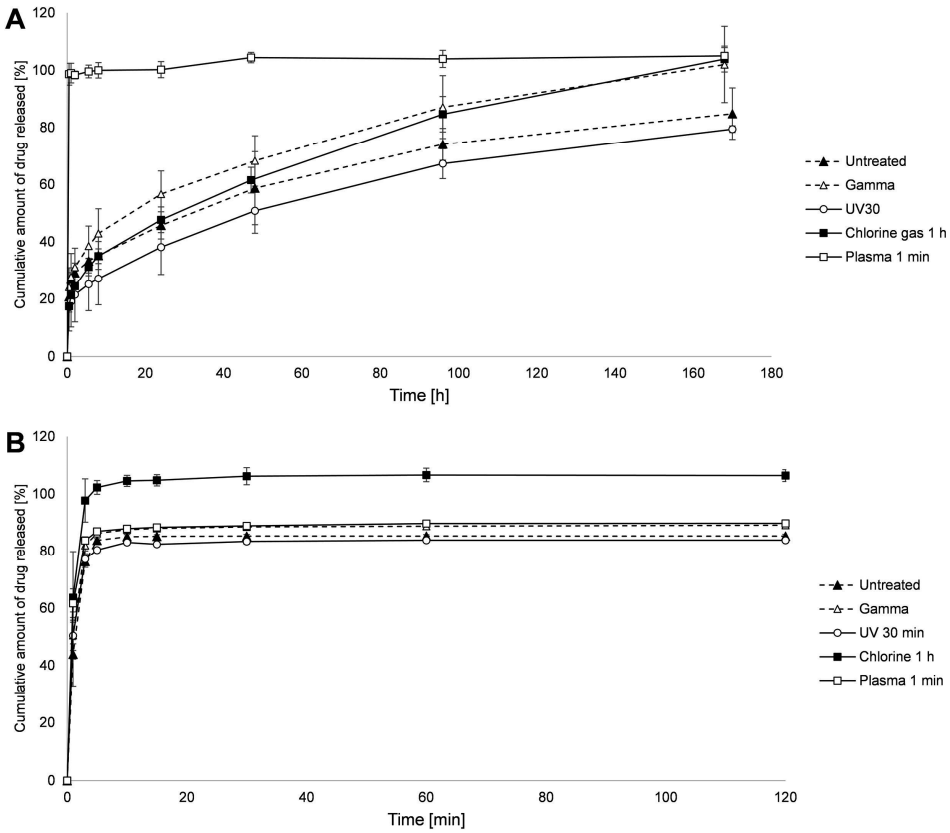

Figure 32. Drug release profiles of untreated and differently treated (gamma irradiation, UV-treatment for 30 min on both sides, *in situ* generated chlorine gas treatment for 1 h and argon plasma treatment for 1 min on both sides) PCL/CAM fiber matrices (A) and PCL/PEO/CAM fiber matrices (B). Data are averages of at least three replicates and error bars denote standard deviation. Key: CAM – chloramphenicol; PCL – poly-caprolactone, PEO – poly(ethylene oxide).

In case of PCL/PEO/CAM matrices, the shape of the release curves does not change after different treatments and most of the drug is rapidly released within the first 5–10 min. Only chlorine treated matrices deviated noticeably as more drug within the same time-period was released compared to the untreated matrices (Figure 32B).

As discussed previously, the hydrophobicity of PCL is the key factor prolonging the drug release from PCL/CAM matrices and thus wetting of the matrix is the major factor triggering drug release. Just as the addition of a hydrophilic polymer PEO, plasma sterilization dramatically improved wetting, which in turn resulted in rapid release of the drug. Plasma is often used for the purpose of modifying the surface properties, most notably to decrease the water contact angle and improve the wettability of the samples (Morent et al., 2011). Unlike untreated PCL and PCL/CAM matrices, plasma treated matrices were

instantly wetted when placed in contact with a buffer solution and swelling indices were remarkably increased. Decreased water contact angle of PCL after plasma treatment could be due to the increased number of carboxyl group end chains on the treated surfaces (Ghobeira et al., 2017). As PCL/PEO and PCL/PEO/CAM matrices were already hydrophilic, plasma treatment did not have such effects on those matrices.

7. CONCLUSIONS

Based on the knowledge gained in the present study, following conclusions can be drawn:

- Hydrophobic PCL is a suitable carrier polymer for a hydrophobic drug CAM to create a slow-release electrospun nanofiber matrix, whereas addition of a hydrophilic polymer PEO greatly changes the matrix properties, e.g. morphology, mechanical properties, wetting and swelling properties, that lead to different drug release profiles and antibacterial activity. Hydrophilic drugs MTZ and CIP can be incorporated into electrospun PCL nanofiber matrices, whereas combining these two drugs alters the buffer uptake and MTZ release profile. Thus, the selection of appropriate materials in the first stage of design is crucial for the production of electrospun DDSs with desired physicochemical, structural, and mechanical properties that further shape the behavior of the matrices in biorelevant conditions.
- The drug can be incorporated into the matrix in an amorphous or crystalline form, depending on its compatibility with the carrier polymer(s). The recrystallization of the drug can take place inside the fibers or on the fiber surface, and this greatly affects matrix interactions with aqueous environment. Electrospinning can also change polymer crystallinity and induce interactions between different components of the fiber matrices. MD simulations provided mechanistic insight into the interactions of different matrix components at molecular level.
- One of the most important, although not universal, factors controlling drug release from electrospun fiber matrices is the wetting and penetration of buffer into the matrices. Buffer penetration is affected by the hydrophilicity/hydrophobicity of the matrix components, matrix thickness and indirectly the solid state of the drug. Thus, for some drug-polymer combinations (e.g. MTZ + PCL) the suitable drug release kinetics can be tailored by altering the matrix thickness.
- Novel hydrogel-based methods to study drug release and diffusion enable to mimic the *in vitro* antibacterial activity testing conditions, and most likely the wound environment, whereas release into the buffer solution overestimated the burst release effects. The developed methods were similar in terms of sensitivity but had different advantages and disadvantages.
- Traditional disc diffusion assay enabled to confirm if the released drugs and their concentrations were effective against tested microbes but did not differentiate between different drug release profiles of electrospun matrices. Advanced antibacterial disc diffusion assays enabled to reveal differences in the antibacterial activity of the differently designed electrospun fiber matrices, even when the differences were only minor.
- To avoid biofilm formation on an electrospun fiber matrix, it has to have sustained antibacterial properties, whereas initial burst release is beneficial to quickly reach effective antibacterial concentrations. As some carrier

polymers can promote biofilm formation, this must be considered in the course of developing wound dressings.
- All developed fiber matrices were safe in *in vitro* cytotoxicity experiments, thus giving an indication that further studies, including *in vivo* tests on animal models, can be continued to elaborate the safety profile of the matrices.
- Different techniques enabled to effectively sterilize electrospun fiber matrices, although the treatment process can alter different fiber matrix properties, including drug content, mechanical properties, interactions with aqueous medium and drug release. The potential effects depend on the specific sterilization method, the polymeric composition of the matrix and the properties of the drug.

To summarize, the design and development of an electrospun DDS is a complex and multifaceted process that needs careful considerations at every step of the way. The knowledge gained in the present dissertation highlights the significance of selecting appropriate materials for the production of electrospun DDSs with desired properties; the need for meticulous characterization to reveal functionality-related characteristics that play an integral part in shaping the performance and quality of an electrospun DDS; the importance of selecting biorelevant conditions for the characterization of electrospun DDSs to better translate the results into *in vivo* conditions depending on the intended application; and the importance of analyzing the effect of post-treatments, e.g., sterilization, as these can cause tremendous changes in the properties and behavior of an electrospun DDS.

8. REFERENCES

Abdelrazek, E. M., Hezma, A. M., El-khodary, A., & Elzayat, A. M. (2016). Spectroscopic studies and thermal properties of PCL/PMMA biopolymer blend. *Egyptian Journal of Basic and Applied Sciences*, *3*(1), 10–15. https://doi.org/10.1016/j.ejbas.2015.06.001

Abrigo, M., Kingshott, P., & McArthur, S. L. (2015). Bacterial response to different surface chemistries fabricated by plasma polymerization on electrospun nanofibers. *Biointerphases*, *10*(4). https://doi.org/10.1116/1.4927218

Abrigo, M., McArthur, S. L., & Kingshott, P. (2014). Electrospun nanofibers as dressings for chronic wound care: Advances, challenges, and future prospects. *Macromolecular Bioscience*, *14*(6), 772–792. https://doi.org/10.1002/mabi.201300561

Alippilakkotte, S., Kumar, S., & Sreejith, L. (2017). Fabrication of PLA/Ag nanofibers by green synthesis method using Momordica charantia fruit extract for wound dressing applications. *Colloids and Surfaces A: Physicochemical and Engineering Aspects*, *529*(May), 771–782. https://doi.org/10.1016/j.colsurfa.2017.06.066

Allafchian, A., Hosseini, H., & Ghoreishi, S. M. (2020). Electrospinning of PVA-carboxymethyl cellulose nanofibers for flufenamic acid drug delivery. *International Journal of Biological Macromolecules*, *163*, 1780–1786. https://doi.org/10.1016/J.IJBIOMAC.2020.09.129

Alwaeli, A. Z. J. (2018). Anaerobic Bacteria Associated with Periodontitis. In S. B. Bhardwaj (Ed.), *Oral Microbiology in Periodontitis*. IntechOpen. https://doi.org/10.5772/intechopen.76352

American Society for Testing Materials (ASTM). (2010). *D3985-05: standard test method for oxygen gas transmission rate through plastic film and sheeting using coulometric sensor*.

American Society for Testing Materials (ASTM). (2013). *D1653-13: standard test methods for water vapor transmission of organic coating filmse*.

Andersson, D. I., & Hughes, D. (2014). Microbiological effects of sublethal levels of antibiotics. *Nature Reviews. Microbiology*, *12*(7), 465–478. https://doi.org/10.1038/nrmicro3270

Anup, N., Chavan, T., Chavan, S., Polaka, S., Kalyane, D., Abed, S. N., Venugopala, K. N., Kalia, K., & Tekade, R. K. (2021). Reinforced electrospun nanofiber composites for drug delivery applications. *Journal of Biomedical Materials Research Part A*, *109*(10), 2036–2064. https://doi.org/10.1002/JBM.A.37187

Augustine, R., Saha, A., Jayachandran, V. P., Thomas, S., & Kalarikkal, N. (2015). Dose-dependent effects of gamma irradiation on the materials properties and cell proliferation of electrospun polycaprolactone tissue engineering scaffolds. *International Journal of Polymeric Materials and Polymeric Biomaterials*, *64*(10), 526–533. https://doi.org/10.1080/00914037.2014.977900

Azimi, B., Maleki, H., Zavagna, L., de la Ossa, J. G., Linari, S., Lazzeri, A., & Danti, S. (2020). Bio-Based Electrospun Fibers for Wound Healing. *Journal of Functional Biomaterials*, *11*(3). https://doi.org/10.3390/JFB11030067

Badami, A. S., Kreke, M. R., Thompson, M. S., Riffle, J. S., & Goldstein, A. S. (2006). Effect of fiber diameter on spreading, proliferation, and differentiation of osteoblastic cells on electrospun poly(lactic acid) substrates. *Biomaterials*, *27*(4), 596–606. https://doi.org/10.1016/J.BIOMATERIALS.2005.05.084

Bae, H.-S., Haider, A., Selim, K. M. K., Kang, D.-Y., Kim, E.-J., & Kang, I.-K. (2013). Fabrication of highly porous PMMA electrospun fibers and their application in the

removal of phenol and iodine. *Journal of Polymer Research 2013 20:7*, *20*(7), 1–7. https://doi.org/10.1007/S10965-013-0158-9

Bakare-Odunola, Bello-Mustapha, & Enemali, I. S. (2009). Light Induced Degradation of Aqueous Solution of Chloramphenicol. In *Nigerian Journal of Pharmaceutical Sciences* (Vol. 8, Issue 1). https://journals.abu.edu.ng/njps/pdf/58.pdf

Baumgarten, P. K. (1971). Electrostatic spinning of acrylic microfibers. *Journal of Colloid and Interface Science*, *36*(1), 71–79. https://doi.org/10.1016/0021-9797(71)90241-4

Beceiro, A., Tomás, M., & Bou, G. (2013). Antimicrobial resistance and virulence: a successful or deleterious association in the bacterial world? *Clinical Microbiology Reviews*, *26*(2), 185–230. https://doi.org/10.1128/CMR.00059-12

Beloin, C., Roux, A., & Ghigo, J. M. (2008). Escherichia coli biofilms. In T. Romeo (Ed.), *Bacterial Biofilms* (Vol. 322, pp. 249–289). https://doi.org/10.1007/978-3-540-75418-3_12

Bhujbal, S. V., Mitra, B., Jain, U., Gong, Y., Agrawal, A., Karki, S., Taylor, L. S., Kumar, S., & (Tony) Zhou, Q. (2021). Pharmaceutical amorphous solid dispersion: A review of manufacturing strategies. *Acta Pharmaceutica Sinica B*, *11*(8), 2505–2536. https://doi.org/10.1016/J.APSB.2021.05.014

Blattner, F. R., Plunkett, G., Bloch, C. A., Perna, N. T., Burland, V., Riley, M., Collado-Vides, J., Glasner, J. D., Rode, C. K., Mayhew, G. F., Gregor, J., Davis, N. W., Kirkpatrick, H. A., Goeden, M. A., Rose, D. J., Mau, B., & Shao, Y. (1997). The complete genome sequence of Escherichia coli K-12. In *Science* (Vol. 277, Issue 5331, pp. 1453–1462). Science. https://doi.org/10.1126/science.277.5331.1453

Boateng, J., & Catanzano, O. (2015). Advanced Therapeutic Dressings for Effective Wound Healing – A Review. *Journal of Pharmaceutical Sciences*, *104*(11), 3653–3680. https://doi.org/10.1002/JPS.24610

Boateng, J. S., Matthews, K. H., Stevens, H. N. E., Eccleston, G. M., Sciences, B., & Building, J. A. (2008). Wound Healing Dressings and Drug Delivery Systems : A Review. *Journal of Pharmaceutical Sciences*, *97*(8), 2892–2923. https://doi.org/10.1002/jps

Bosworth, L. A., Gibb, A., & Downes, S. (2012). Gamma irradiation of electrospun poly(ε-caprolactone) fibers affects material properties but not cell response. *Journal of Polymer Science Part B: Polymer Physics*, *50*(12), 870–876. https://doi.org/10.1002/polb.23072

Bowler, P. G., Duerden, B. I., & Armstrong, D. G. (2001). Wound microbiology and associated approaches to wound management. *Clinical Microbiology Reviews*, *14*(2), 244–269. https://doi.org/10.1128/CMR.14.2.244-269.2001

Bowler, Philip G. (2003). The 10(5) bacterial growth guideline: reassessing its clinical relevance in wound healing. *Ostomy Wound Management*, *49*(1), 44–53.

Brackman, G., Cos, P., Maes, L., Nelis, H. J., & Coenye, T. (2011). Quorum sensing inhibitors increase the susceptibility of bacterial biofilms to antibiotics in vitro and in vivo. *Antimicrobial Agents and Chemotherapy*, *55*(6), 2655–2661. https://doi.org/10.1128/AAC.00045-11

Brady, R. A., Leid, J. G., Calhoun, J. H., Costerton, J. W., & Shirtliff, M. E. (2008). Osteomyelitis and the role of biofilms in chronic infection. *FEMS Immunology and Medical Microbiology*, *52*(1), 13–22. https://doi.org/10.1111/j.1574-695X.2007.00357.x

Brunauer, S., Emmett, P. H., & Teller, E. (1938). Adsorption of Gases in Multimolecular Layers. *Journal of the American Chemical Society*, *60*(2), 309–319. https://doi.org/10.1021/ja01269a023

Bunaciu, A. A., Aboul-Enein, H. Y., & Hoang, V. D. (2015). Vibrational spectroscopy used in polymorphic analysis. *Trends in Analytical Chemistry*, *69*, 14–22. https://doi.org/10.1016/J.TRAC.2015.02.006

Campiglio, C. E., Negrini, N. C., Farè, S., & Draghi, L. (2019). Cross-Linking Strategies for Electrospun Gelatin Scaffolds. *Materials*, *12*(15). https://doi.org/10.3390/MA12152476

Centers for Disease Contol and Prevention (CDC). (2002a). Staphylococcus aureus resistant to vancomycin – United States, 2002. In *Journal of the American Medical Association* (Vol. 288, Issue 7). American Medical Association. https://doi.org/10.1001/jama.288.7.824

Centers for Disease Contol and Prevention (CDC). (2002b). Vancomycin-Resistant Staphylococcus aureus – Pennsylvania, 2002. In *Journal of the American Medical Association* (Vol. 288, Issue 17). American Medical Association. https://doi.org/10.1001/JAMA.288.17.2116-JWR1106-3-1

Chamundeeswari, S. V., Chamundeeswari, S. P. V., Samuel, E. R. J. J., & Sundaraganesan, N. (2011). Theoretical and experimental studies on 2-(2-methyl-5-nitro-1-imidazolyl)ethanol. *European Journal of Chemistry*, *2*(2), 136–145. https://doi.org/10.5155/eurjchem.2.2.136-145.169

Chen, X., Zhao, R., Wang, X., Li, X., Peng, F., Jin, Z., Gao, X., Yu, J., & Wang, C. (2017). Electrospun mupirocin loaded polyurethane fiber mats for anti-infection burn wound dressing application. *Journal of Biomaterials Science, Polymer Edition*, *28*(2), 162–176. https://doi.org/10.1080/09205063.2016.1262158

Chou, S.-F., & Woodrow, K. A. (2017). Relationships between mechanical properties and drug release from electrospun fibers of PCL and PLGA blends. *Journal of the Mechanical Behavior of Biomedical Materials*, *65*, 724–733. https://doi.org/10.1016/j.jmbbm.2016.09.004

Cipitria, A., Skelton, A., Dargaville, T. R., Dalton, P. D., & Hutmacher, D. W. (2011). Design, fabrication and characterization of PCL electrospun scaffolds – a review. *Journal of Materials Chemistry*, *21*(26), 9419. https://doi.org/10.1039/c0jm04502k

Corsaro, C., Mallamace, D., Neri, G., & Fazio, E. (2021). Hydrophilicity and hydrophobicity: Key aspects for biomedical and technological purposes. *Physica A: Statistical Mechanics and Its Applications*, *580*, 126189. https://doi.org/10.1016/J.PHYSA.2021.126189

Cortez Tornello, P. R., Caracciolo, P. C., Cuadrado, T. R., & Abraham, G. A. (2014). Structural characterization of electrospun micro/nanofibrous scaffolds by liquid extrusion porosimetry: A comparison with other techniques. *Materials Science and Engineering: C*, *41*, 335–342. https://doi.org/10.1016/j.msec.2014.04.065

Cottam, E., Hukins, D. W. L., Lee, K., Hewitt, C., & Jenkins, M. J. (2009). Effect of sterilisation by gamma irradiation on the ability of polycaprolactone (PCL) to act as a scaffold material. *Medical Engineering & Physics*, *31*(2), 221–226. https://doi.org/10.1016/J.MEDENGPHY.2008.07.005

Cui, W., Li, X., Zhu, X., Yu, G., Zhou, S., & Weng, J. (2006). Investigation of drug release and matrix degradation of electrospun poly(DL-lactide) fibers with paracetanol inoculation. *Biomacromolecules*, *7*(5), 1623–1629. https://doi.org/10.1021/bm060057z

Daeschlein, G. (2013). Antimicrobial and antiseptic strategies in wound management. In *International Wound Journal* (Vol. 10, Issue S1, pp. 9–14). Int Wound J. https://doi.org/10.1111/iwj.12175

Dai, Y., Xia, Y., Chen, H.-B., Li, N., Chen, G., Zhang, F.-M., & Gu, N. (2016). Optimization of sterilization methods for electrospun poly(ε-caprolactone) to enhance pre-osteoblast cell behaviors for guided bone regeneration. *Journal of Bioactive and Compatible Polymers*, *31*(2), 152–166. https://doi.org/10.1177/ 0883911515598795

Darouiche, R. O., & Darouiche, R. O. (2001). Device-Associated Infections: A Macroproblem that Starts with Microadherence. *Clinical Infectious Diseases*, *33*(9), 1567–1572. https://doi.org/10.1086/323130

Dash, S., Murthy, P. N., Nath, L., & Chowdhury, P. (2010). Kinetic modeling on drug release from controlled drug delivery systems. *Acta Poloniae Pharmaceutica*, *67*(3), 217–223. https://doi.org/10.1016/S0928-0987(01)00095-1

Davidson, C. A. B., & Lowe, C. R. (2004). Optimisation of polymeric surface pretreatment to prevent bacterial biofilm formation for use in microfluidics. *Journal of Molecular Recognition*, *17*(3), 180–185. https://doi.org/10.1002/jmr.662

Davies, C. E., Wilson, M. J., Hill, K. E., Stephens, P., Hill, C. M., Harding, K. G., & Thomas, D. W. (2001). Use of molecular techniques to study microbial diversity in the skin: Chronic wounds reevaluated. In *Wound Repair and Regeneration* (Vol. 9, Issue 5, pp. 332–340). Wound Repair Regen. https://doi.org/10.1046/j.1524-475x.2001.00332.x

Davison, W. H. T. (1955). Infrared spectra and crystallinity. Part III. Poly(ethylene glycol). *Journal of the Chemical Society (Resumed)*, 3270–3274. https://doi.org/10.1039/JR9550003270

Demirci, S., Celebioglu, A., & Uyar, T. (2014). pH-responsive nanofibers with controlled drug release properties. *Polymer Chemistry*, 2050–2056. https://doi.org/10.1039/c3py01276j

Deo, P. N., & Deshmukh, R. (2019). Oral microbiome: Unveiling the fundamentals. *Journal of Oral and Maxillofacial Pathology*, *23*(1), 122–128. https://doi.org/10.4103/jomfp.JOMFP_304_18

Dhand, C., Venkatesh, M., Barathi, V. A., Harini, S., Bairagi, S., Goh Tze Leng, E., Muruganandham, N., Low, K. Z. W., Fazil, M. H. U. T., Loh, X. J., Srinivasan, D. K., Liu, S. P., Beuerman, R. W., Verma, N. K., Ramakrishna, S., & Lakshminarayanan, R. (2017). Bio-inspired crosslinking and matrix-drug interactions for advanced wound dressings with long-term antimicrobial activity. *Biomaterials*, *138*, 153–168. https://doi.org/10.1016/j.biomaterials.2017.05.043

Doumeng, M., Makhlouf, L., Berthet, F., Marsan, O., Delbé, K., Denape, J., & Chabert, F. (2021). A comparative study of the crystallinity of polyetheretherketone by using density, DSC, XRD, and Raman spectroscopy techniques. *Polymer Testing*, *93*, 106878. https://doi.org/10.1016/J.POLYMERTESTING.2020.106878

Dowd, S. E., Wolcott, R. D., Kennedy, J., Jones, C., & Cox, S. B. (2011). Molecular diagnostics and personalised medicine in wound care: Assessment of outcomes. *Journal of Wound Care*, *20*(5), 232–239. https://doi.org/10.12968/jowc.2011.20.5.232

Drobnik, J., Krucinska, I., Komisarczyk, A., Sporny, S., Szczepanowska, A., & Ciosek, J. (2017). Effects of electrospun scaffolds of di-O-butyrylchitin and poly-(ϵ-caprolactone) on wound healing. *Canadian Journal of Surgery*, *60*(3), 162–171. https://doi.org/10.1503/CJS.010116

Drosou, A., Falabella, A., & Kirsner, R. S. (2003). Antiseptics on wounds: An area of controversy. *Wounds*, *15*(5), 149–166.

Dulnik, J., Denis, P., Sajkiewicz, P., Kołbuk, D., & Choińska, E. (2016). Biodegradation of bicomponent PCL/gelatin and PCL/collagen nanofibers electrospun

from alternative solvent system. *Polymer Degradation and Stability*, *130*, 10–21. https://doi.org/10.1016/j.polymdegradstab.2016.05.022

Edwards, R., & Harding, K. G. (2004). Bacteria and wound healing. *Current Opinion in Infectious Diseases*, *17*(2), 91–96. https://doi.org/10.1097/00001432-200404000-00004

Elzein, T., Nasser-Eddine, M., Delaite, C., Bistac, S., & Dumas, P. (2004). FTIR study of polycaprolactone chain organization at interfaces. *Journal of Colloid and Interface Science*, *273*(2), 381–387. https://doi.org/10.1016/j.jcis.2004.02.001

European Medicines Agency. (2016). *Guideline on the sterilisation of the medicinal product , active substance , excipient and primary container.*

Fahimirad, S., Fahimirad, Z., & Sillanpää, M. (2021). Efficient removal of water bacteria and viruses using electrospun nanofibers. *Science of The Total Environment*, *751*, 141673. https://doi.org/10.1016/J.SCITOTENV.2020.141673

Falde, E. J., Freedman, J. D., Herrera, V. L. M., Yohe, S. T., Colson, Y. L., & Grinstaff, M. W. (2015). Layered superhydrophobic meshes for controlled drug release. *Journal of Controlled Release*, *214*, 23–29. https://doi.org/10.1016/j.jconrel.2015.06.042

Fathi-Azarbayjani, A., & Chan, S. Y. (2010). Single and multi-layered nanofibers for rapid and controlled drug delivery. *Chemical and Pharmaceutical Bulletin*, *58*(2), 143–146. https://doi.org/10.1248/cpb.58.143

Fazli, Y., & Shariatinia, Z. (2017). Controlled release of cefazolin sodium antibiotic drug from electrospun chitosan-polyethylene oxide nanofibrous Mats. *Materials Science and Engineering C*, *71*, 641–652. https://doi.org/10.1016/j.msec.2016.10.048

Food and Drug Administration. (2016a). *Use of International Standard ISO 10993-1, "Biological evaluation of medical devices -Part 1: Evaluation and testing within a risk management process"; Guidance for Industry and Food and Drug Administration Staff*.

Food and Drug Administration. (2016b). FDA Executive Summary: Classification of Wound Dressings Combined with Drugs. *Meeting of the General and Plastic Surgery Devices Advisory Panel*, 1–83.

Forward, K. M., & Rutledge, G. C. (2012). Free surface electrospinning from a wire electrode. *Chemical Engineering Journal*, *183*, 492–503. https://doi.org/10.1016/J.CEJ.2011.12.045

Fu, Y., & Kao, W. J. (2010). Drug release kinetics and transport mechanisms of non-degradable and degradable polymeric delivery systems. *Expert Opinion on Drug Delivery*, *7*(4), 429–444. https://doi.org/10.1517/17425241003602259

Gefen, O., Chekol, B., Strahilevitz, J., Balaban, N. Q., & Balaban, N. Q. (2017). TDtest: easy detection of bacterial tolerance and persistence in clinical isolates by a modified disk-diffusion assay. *Scientific Reports*, *7*, 41284. https://doi.org/10.1038/srep41284

Ghobeira, R., Philips, C., Declercq, H., Cools, P., De Geyter, N., Cornelissen, R., & Morent, R. (2017). Effects of different sterilization methods on the physico-chemical and bioresponsive properties of plasma-treated polycaprolactone films. *Biomedical Materials*, *12*(1), 015017. https://doi.org/10.1088/1748-605X/aa51d5

Guerra, A. J., Cano, P., Rabionet, M., Puig, T., & Ciurana, J. (2018). Effects of different sterilization processes on the properties of a novel 3D-printed polycaprolactone stent. *Polymers for Advanced Technologies*, *29*(8), 2327–2335. https://doi.org/10.1002/pat.4344

Guo, S., & DiPietro, L. A. (2010). Factors Affecting Wound Healing. *Journal of Dental Research*, *89*(3), 219. https://doi.org/10.1177/0022034509359125

Haider, A., Haider, S., & Kang, I. K. (2018). A comprehensive review summarizing the effect of electrospinning parameters and potential applications of nanofibers in biomedical and biotechnology. *Arabian Journal of Chemistry*, *11*(8), 1165–1188. https://doi.org/10.1016/j.arabjc.2015.11.015

Haider, S., Al-Zeghayer, Y., Ahmed Ali, F. A., Haider, A., Mahmood, A., Al-Masry, W. A., Imran, M., & Aijaz, M. O. (2013). Highly aligned narrow diameter chitosan electrospun nanofibers. *Journal of Polymer Research 2013 20:4*, *20*(4), 1–11. https://doi.org/10.1007/S10965-013-0105-9

Hall Barrientos, I. J., Paladino, E., Brozio, S., Passarelli, M. K., Moug, S., Black, R. A., Wilson, C. G., & Lamprou, D. A. (2017). Fabrication and characterisation of drug-loaded electrospun polymeric nanofibers for controlled release in hernia repair. *International Journal of Pharmaceutics*, *517*(1–2), 329–337. https://doi.org/10.1016/J.IJPHARM.2016.12.022

Han, J., Zhang, H., Zhu, L., & Branford-white, C. J. (2009). Electrospun biodegradable nanofiber mats for controlled release of herbal medicine. *3rd International Conference on Bioinformatics and Biomedical Engineering*, 3–6. https://doi.org/10.1109/ICBBE.2009.5162767

Harding, K. G., Morris, H. L., & Patel, G. K. (2002). Science, medicine and the future: healing chronic wounds. *British Medical Journal*, *324*(7330), 160–163. https://doi.org/10.1136/bmj.324.7330.160

Hartgerink, J. D., Beniash, E., & Stupp, S. I. (2001). Self-assembly and mineralization of peptide-amphiphile nanofibers. *Science*, *294*(5547), 1684–1688. https://doi.org/10.1126/science.1063187.

Hartman, O., Zhang, C., Adams, E. L., Farach-Carson, M. C., Petrelli, N. J., Chase, B. D., & Rabolt, J. F. (2010). Biofunctionalization of electrospun PCL-based scaffolds with perlecan domain IV peptide to create a 3-D pharmacokinetic cancer model. *Biomaterials*, *31*(21), 5700–5718. https://doi.org/10.1016/J.BIOMATERIALS.2010.03.017

Hassounah, I. A., Shehata, N. A., Kimsawatde, G. C., Hudson, A. G., Sriranganathan, N., Joseph, E. G., & Mahajan, R. L. (2014). Studying the activity of antitubercluosis drugs inside electrospun polyvinyl alcohol, polyethylene oxide, and polycaprolacton nanofibers. *Journal of Biomedical Materials Research - Part A*, *102*(11), 4009–4016. https://doi.org/10.1002/jbm.a.35070

He, T., Wang, J., Huang, P., Zeng, B., Li, H., Cao, Q., Zhang, S., Luo, Z., Deng, D. Y. B., Zhang, H., & Zhou, W. (2015). Electrospinning polyvinylidene fluoride fibrous membranes containing anti-bacterial drugs used as wound dressing. *Colloids and Surfaces B: Biointerfaces*, *130*, 278–286. https://doi.org/10.1016/j.colsurfb.2015.04.026

Hemmi, H., Takeuchi, O., Kawai, T., Kaisho, T., Sato, S., Sanjo, H., Matsumoto, M., Hoshino, K., Wagner, H., Takeda, K., & Akira, S. (2000). A Toll-like receptor recognizes bacterial DNA. *Nature 2000 408:6813*, *408*(6813), 740–745. https://doi.org/10.1038/35047123

Herrero-Herrero, M., Gómez-Tejedor, J. A., & Vallés-Lluch, A. (2018). PLA/PCL electrospun membranes of tailored fibres diameter as drug delivery systems. *European Polymer Journal*, *99*, 445–455. https://doi.org/10.1016/J.EURPOLYMJ.2017.12.045

Høiby, N., Ciofu, O., Krogh Johansen, H., Song, Z.-J., Moser, C., Jensen, P. Ø., Molin, S., Givskov, M., Tolker-Nielsen, T., & Bjarnsholt, T. (2011). The clinical impact of bacterial biofilms. *International Journal of Oral Science*, *3*, 55–65. https://doi.org/10.4248/IJOS11026

Holy, C. E., Cheng, C., Davies, J. E., & Shoichet, M. S. (2000). Optimizing the sterilization of PLGA scaffolds for use in tissue engineering. *Biomaterials*, *22*(1), 25–31. https://doi.org/10.1016/S0142-9612(00)00136-8

Hong, L., Horni, A., Hesse, M., & Altorfer, H. (2002). Identification and evaluation of radiolysis products of irradiated chloramphenicol by HPLC-MS and HPLC-DAD. *Chromatographia*, *55*(1–2), 13–18. https://doi.org/10.1007/BF02492308

Horakova, J., Mikes, P., Saman, A., Jencova, V., Klapstova, A., Svarcova, T., Ackermann, M., Novotny, V., Suchy, T., & Lukas, D. (2018). The effect of ethylene oxide sterilization on electrospun vascular grafts made from biodegradable polyesters. *Materials Science and Engineering: C*, *92*, 132–142. https://doi.org/10.1016/J.MSEC.2018.06.041

Howell-Jones, R. S., Wilson, M. J., Hill, K. E., Howard, A. J., Price, P. E., & Thomas, D. W. (2005). A review of the microbiology, antibiotic usage and resistance in chronic skin wounds. *Journal of Antimicrobial Chemotherapy*, *55*(55), 143–149.

Hu, J., Prabhakaran, M. P., Tian, L., Ding, X., & Ramakrishna, S. (2015). Drug-loaded emulsion electrospun nanofibers: Characterization, drug release and in vitro biocompatibility. *RSC Advances*, *5*(121), 100256–100267. https://doi.org/10.1039/c5ra18535a

Huang, Z.-M. M., Zhang, Y.-Z. Z., Kotaki, M., & Ramakrishna, S. (2003). A review on polymer nanofibers by electrospinning and their applications in nanocomposites. *Composites Science and Technology*, *63*(15), 2223–2253. https://doi.org/10.1016/S0266-3538(03)00178-7

Ibrahim, H. M., Dakrory, A., & Klingner, A. (2015). Carboxymethyl Chitosan Electrospun Nanofibers: Preparation and its Antibacterial Activity. *Journal of Textile and Apparel, Technology and Management*, *9*(2), 1–13.

Ignatova, M., Manolova, N., & Rashkov, I. (2013). Electrospun Antibacterial Chitosan-Based Fibers. *Macromolecular Bioscience*, *13*(7), 860–872. https://doi.org/10.1002/mabi.201300058

Islam, M. S., Ang, B. C., Andriyana, A., & Afifi, A. M. (2019). A review on fabrication of nanofibers via electrospinning and their applications. *SN Applied Sciences 2019 1:10*, *1*(10), 1–16. https://doi.org/10.1007/S42452-019-1288-4

James, G. A., Swogger, E., Wolcott, R., Pulcini, E. deLancey, Secor, P., Sestrich, J., Costerton, J. W., & Stewart, P. S. (2008). Biofilms in chronic wounds. *Wound Repair and Regeneration*, *16*(1), 37–44. https://doi.org/10.1111/j.1524-475X.2007.00321.x

Jang, C. H., Cho, Y. B., Jang, Y. S., Kim, M. S., & Kim, G. H. (2015). Antibacterial effect of electrospun polycaprolactone/polyethylene oxide/vancomycin nanofiber mat for prevention of periprosthetic infection and biofilm formation. *International Journal of Pediatric Otorhinolaryngology*, *79*(8), 1299–1305. https://doi.org/10.1016/j.ijporl.2015.05.037

Järbrink, K., Ni, G., Sönnergren, H., Schmidtchen, A., Pang, C., Bajpai, R., & Car, J. (2017). The humanistic and economic burden of chronic wounds: A protocol for a systematic review. *Systematic Reviews*, *6*(15). https://doi.org/10.1186/s13643-016-0400-8

Jeong, J. C., Lee, J., & Cho, K. (2003). Effects of crystalline microstructure on drug release behavior of poly(ε-caprolactone) microspheres. *Journal of Controlled Release*, *92*(3), 249–258. https://doi.org/10.1016/S0168-3659(03)00367-5

Kaczmarek, H., Sionkowska, A., Kamińska, A., Kowalonek, J., Świątek, M., & Szalla, A. (2001). The influence of transition metal salts on photo-oxidative degradation of poly(ethylene oxide). *Polymer Degradation and Stability*, *73*(3), 437–441. https://doi.org/10.1016/S0141-3910(01)00125-2

Kajdič, S., Planinšek, O., Gašperlin, M., & Kocbek, P. (2019). Electrospun nanofibers for customized drug-delivery systems. *Journal of Drug Delivery Science and Technology*, *51*, 672–681. https://doi.org/10.1016/J.JDDST.2019.03.038

Kajdič, S., Vrečer, F., & Kocbek, P. (2018). Preparation of poloxamer-based nanofibers for enhanced dissolution of carvedilol. *European Journal of Pharmaceutical Sciences*, *117*, 331–340. https://doi.org/10.1016/J.EJPS.2018.03.006

Kakkar, A. P., Singh, M., & Mendiratta, A. (1997). Isolation and characterization of Ciprofloxacin-HCL crystals. *Drug Development and Industrial Pharmacy*, *23*(11), 1063–1067. https://doi.org/10.3109/03639049709150494

Kamath, S. M., Sridhar, K., Jaison, D., Gopinath, V., Ibrahim, B. K. M., Gupta, N., Sundaram, A., Sivaperumal, P., Padmapriya, S., & Patil, S. S. (2020). Fabrication of tri-layered electrospun polycaprolactone mats with improved sustained drug release profile. *Scientific Reports 2020 10:1*, *10*(1), 1–13. https://doi.org/10.1038/s41598-020-74885-1

Kampf, G. (2016). Acquired resistance to chlorhexidine – is it time to establish an 'antiseptic stewardship' initiative? *Journal of Hospital Infection*, *94*(3), 213–227. https://doi.org/10.1016/j.jhin.2016.08.018

Karuppuswamy, P., Reddy Venugopal, J., Navaneethan, B., Luwang Laiva, A., & Ramakrishna, S. (2015). Polycaprolactone nanofibers for the controlled release of tetracycline hydrochloride. *Materials Letters*, *141*, 180–186. https://doi.org/10.1016/j.matlet.2014.11.044

Keshvardoostchokami, M., Majidi, S. S., Huo, P., Ramachandran, R., Chen, M., & Liu, B. (2020). Electrospun Nanofibers of Natural and Synthetic Polymers as Artificial Extracellular Matrix for Tissue Engineering. *Nanomaterials 2021, Vol. 11, Page 21*, *11*(1), 21. https://doi.org/10.3390/NANO11010021

Ko, S. W., Lee, J. Y., Lee, J., Son, B. C., Jang, S. R., Aguilar, L. E., Oh, Y. M., Park, C. H., & Kim, C. S. (2019). Analysis of drug release behavior utilizing the swelling characteristics of cellulosic nanofibers. *Polymers*, *11*(9). https://doi.org/10.3390/polym11091376

Kosmidis, K., Argyrakis, P., & Macheras, P. (2003a). A reappraisal of drug release laws using Monte Carlo simulations: The prevalence of the Weibull function. *Pharmaceutical Research*, *20*(7), 988–995. https://doi.org/10.1023/A:1024497920145

Kosmidis, K., Argyrakis, P., & Macheras, P. (2003b). Fractal kinetics in drug release from finite fractal matrices. *Journal of Chemical Physics*, *119*(12), 6373–6377. https://doi.org/10.1063/1.1603731

Kuang, G., Zhang, Z., Liu, S., Zhou, D., Lu, X., Jing, X., & Huang, Y. (2018). Biphasic drug release from electrospun polyblend nanofibers for optimized local cancer treatment. *Biomaterials Science*, *6*(2), 324–331. https://doi.org/10.1039/C7BM01018D

Kuzelova Kostakova, E., Meszaros, L., Maskova, G., Blazkova, L., Turcsan, T., & Lukas, D. (2017). Crystallinity of Electrospun and Centrifugal Spun Polycaprolactone Fibers: A Comparative Study. *Journal of Nanomaterials*, *2017*, 1–9. https://doi.org/10.1155/2017/8952390

Laheij, A. M. G. A., Soet, J. J. de, Veerman, E. C. I., Bolscher, J. G. M., & Loveren, C. van. (2013). The Influence of Oral Bacteria on Epithelial Cell Migration In Vitro. *Mediators of Inflammation*, *2013*. https://doi.org/10.1155/2013/154532

Laidmäe, I., Nieminen, H., Salmi, A., Paulin, T., Rauhala, T., Falk, K., Yliruusi, J., Heinämäki, J., Haeggström, E., & Veski, P. (2016). *Device and method to produce nanofibers and constructs thereof* (Patent No. PCT/FI2016/050170).

Lam, J., Chan, R., Lam, K., & Costerton, J. W. (1980). Production of mucoid microcolonies by Pseudomonas aeruginosa within infected lungs in cystic fibrosis. *Infection and Immunity*, *28*(2), 546–556. https://doi.org/10.1128/iai.28.2.546-556.1980

Lanno, G.-M., Ramos, C., Preem, L., Putrinš, M., Laidmäe, I., Tenson, T., & Kogermann, K. (2020). Antibacterial Porous Electrospun Fibers as Skin Scaffolds for Wound Healing Applications. *ACS Omega*, *5*(46), 30011–30022. https://doi.org/10.1021/ACSOMEGA.0C04402

Leaper, D., Assadian, O., & Edmiston, C. E. (2015). Approach to chronic wound infections. *British Journal of Dermatology*, *173*(2), 351–358. https://doi.org/10.1111/bjd.13677

Leaper, D. J., Schultz, G., Carville, K., Fletcher, J., Swanson, T., & Drake, R. (2012). Extending the TIME concept: What have we learned in the past 10 years? *International Wound Journal*, *9*(SUPPL. 2), 1–19. https://doi.org/10.1111/j.1742-481X.2012.01097.x

Lee, S. Y., Kuti, J. L., & Nicolau, D. P. (2005). Antimicrobial management of complicated skin and skin structure infections in the era of emerging resistance. *Surgical Infections*, *6*(3), 283–295. https://doi.org/10.1089/sur.2005.6.283

Lembach, A. N., Tan, H.-B., Roisman, I. V., Gambaryan-Roisman, T., Zhang, Y., Tropea, C., & Yarin, A. L. (2010). Drop Impact, Spreading, Splashing, and Penetration into Electrospun Nanofiber Mats. *Langmuir*, *26*(12), 9516–9523. https://doi.org/10.1021/LA100031D

Li, J. L., Cai, Y. L., Guo, Y. L., Fuh, J. Y. H., Sun, J., Hong, G. S., Lam, R. N., Wong, Y. S., Wang, W., Tay, B. Y., & Thian, E. S. (2014). Fabrication of three-dimensional porous scaffolds with controlled filament orientation and large pore size via an improved E-jetting technique. *Journal of Biomedical Materials Research B: Applied Biomaterials*, *102*(4), 651–658. https://doi.org/10.1002/jbm.b.33043

Li, T., Ding, X., Tian, L., Hu, J., Yang, X., & Ramakrishna, S. (2017). The control of beads diameter of bead-on-string electrospun nanofibers and the corresponding release behaviors of embedded drugs. *Materials Science and Engineering C*, *74*, 471–477. https://doi.org/10.1016/j.msec.2016.12.050

Li, Z., & Wang, C. C. (2013). Effects of Working Parameters on Electrospinning. In *One-Dimensional Nanostructures* (pp. 15–28). https://doi.org/10.1007/978-3-642-36427-3_2

Liao, N., Unnithan, A. R., Joshi, M. K., Tiwari, A. P., Hong, S. T., Park, C.-H., & Kim, C. S. (2015). Electrospun bioactive poly (ε-caprolactone)–cellulose acetate–dextran antibacterial composite mats for wound dressing applications. *Colloids and Surfaces A: Physicochemical and Engineering Aspects*, *469*, 194–201. https://doi.org/10.1016/j.colsurfa.2015.01.022

Lipsky, B. A., & Hoey, C. (2009). Topical antimicrobial therapy for treating chronic wounds. *Clinical Infectious Diseases*, *49*(10), 1541–1549. https://doi.org/10.1086/644732

Liu, X., Xu, H., Zhang, M., & Yu, D.-G. (2021). Electrospun Medicated Nanofibers for Wound Healing: Review. *Membranes*, *11*(10), 770. https://doi.org/10.3390/MEMBRANES11100770

Liu, Z., Ramakrishna, S., & Liu, X. (2020). Electrospinning and emerging healthcare and medicine possibilities. *APL Bioengineering*, *4*(3), 30901. https://doi.org/10.1063/5.0012309

Lowery, J. L., Datta, N., & Rutledge, G. C. (2010). Effect of fiber diameter, pore size and seeding method on growth of human dermal fibroblasts in electrospun poly(ε-caprolactone) fibrous mats. *Biomaterials*, *31*(3), 491–504. https://doi.org/10.1016/j.biomaterials.2009.09.072

Maker, J. H., Stroup, C. M., Huang, V., & James, S. F. (2019). Antibiotic Hypersensitivity Mechanisms. *Pharmacy: Journal of Pharmacy Education and Practice*, *7*(3), 122. https://doi.org/10.3390/PHARMACY7030122

Martínez-Alejo, J. M., Domínguez-Chávez, J. G., Rivera-Islas, J., Herrera-Ruiz, D., Höpfl, H., Morales-Rojas, H., & Senosiain, J. P. (2014). A Twist in Cocrystals of Salts: Changes in Packing and Chloride Coordination Lead to Opposite Trends in the Biopharmaceutical Performance of Fluoroquinolone Hydrochloride Cocrystals. *Crystal Growth and Design*, *14*(6), 3078–3095. https://doi.org/10.1021/CG500345A

McNamara, P. J., & Levy, S. B. (2016). Triclosan: An instructive tale. *Antimicrobial Agents and Chemotherapy*, *60*(12), 7015–7016. https://doi.org/10.1128/AAC.02105-16

Medical Device Coordination Group. (2021). *Guidance on classification of medical devices*. https://ec.europa.eu/health/sites/default/files/md_sector/docs/mdcg_2021-24_en.pdf

Megelski, S., Stephens, J. S., Chase, D. B., & Rabolt, J. F. (2002). Micro- and Nanostructured Surface Morphology on Electrospun Polymer Fibers. *Macromolecules*, *35*(22), 8456–8466. https://doi.org/10.1021/MA020444A

Mekkawy, A. I., El-Mokhtar, M. A., Nafady, N. A., Yousef, N., Hamad, M. A., El-Shanawany, S. M., Ibrahim, E. H., & Elsabahy, M. (2017). In vitro and in vivo evaluation of biologically synthesized silver nanoparticles for topical applications: effect of surface coating and loading into hydrogels. *International Journal of Nanomedicine*, *12*, 759–777. https://doi.org/10.2147/IJN.S124294

Melamed, S., Lalush, C., Elad, T., Yagur-Kroll, S., Belkin, S., & Pedahzur, R. (2012). A bacterial reporter panel for the detection and classification of antibiotic substances. *Microbial Biotechnology*, *5*(4), 536. https://doi.org/10.1111/J.1751-7915.2012.00333.X

Mele, E. (2016). Electrospinning of natural polymers for advanced wound care: Towards responsive and adaptive dressings. *Journal of Materials Chemistry B*, *4*(28), 4801–4812. https://doi.org/10.1039/c6tb00804f

Miyazawa, T., Fukushima, K., & Ideguchi, Y. (1962). Molecular vibrations and structure of high polymers. III. Polarized infrared spectra, normal vibrations, and helical conformation of polyethylene glycol. *The Journal of Chemical Physics*, *37*(12), 2764–2776. https://doi.org/10.1063/1.1733103

Mobley, H. L., Green, D. M., Trifillis, A. L., Johnson, D. E., Chippendale, G. R., Lockatell, C. V, Jones, B. D., & Warren, J. W. (1990). Pyelonephritogenic Escherichia coli and killing of cultured human renal proximal tubular epithelial cells: role of hemolysin in some strains. *Infection and Immunity*, *58*(5), 1281–1289. https://doi.org/https://doi.org/10.1128/iai.58.5.1281-1289.1990

Molnar, K., & Nagy, Z. K. (2016). Corona-electrospinning: Needleless method for high-throughput continuous nanofiber production. *European Polymer Journal*, *74*, 279–286. https://doi.org/10.1016/J.EURPOLYMJ.2015.11.028

Mordor Intelligence. (2020). *Nanofiber Market | 2021 – 26 | Industry Share, Size, Growth*. https://www.mordorintelligence.com/industry-reports/nanofiber-market

Morent, R., De Geyter, N., Desmet, T., Dubruel, P., & Leys, C. (2011). Plasma Surface Modification of Biodegradable Polymers: A Review. *Plasma Processes and Polymers*, *8*(3), 171–190. https://doi.org/10.1002/ppap.201000153

Mucha, M., Tylman, M., & Mucha, J. (2015). Crystallization kinetics of polycaprolactone in nanocomposites. *Polimery*, *61*(11/12), 686–692. https://doi.org/10.14314/polimery.2015.686

Munj, H. R., Lannutti, J. J., & Tomasko, D. L. (2017). Understanding drug release from PCL/gelatin electrospun blends. *Journal of Biomaterials Applications*, *31*(6), 933–949. https://doi.org/10.1177/0885328216673555

Munson, E. J. (2009). Analytical Techniques in Solid-state Characterization. In *Developing Solid Oral Dosage Forms* (pp. 61–74). Academic Press. https://doi.org/10.1016/B978-0-444-53242-8.00003-5

Murugan, R., & Ramakrishna, S. (2006). Nano-Featured Scaffolds for Tissue Engineering: A Review of Spinning Methodologies. *Tissue Engineering*, *12*(3), 435–447. https://doi.org/10.1089/ten.2006.12.435

Nada, A. A., Hassabo, A. G., Mohamed, A. L., & Zaghloul, S. (2016). Encapsulation of nicotinamide into cellulose based electrospun fibers. *Journal of Applied Pharmaceutical Science*, *6*(8), 13–21. https://doi.org/10.7324/JAPS.2016.60803

Natu, M. V., de Sousa, H. C., & Gil, M. H. (2010). Effects of drug solubility, state and loading on controlled release in bicomponent electrospun fibers. *International Journal of Pharmaceutics*, *397*(1–2), 50–58. https://doi.org/10.1016/J.IJPHARM.2010.06.045

Nazemi, K., Moztarzadeh, F., Jalali, N., Asgari, S., & Mozafari, M. (2014). Synthesis and characterization of poly(lactic-co-glycolic) acid nanoparticles-loaded chitosan/bioactive glass scaffolds as a localized delivery system in the bone defects. *BioMed Research International*, 898930. https://doi.org/10.1155/2014/898930

Neidhardt, F. C., Bloch, P. L., & Smith, D. F. (1974). Culture medium for enterobacteria. *Journal of Bacteriology*, *119*(3), 736–747. https://doi.org/10.1128/jb.119.3.736-747.1974

Nguyen, T. T. T., Ghosh, C., Hwang, S. G., Chanunpanich, N., & Park, J. S. (2012). Porous core/sheath composite nanofibers fabricated by coaxial electrospinning as a potential mat for drug release system. *International Journal of Pharmaceutics*, *439*(1–2), 296–306. https://doi.org/10.1016/J.IJPHARM.2012.09.019

Nikmaram, N., Roohinejad, S., Hashemi, S., Koubaa, M., Barba, F. J., Abbaspourrad, A., & Greiner, R. (2017). Emulsion-based systems for fabrication of electrospun nanofibers: food, pharmaceutical and biomedical applications. *RSC Advances*, *7*(46), 28951–28964. https://doi.org/10.1039/C7RA00179G

Nussbaum, S. R., Carter, M. J., Fife, C. E., DaVanzo, J., Haught, R., Nusgart, M., & Cartwright, D. (2018). An Economic Evaluation of the Impact, Cost, and Medicare Policy Implications of Chronic Nonhealing Wounds. *Value in Health*, *21*(1), 27–32. https://doi.org/10.1016/J.JVAL.2017.07.007

Oates, A., Bowling, F. L., Boulton, A. J. M., Bowler, P. G., Metcalf, D. G., & McBain, A. J. (2014). The visualization of biofilms in chronic diabetic foot wounds using

routine diagnostic microscopy methods. *Journal of Diabetes Research*, 153586. https://doi.org/10.1155/2014/153586

Ochoa Machiste, E., Segale, L., Conti, S., Fasani, E., Albini, A., Conte, U., & Maggi, L. (2005). Effect of UV light exposure on hydrophilic polymers used as drug release modulators in solid dosage forms. *Journal of Drug Delivery Science and Technology*, *15*(2), 151–157. https://doi.org/10.1016/S1773-2247(05)50020-0

Odelius, K., Plikk, P., & Albertsson, A.-C. (2008). The influence of composition of porous copolyester scaffolds on reactions induced by irradiation sterilization. *Biomaterials*, *29*(2), 129–140. https://doi.org/10.1016/J.BIOMATERIALS.2007.08.046

Okuda, T., Tominaga, K., & Kidoaki, S. (2010). Time-programmed dual release formulation by multilayered drug-loaded nanofiber meshes. *Journal of Controlled Release*, *143*(2), 258–264. https://doi.org/10.1016/J.JCONREL.2009.12.029

Oliveira, J. E., Mattoso, L. H. C., Orts, W. J., & Medeiros, E. S. (2013). Structural and Morphological Characterization of Micro and Nanofibers Produced by Electrospinning and Solution Blow Spinning : A Comparative Study. *Advances in Materials Science and Engineering*, *2013*, 1–14. https://doi.org/10.1155/2013/409572

Olivera, M. E., Manzo, R. H., Junginger, H. E., Midha, K. K., Shah, V. P., Stavchansky, S., Dressman, J. B., & Barends, D. M. (2011). Biowaiver Monographs for Immediate Release Solid Oral Dosage Forms: Ciprofloxacin Hydrochloride. *Journal of Pharmaceutical Sciences*, *100*(1), 22–33. https://doi.org/10.1002/JPS.22259

Omer, S., Forgách, L., Zelkó, R., & Sebe, I. (2021). Scale-up of Electrospinning: Market Overview of Products and Devices for Pharmaceutical and Biomedical Purposes. *Pharmaceutics*, *13*(2), 1–21. https://doi.org/10.3390/PHARMACEUTICS13020286

Ousey, K., & McIntosh, C. (2010). Understanding wound bed preparation and wound debridement. *British Journal of Community Nursing*, *15*(12 SUPPL.). https://doi.org/10.12968/bjcn.2010.15.Sup12.S22

Ovington, L. (2003). Bacterial toxins and wound healing. *Ostomy Wound Management*, *49*(7 A Suppl), 8–12.

Paaver, U., Heinämäki, J., Laidmäe, I., Lust, A., Kozlova, J., Sillaste, E., Kirsimäe, K., Veski, P., & Kogermann, K. (2015). Electrospun nanofibers as a potential controlled-release solid dispersion system for poorly water-soluble drugs. *International Journal of Pharmaceutics*, *479*(1), 252–260. https://doi.org/10.1016/j.ijpharm.2014.12.024

Papadopoulou, V., Kosmidis, K., Vlachou, M., & Macheras, P. (2006). On the use of the Weibull function for the discernment of drug release mechanisms. *International Journal of Pharmaceutics*, *309*(1), 44–50. https://doi.org/10.1016/j.ijpharm.2005.10.044

Paskiabi, F. A., Bonakdar, S., Shokrgozar, M. A., Imani, M., Jahanshiri, Z., Shams-Ghahfarokhi, M., & Razzaghi-Abyaneh, M. (2017). Terbinafine-loaded wound dressing for chronic superficial fungal infections. *Materials Science and Engineering: C*, *73*, 130–136. https://doi.org/10.1016/J.MSEC.2016.12.078

Pavicic, M. J. A. M. P., Van Winkelhoff, A. J., & De Graaff, J. (1991). Synergistic effects between amoxicillin, metronidazole, and the hydroxymetabolite of metronidazole against Actinobacillus actinomycetemcomitans. *Antimicrobial Agents and Chemotherapy*, *35*(5), 961–966. https://doi.org/10.1128/AAC.35.5.961

Pelipenko, J., Kristl, J., Janković, B., Baumgartner, S., & Kocbek, P. (2013). The impact of relative humidity during electrospinning on the morphology and mechanical

properties of nanofibers. *International Journal of Pharmaceutics*, *456*(1), 125–134. https://doi.org/10.1016/J.IJPHARM.2013.07.078

Percival, N. J. (2002). Classification of Wounds and their Management. *Surgery*, *20*(5), 114–117. https://doi.org/10.1383/SURG.20.5.114.14626

Percival, S. L., & Suleman, L. (2015). Slough and biofilm: Removal of barriers to wound healing by desloughing. *Journal of Wound Care*, *24*(11), 498–510. https://doi.org/10.12968/jowc.2015.24.11.498

Percival, Steven L., Mayer, D., Kirsner, R. S., Schultz, G., Weir, D., Roy, S., Alavi, A., & Romanelli, M. (2019). Surfactants: Role in biofilm management and cellular behaviour. *International Wound Journal*, *16*(3), 753–760. https://doi.org/10.1111/IWJ.13093

Percival, Steven L, McCarty, S. M., & Lipsky, B. (2015). Biofilms and Wounds: An Overview of the Evidence. *Advances in Wound Care*, *4*(7), 373–381. https://doi.org/10.1089/wound.2014.0557

Petlin, D. G., Amarah, A. A., Tverdokhlebov, S. I., & Anissimov, Y. G. (2017). A fiber distribution model for predicting drug release rates. *Journal of Controlled Release*, *258*, 218–225. https://doi.org/10.1016/J.JCONREL.2017.05.021

Phillips, C. J., Humphreys, I., Fletcher, J., Harding, K., Chamberlain, G., & Macey, S. (2016). Estimating the costs associated with the management of patients with chronic wounds using linked routine data. *International Wound Journal*, *13*(6), 1193–1197. https://doi.org/10.1111/iwj.12443

Pillay, V., Dott, C., Choonara, Y. E., Tyagi, C., Tomar, L., Kumar, P., Du Toit, L. C., & Ndesendo, V. M. K. (2013). A review of the effect of processing variables on the fabrication of electrospun nanofibers for drug delivery applications. *Journal of Nanomaterials*, *2013*, 1–22. https://doi.org/10.1155/2013/789289

Preem, L., Mahmoudzadeh, M., Putrinš, M., Meos, A., Laidmäe, I., Romann, T., Aruväli, J., Härmas, R., Koivuniemi, A., Bunker, A., Tenson, T., & Kogermann, K. (2017). Interactions between Chloramphenicol, Carrier Polymers, and Bacteria-Implications for Designing Electrospun Drug Delivery Systems Countering Wound Infection. *Molecular Pharmaceutics*, *14*(12). https://doi.org/10.1021/acs.molpharmaceut.7b00524

Preem, Liis, & Kogermann, K. (2018). Electrospun Antimicrobial Wound Dressings: Novel Strategies to Fight Against Wound Infections. In *Chronic Wounds, Wound Dressings and Wound Healing* (pp. 213–253). Springer, Cham. https://doi.org/10.1007/15695_2018_133

Rainer, A., Centola, M., Spadaccio, C., Gherardi, G., Genovese, J. A., Licoccia, S., & Trombetta, M. (2010). Comparative study of different techniques for the sterilization of poly-L-lactide electrospun microfibers: effectiveness vs. material degradation. *The International Journal of Artificial Organs*, *33*(2), 76–85. https://doi.org/10.1177/039139881003300203

Rambhia, K. J., & Ma, P. X. (2015). Controlled drug release for tissue engineering. *Journal of Controlled Release*, *219*, 119–128. https://doi.org/10.1016/j.jconrel.2015.08.049

Ramos, C., Lanno, G. M., Laidmäe, I., Meos, A., Härmas, R., & Kogermann, K. (2021). High humidity electrospinning of porous fibers for tuning the release of drug delivery systems. *International Journal of Polymeric Materials and Polymeric Biomaterials*, *70*(12), 880–892. https://doi.org/10.1080/00914037.2020.1765361

Rediguieri, Camila F., Porta, V., Diana, D. S., Nunes, T. M., Junginger, H. E., Kopp, S., Midha, K. K., Shah, V. P., Stavchansky, S., Dressman, J. B., & Barends, D. M.

(2011). Biowaiver Monographs for Immediate Release Solid Oral Dosage Forms: Metronidazole. *Journal of Pharmaceutical Sciences*, *100*(5), 1618–1627. https://doi.org/10.1002/JPS.22409

Rediguieri, Carolina Fracalossi, Sassonia, R. C., Dua, K., Kikuchi, I. S., & de Jesus Andreoli Pinto, T. (2016). Impact of sterilization methods on electrospun scaffolds for tissue engineering. *European Polymer Journal*, *82*, 181–195. https://doi.org/10.1016/j.eurpolymj.2016.07.016

Reneker, D. H., & Yarin, A. L. (2008). Electrospinning jets and polymer nanofibers. *Polymer*, *49*(10), 2387–2425. https://doi.org/10.1016/J.POLYMER.2008.02.002

Rhoads, D. D., Wolcott, R. D., & Percival, S. L. (2008). Biofilms in wounds: management strategies. *Journal of Wound Care*, *17*(11), 502–508. https://doi.org/http://dx.doi.org/10.12968/jowc.2008.17.11.31479

Rhoads, D. D., Wolcott, R. D., Sun, Y., & Dowd, S. E. (2012). Comparison of Culture and Molecular Identification of Bacteria in Chronic Wounds. *International Journal of Molecular Sciences*, *13*(3), 2535–2550. https://doi.org/10.3390/IJMS13032535

Rieger, K. A., Birch, N. P., & Schiffman, J. D. (2013). Designing electrospun nanofiber mats to promote wound healing – a review. *Journal of Materials Chemistry B*, *1*(36), 4531. https://doi.org/10.1039/c3tb20795a

Roberts, C. D., Leaper, D. J., & Assadian, O. (2017). The Role of Topical Antiseptic Agents Within Antimicrobial Stewardship Strategies for Prevention and Treatment of Surgical Site and Chronic Open Wound Infection. *Advances in Wound Care*, *6*(2), 63–71. https://doi.org/10.1089/wound.2016.0701.

Rocco, A. M., Da Fonseca, C. P., & Pereira, R. P. (2002). A polymeric solid electrolyte based on a binary blend of poly(ethylene oxide), poly(methyl vinyl ether-maleic acid) and LiClO4. *Polymer*, *43*(13), 3601–3609. https://doi.org/10.1016/S0032-3861(02)00173-8

Rutledge, G. C., Lowery, J. L., & Pai, C. (2009). Characterization by Mercury Porosimetry of Nonwoven Fiber Media with Deformation. *Journal of Engineered Fibers and Fabrics*, *4*(3), 1–13. https://doi.org/10.1177/155892500900400301

Ruzicka, T., Seegräber, M., Bieber, T., Homey, B., Riordain, R. N. I., Madsen, L. S., & Hansen, J. (2018). The Rivelin Patch – A New Treatment Strategy for Oral Lichen Planus. *Oral Surgery, Oral Medicine, Oral Pathology and Oral Radiology*, *126*(4), e204. https://doi.org/10.1016/J.OOOO.2018.05.038

Sadri, M., Mohammadi, A., & Hosseini, H. (2016). Drug release rate and kinetic investigation of composite polymeric nanofibers. *Nanomedicine Research Journal*, *1*(2), 112–121. https://doi.org/10.7508/NMRJ.2016.02.008

Sahoo, S., Chakraborti, C. K., & Mishra, S. C. (2011). Qualitative analysis of controlled release ciprofloxacin/carbopol 934 mucoadhesive suspension. *Journal of Advanced Pharmaceutical Technology & Research*, *2*(3), 195–204. https://doi.org/10.4103/2231-4040.85541

Said, S. S., Aloufy, A. K., El-Halfawy, O. M., Boraei, N. A., & El-Khordagui, L. K. (2011). Antimicrobial PLGA ultrafine fibers: interaction with wound bacteria. *European Journal of Pharmaceutics and Biopharmaceutics*, *79*(1), 108–118. https://doi.org/10.1016/j.ejpb.2011.03.002

Sajan, D., Sockalingum, G. D., Manfait, M., Hubert Joe, I., & Jayakumar, V. S. (2008). NIR-FT Raman, FT-IR and surface-enhanced Raman scattering spectra, with theoretical simulations on chloramphenicol. *Journal of Raman Spectroscopy*, *39*(12), 1772–1783. https://doi.org/10.1002/jrs.2033

Sambrook, J., & D, R. (Eds.). (2001). *Molecular Cloning: A Laboratory Manual, 3rd ed* (3rd ed.). Cold Spring Harbor Laboratory Press. www.cshlpress.org

Schierle, C. F., De la Garza, M., Mustoe, T. A., & Galiano, R. D. (2009). Staphylococcal biofilms impair wound healing by delaying reepithelialization in a murine cutaneous wound model. *Wound Repair and Regeneration*, *17*(3), 354–359. https://doi.org/10.1111/j.1524-475X.2009.00489.x

Schraibman, I. G. (1990). The significance of beta-haemolytic streptococci in chronic leg ulcers. *Annals of The Royal College of Surgeons of England*, *72*(2), 123.

Seif, S., Franzen, L., & Windbergs, M. (2015). Overcoming drug crystallization in electrospun fibers – Elucidating key parameters and developing strategies for drug delivery. *International Journal of Pharmaceutics*, *478*(1), 390–397. https://doi.org/10.1016/J.IJPHARM.2014.11.045

Shahriar, S. M. S., Mondal, J., Hasan, M. N., Revuri, V., Lee, D. Y., & Lee, Y.-K. (2019). Electrospinning Nanofibers for Therapeutics Delivery. *Nanomaterials 2019, Vol. 9, Page 532*, *9*(4), 532. https://doi.org/10.3390/NANO9040532

Shi, R., Geng, H., Gong, M., Ye, J., Wu, C., Hu, X., & Zhang, L. (2018). Long-acting and broad-spectrum antimicrobial electrospun poly (ε-caprolactone)/gelatin micro/nanofibers for wound dressing. *Journal of Colloid and Interface Science*, *509*, 275–284. https://doi.org/10.1016/j.jcis.2017.08.092

Si, M. Z., Kang, Y. P., & Zhang, Z. G. (2009). Surface-enhanced Raman scattering (SERS) spectra of chloramphenicol in Ag colloids prepared by microwave heating method. *Journal of Raman Spectroscopy*, *40*(9), 1319–1323. https://doi.org/10.1002/jrs.2286

Siddiqui, A. R., & Bernstein, J. M. (2010). Chronic wound infection: Facts and controversies. *Clinics in Dermatology*, *28*(5), 519–526. https://doi.org/10.1016/j.clindermatol.2010.03.009

Sill, T. J., & von Recum, H. A. (2008). Electrospinning: Applications in drug delivery and tissue engineering. *Biomaterials*, *29*(13), 1989–2006. https://doi.org/10.1016/J.BIOMATERIALS.2008.01.011

Singh, R., Ahmed, F., Polley, P., & Giri, J. (2018). Fabrication and Characterization of Core–Shell Nanofibers Using a Next-Generation Airbrush for Biomedical Applications. *ACS Applied Materials & Interfaces*, *10*(49), 41924–41934. https://doi.org/10.1021/ACSAMI.8B13809

Širc, J., Hobzová, R., Kostina, N., Munzarová, M., Juklíčková, M., Lhotka, M., Kubinová, Š., Zajícová, A., & Michálek, J. (2012). Morphological characterization of nanofibers: Methods and application in practice. *Journal of Nanomaterials*, *2012*, 1–14. https://doi.org/10.1155/2012/327369

Slots, J. (2004). Systemic Antibiotics in Periodontics. *Journal of Periodontology*, *75*(11), 1553–1565. https://doi.org/10.1902/jop.2004.75.11.1553

Smith, G. P. S., McLaughlin, A. W., Clarkson, A. N., Gordon, K. C., & Walker, G. F. (2017). Raman microscopic imaging of electrospun fibers made from a polycaprolactone and polyethylene oxide blend. *Vibrational Spectroscopy*, *92*, 27–34. https://doi.org/10.1016/J.VIBSPEC.2017.05.002

Socransky, S. S., & Haffajee, A. D. (2005). Periodontal microbial ecology. *Periodontology 2000*, *38*, 135–187. https://doi.org/10.1111/j.1600-0757.2005.00107.x

Sønderholm, M., Kragh, K. N., Koren, K., Jakobsen, T. H., Darch, S. E., Alhede, M., Jensen, P. Ø., Whiteley, M., Kühl, M., & Bjarnsholt, T. (2017). Pseudomonas aeruginosa Aggregate Formation in an Alginate Bead Model System Exhibits In

Vivo-Like Characteristics. *Applied and Environmental Microbiology*, *83*(9). https://doi.org/10.1128/AEM.00113-17

Steed, D. L., Donohoe, D., Webster, M. W., & Lindsley, L. (1996). Effect of extensive debridement and treatment on the healing of diabetic foot ulcers. *Journal of the American College of Surgeons*, *183*(1), 61–64.

Stewart, P. S., Costerton, J. W., Koga, T., Kawada, H., Yokota, T., & Usui, T. (2001). Antibiotic resistance of bacteria in biofilms. *The Lancet*, *358*(9276), 135–138. https://doi.org/10.1016/S0140-6736(01)05321-1

Sultanova, Z., Kaleli, G., Kabay, G., & Mutlu, M. (2016). Controlled release of a hydrophilic drug from coaxially electrospun polycaprolactone nanofibers. *International Journal of Pharmaceutics*, *505*(1), 133–138. https://doi.org/10.1016/j.ijpharm.2016.03.032

Sun, L., Gao, W., Fu, X., Shi, M., Xie, W., Zhang, W., Zhao, F., & Chen, X. (2018). Enhanced wound healing in diabetic rats by nanofibrous scaffolds mimicking the basketweave pattern of collagen fibrils in native skin. *Biomaterials Science*. https://doi.org/10.1039/C7BM00545H

Sun, Z., Zussman, E., Yarin, A. L., Wendorff, J. H., & Greiner, A. (2003). Compound Core–Shell Polymer Nanofibers by Co-Electrospinning. *Advanced Materials*, *15*(22), 1929–1932. https://doi.org/10.1002/adma.200305136

Sun, Zhaoyang, Fan, C., Tang, X., Zhao, J., Song, Y., Shao, Z., & Xu, L. (2016). Characterization and antibacterial properties of porous fibers containing silver ions. *Applied Surface Science*, *387*, 828–838. https://doi.org/10.1016/j.apsusc.2016.07.015

Supe, S., & Takudage, P. (2021). Methods for evaluating penetration of drug into the skin: A review. *Skin Research and Technology*, *27*(3), 299–308. https://doi.org/10.1111/SRT.12968

Szakonyi, G., & Zelkó, R. (2012). The effect of water on the solid state characteristics of pharmaceutical excipients: Molecular mechanisms, measurement techniques, and quality aspects of final dosage form. *International Journal of Pharmaceutical Investigation*, *2*(1), 18–25. https://doi.org/10.4103/2230-973X.96922

Szewczyk, P. K., & Stachewicz, U. (2020). The impact of relative humidity on electrospun polymer fibers: From structural changes to fiber morphology. *Advances in Colloid and Interface Science*, *286*, 102315. https://doi.org/10.1016/J.CIS.2020.102315

Tamm, I., Heinämäki, J., Laidmäe, I., Rammo, L., Paaver, U., Ingebrigtsen, S. G., Škalko-Basnet, N., Halenius, A., Yliruusi, J., Pitkänen, P., Alakurtti, S., & Kogermann, K. (2016). Development of Suberin Fatty Acids and Chloramphenicol-Loaded Antimicrobial Electrospun Nanofibrous Mats Intended for Wound Therapy. *Journal of Pharmaceutical Sciences*, *105*(3), 1239–1247. https://doi.org/10.1016/j.xphs.2015.12.025

Tan, Z., Tan, F., Zhao, L., & Li, J. (2012). The Synthesis, Characterization and Application of Ciprofloxacin Complexes and Its Coordination with Copper, Manganese and Zirconium Ions. *Journal of Crystallization Process and Technology*, *02*(02), 55–63. https://doi.org/10.4236/jcpt.2012.22008

Teo, W.-E., Inai, R., & Ramakrishna, S. (2011). Technological advances in electrospinning of nanofibers. *Science and Technology of Advanced Materials*, *12*(1). https://doi.org/10.1088/1468-6996/12/1/11660944

Thakkar, S., & Misra, M. (2017). Electrospun polymeric nanofibers: New horizons in drug delivery. *European Journal of Pharmaceutical Sciences*, *107*(May), 148–167. https://doi.org/10.1016/j.ejps.2017.07.001

Theocharis, A. D., Skandalis, S. S., Gialeli, C., & Karamanos, N. K. (2016). Extracellular matrix structure. *Advanced Drug Delivery Reviews*, *97*, 4–27. https://doi.org/10.1016/J.ADDR.2015.11.001

Toma, A. I., Fuller, J. M., Willett, N. J., & Goudy, S. L. (2021). Oral wound healing models and emerging regenerative therapies. *Translational Research*, *236*, 17–34. https://doi.org/10.1016/J.TRSL.2021.06.003

Tsekova, P. B., Spasova, M. G., Manolova, N. E., Markova, N. D., & Rashkov, I. B. (2017). Electrospun curcumin-loaded cellulose acetate/polyvinylpyrrolidone fibrous materials with complex architecture and antibacterial activity. *Materials Science and Engineering: C*, *73*, 206–214. https://doi.org/10.1016/j.msec.2016.12.086

Unnithan, A. R., Gnanasekaran, G., Sathishkumar, Y., Lee, Y. S., & Kim, C. S. (2014). Electrospun antibacterial polyurethane-cellulose acetate-zein composite mats for wound dressing. *Carbohydrate Polymers*, *102*(1), 884–892. https://doi.org/10.1016/j.carbpol.2013.10.070

Ushiki, T. (2002). Collagen fibers, reticular fibers and elastic fibers. A comprehensive understanding from a morphological viewpoint. *Archives of Histology and Cytology*, *65*(2), 109–126. https://doi.org/10.1679/AOHC.65.109

Valente, T. A. M., Silva, D. M., Gomes, P. S., Fernandes, M. H., Santos, J. D., & Sencadas, V. (2016). Effect of sterilization methods on electrospun poly(lactic acid) (PLA) fiber alignment for biomedical applications. *ACS Applied Materials and Interfaces*, *8*(5), 3241–3249. https://doi.org/10.1021/acsami.5b10869

Vasireddi, R., Kruse, J., Vakili, M., Kulkarni, S., Keller, T. F., Monteiro, D. C. F., & Trebbin, M. (2019). Solution blow spinning of polymer/nanocomposite micro-/nanofibers with tunable diameters and morphologies using a gas dynamic virtual nozzle. *Scientific Reports 2019 9:1*, *9*(1), 1–10. https://doi.org/10.1038/s41598-019-50477-6

Vasita, R., & Katti, D. S. (2006). Nanofibers and their applications in tissue engineering. *International Journal of Nanomedicine*, *1*(1), 15–30. https://doi.org/10.2147/nano.2006.1.1.15

Verreck, G., Chun, I., Peeters, J., Rosenblatt, J., & Brewster, M. E. (2003). Preparation and characterization of nanofibers containing amorphous drug dispersions generated by electrostatic spinning. *Pharmaceutical Research*, *20*(5), 810–817. https://doi.org/10.1023/A:1023450006281

Vineis, C., & Varesano, A. (2018). Natural polymer-based electrospun fibers for antibacterial uses. *Electrofluidodynamic Technologies (EFDTs) for Biomaterials and Medical Devices: Principles and Advances*, 275–294. https://doi.org/10.1016/B978-0-08-101745-6.00014-1

Vonasek, E., Lu, P., Hsieh, Y.-L., & Nitin, N. (2017). Bacteriophages immobilized on electrospun cellulose microfibers by non-specific adsorption, protein–ligand binding, and electrostatic interactions. *Cellulose 2017 24:10*, *24*(10), 4581–4589. https://doi.org/10.1007/S10570-017-1442-3

Wang, J., & Windbergs, M. (2018). Influence of polymer composition and drug loading procedure on dual drug release from PLGA:PEG electrospun fibers. *European Journal of Pharmaceutical Sciences*, *124*, 71–79. https://doi.org/10.1016/J.EJPS.2018.08.028

Wang, K., Liu, X.-K., Chen, X.-H., Yu, D.-G., Yang, Y.-Y., & Liu, P. (2018). Electrospun Hydrophilic Janus Nanocomposites for the Rapid Onset of Therapeutic Action of Helicid. *ACS Applied Materials and Interfaces*, *10*(3), 2859–2867. https://doi.org/10.1021/ACSAMI.7B17663

Wang, T., & Kumar, S. (2006). Electrospinning of polyacrylonitrile nanofibers. *Journal of Applied Polymer Science*, *102*(2), 1023–1029. https://doi.org/10.1002/APP.24123

Wang, X., Zhao, H., Turng, L. S., & Li, Q. (2013). Crystalline morphology of electrospun poly(ε-caprolactone) (PCL) nanofibers. *Industrial and Engineering Chemistry Research*, *52*(13). https://doi.org/10.1021/ie302185e

Wang, Y., Qiao, W., Wang, B., Zhang, Y., Shao, P., & Yin, T. (2011). Electrospun composite nanofibers containing nanoparticles for the programmable release of dual drugs. *Polymer Journal 2011 43:5*, *43*(5), 478–483. https://doi.org/10.1038/pj.2011.11

Wei, Q. (2012). *Functional nanofibers and their applications* (W. Qufu (Ed.)). Woodhead Publishing Limited, 2012.

Weiser, J. R., & Saltzman, W. M. (2014). Controlled release for local delivery of drugs: barriers and models. *Journal of Controlled Release*, *190*, 664–673. https://doi.org/10.1016/J.JCONREL.2014.04.048

Williamson, D. A., Carter, G. P., & Howden, B. P. (2017). Current and emerging topical antibacterials and antiseptics: Agents, action, and resistance patterns. In *Clinical Microbiology Reviews* (Vol. 30, Issue 3, pp. 827–860). Clin Microbiol Rev. https://doi.org/10.1128/CMR.00112-16

Winter, G. D. (1962). Formation of the scab and the rate of epithelization of superficial wounds in the skin of the young domestic pig. *Nature*, *193*, 293–294.

Wolcott, R. D., Kennedy, J. P., & Dowd, S. E. (2009). Regular debridement is the main tool for maintaining a healthy wound bed in most chronic wounds. *Journal of Wound Care*, *18*(2), 54–56. https://doi.org/10.12968/jowc.2009.18.2.38743

Wolcott, R. D., Rumbaugh, K. P., James, G., Schultz, G., Phillips, P., Yang, Q., Watters, C., Stewart, P. S., & Dowd, S. E. (2010). Biofilm maturity studies indicate sharp debridement opens a time-dependent therapeutic window. *Journal of Wound Care*, *19*(8), 320–328. https://doi.org/10.12968/jowc.2010.19.8.77709

Wong, S.-C., Baji, A., & Leng, S. (2008). Effect of fiber diameter on tensile properties of electrospun poly(ε-caprolactone). *Polymer*, *49*(21), 4713–4722. https://doi.org/10.1016/j. polymer.2008.08.022

Wu, J., Zhang, Z., Gu, J., Zhou, W., Liang, X., Zhou, G., Han, C. C., Xu, S., & Liu, Y. (2020). Mechanism of a long-term controlled drug release system based on simple blended electrospun fibers. *Journal of Controlled Release*, *320*, 337–346. https://doi.org/10.1016/J.JCONREL.2020.01.020

Xie, Z., & Buschle-Diller, G. (2010). Electrospun poly(D,L-lactide) fibers for drug delivery: The influence of cosolvent and the mechanism of drug release. *Journal of Applied Polymer Science*, *115*(1), 1–8. https://doi.org/10.1002/app.31026

Xu, X., Wang, H., Jiang, L., Wang, X., Payne, S. A., Zhu, J. Y., & Li, R. (2014). Comparison between cellulose nanocrystal and cellulose nanofibril reinforced poly(ethylene oxide) nanofibers and their novel shish-kebab-like crystalline structures. *Macromolecules*, *47*(10), 3409–3416. https://doi.org/10.1021/ma402627j

Xue, J., He, M., Niu, Y., Liu, H., Crawford, A., Coates, P., Chen, D., Shi, R., & Zhang, L. (2014). Preparation and in vivo efficient anti-infection property of GTR/GBR implant made by metronidazole loaded electrospun polycaprolactone nanofiber

membrane. *International Journal of Pharmaceutics*, *475*(1), 566–577. https://doi.org/10.1016/j.ijpharm.2014.09.026

Yang, G., Li, X., He, Y., Ma, J., Ni, G., & Zhou, S. (2018). From nano to micro to macro: Electrospun hierarchically structured polymeric fibers for biomedical applications. *Progress in Polymer Science*, *81*, 80–113. https://doi.org/10.1016/J.PROGPOLYMSCI.2017.12.003

Yang, J., Wang, K., Yu, D. G., Yang, Y., Bligh, S. W. A., & Williams, G. R. (2020). Electrospun Janus nanofibers loaded with a drug and inorganic nanoparticles as an effective antibacterial wound dressing. *Materials Science and Engineering: C*, *111*, 110805. https://doi.org/10.1016/J.MSEC.2020.110805

Yang, L., Chen, J., & Gao, J. (2009). Low temperature argon plasma sterilization effect on Pseudomonas aeruginosa and its mechanisms. *Journal of Electrostatics*, *67*(4), 646–651. https://doi.org/10.1016/J.ELSTAT.2009.01.060

Yang, T., Sun, X., Ren, Z., Li, H., & Yan, S. (2014). Crystallizability of poly(ε-caprolactone) blends with poly(vinylphenol) under different conditions. *Chinese Journal of Polymer Science*, *32*(9), 1119–1127. https://doi.org/10.1007/s10118-014-1492-z

Yarin, A. L. (2011). Coaxial electrospinning and emulsion electrospinning of core-shell fibers. *Polymers for Advanced Technologies*, *22*(3), 310–317. https://doi.org/10.1002/ pat.1781

Yarin, A. L., & Zussman, E. (2004). Upward needleless electrospinning of multiple nanofibers. *Polymer*, *45*(9), 2977–2980. https://doi.org/10.1016/j.polymer.2004.02.066

Yohe, S. T., Colson, Y. L., & Grinstaff, M. W. (2012). Superhydrophobic materials for tunable drug release: Using displacement of air to control delivery rates. *Journal of the American Chemical Society*, *134*(4), 2016–2019. https://doi.org/10.1021/ja211148a

Zahedi, P., Rezaeian, I., Ranaei-Siadat, S.-O., Jafari, S.-H., & Supaphol, P. (2009). A review on wound dressings with an emphasis on electrospun nanofibrous polymeric bandages. *Polymers for Advanced Technologies*, *21*(2). https://doi.org/10.1002/pat.1625

Zamani, M., Prabhakaran, M. P., & Ramakrishna, S. (2013). Advances in drug delivery via electrospun and electrosprayed nanomaterials. *International Journal of Nanomedicine*, *8*, 2997–3017. https://doi.org/10.2147/IJN.S43575

Zargham, S., Bazgir, S., Tavakoli, A., Rashidi, A. S., & Damerchely, R. (2012). The effect of flow rate on morphology and deposition area of electrospun nylon 6 nanofiber. *Journal of Engineered Fibers and Fabrics*, *7*(4), 42–49. https://doi.org/10.1177/155892501200700414

Zdarta, J., Jankowska, K., Wyszowska, M., Kijeńska-Gawrońska, E., Zgoła-Grześkowiak, A., Pinelo, M., Meyer, A. S., Moszyński, D., & Jesionowski, T. (2019). Robust biodegradation of naproxen and diclofenac by laccase immobilized using electrospun nanofibers with enhanced stability and reusability. *Materials Science and Engineering: C*, *103*, 109789. https://doi.org/10.1016/J.MSEC.2019. 109789

Zeng, J., Yang, L., Liang, Q., Zhang, X., Guan, H., Xu, X., Chen, X., & Jing, X. (2005). Influence of the drug compatibility with polymer solution on the release kinetics of electrospun fiber formulation. *Journal of Controlled Release*, *105*(1–2), 43–51. https://doi.org/10.1016/J.JCONREL.2005.02.024

Zhang, X., Guo, R., Xu, J., Lan, Y., Jiao, Y., Zhou, C., & Zhao, Y. (2015). Poly(L-lactide)/halloysite nanotube electrospun mats as dual-drug delivery systems and their therapeutic efficacy in infected full-thickness burns. *Journal of Biomaterials Applications*, *30*(5), 512–525. https://doi.org/10.1177/0885328215593837

Zhang, Y., Lim, C. T., Ramakrishna, S., & Huang, Z.-M. (2005). Recent development of polymer nanofibers for biomedical and biotechnological applications. *Journal of Materials Science. Materials in Medicine*, *16*(10), 933–946. https://doi.org/10.1007/s10856-005-4428-x.

Zhao, R., Li, X., Sun, B., Tong, Y., Jiang, Z., & Wang, C. (2015). Nitrofurazone-loaded electrospun PLLA/sericin-based dual-layer fiber mats for wound dressing applications. *RSC Adv.*, *5*(22), 16940–16949. https://doi.org/10.1039/C4RA16208K

Zupančič, Š., Preem, L., Kristl, J., Putrinš, M., Tenson, T., Kocbek, P., & Kogermann, K. (2018). Impact of PCL nanofiber mat structural properties on hydrophilic drug release and antibacterial activity on periodontal pathogens. *European Journal of Pharmaceutical Sciences*, *122*, 347–358. https://doi.org/10.1016/j.ejps.2018.07.024

Zupančič, Š., Sinha-Ray, S., Sinha-Ray, S., Kristl, J., & Yarin, A. L. (2016). Long-Term Sustained Ciprofloxacin Release from PMMA and Hydrophilic Polymer Blended Nanofibers. *Molecular Pharmaceutics*, *13*(1), 295–305. https://doi.org/10.1021/acs.molpharmaceut.5b00804

9. SUMMARY IN ESTONIAN

Infitseerunud haavadel kasutatavate antibakteriaalsete elektrospinnitud ravimkandursüsteemide disain ja omaduste analüüs

Sissejuhatus

Halvasti paranevad haavad on kaasaegses ühiskonnas kiiresti kasvav sotsiaalmajanduslik probleem (Järbrink et al., 2017). Haavapatoloogiate kujunemises mängivad rolli mitmed faktorid, kuid järjest suuremat tähtsust selles omistatakse biokilele ja mikrobioloogilise tasakaalu häirumisele haavakeskkonnas, mis loovad paranemiseks ebasoodsa mikrokeskkonna (P. G. Bowler et al., 2001; D. Leaper et al., 2015). Seega on selliste haavade ravis asendamatu koht antimikroobsetel strateegiatel. (Daeschlein, 2013).

Infitseerunud haavade raviks on näidustatud süsteemne antibiootikumravi (Lee et al., 2005), mis võib aga põhjustada tõsiseid kõrvaltoimeid, samuti võivad antibiootikumide kontsentratsioonid haavas jääda ebapiisavaks (P. G. Bowler et al., 2001; Rhoads et al., 2008). Subterapeutilised antibiootikumide kontsentratsioonid aga tõstavad oluliselt antibiootikumresistentsuse ja persisteerivate bakterite tekkimise riski (Andersson & Hughes, 2014). Alternatiivselt saab raviks kasutada paikseid ravimvorme, nagu lahused, kreemid, salvid jt, kuigi need vajavad sagedast manustamist, nende reoloogilised omadused muutuvad haavaeksudaadi juuresolekul ning samuti väheneb nende toimeefektiivsus biokile ja haavaeksudaadi tõttu (J. S. Boateng et al., 2008; Siddiqui & Bernstein, 2010). Raviaine ei saa avaldada oma maksimaalset terapeutilist potentsiaali, kui seda pole viidud sobivasse ravimvormi ega manustatud sobival viisil. Seetõttu võiks kaasaegsed haavakatted, kuhu on võimalik viia ka raviaineid ning kontrollida nende vabanemiskineetikat, saavutamaks lokaalseid kliiniliselt olulisi antibakteriaalse aine kontsentratsioone pikema aja vältel, oluliselt parandada raviefektiivsust, vähendada kõrvaltoimeid ning parandada ravisoostumust (J. Boateng & Catanzano, 2015; Rambhia & Ma, 2015).

Elektrospinnimine on paindlik ja perspektiivikas meetod polümeersete nano- ja mikrofiibermaatriksite valmistamiseks, võimaldades suhteliselt lihtsalt inkorporeerida ka erinevaid raviaineid ning seeläbi luua mitmekülgsete omadustega ning soovitud raviaine vabanemiskineetikaga ravimkandursüsteeme (Kajdič et al., 2019). Lisaks on elektrospinnitud fiibritel mitmeid omadusi, mis muudavad nende kasutamise haavaravis väga atraktiivseks. Fiibermaatriksi poorne struktuur võimaldab efektiivset hapniku juurdepääsu haavale, lisaks soodustab fiibrite suur eripind hemostaasi ning haavaeksudaadi absorbeerimist (Rieger et al., 2013). Lisaks on elektrospinnitud fiibermaatriksid morfoloogiliselt sarnased naha enda ekstratsellulaarse maatriksiga, mis soodustab rakkude adhesiooni, migratsiooni ja proliferatsiooni ning aitab vähendada armistumist (Vasita & Katti, 2006; Zahedi et al., 2009). Seega on elektrospinnitud fiibermaatriksid samaaegselt suure potentsiaaliga ravimkandursüsteemid ja haavakatted.

Kuna elektrospinnimine on uudne meetod ravimkandursüsteemide valmistamiseks, on endiselt palju teadmata nii erinevate materjali kui ka protsessitingimuste mõjust fiibermaatriksite struktuursetele, füsikokeemilistele ja biofarmatseutilistele omadustele ning sellele, kuidas need omadused mõjutavad ravimkandursüsteemide kasutamist *in vivo* tingimustes. Parem arusaam neist mõjudest aitaks oluliselt kaasa ohutute ja efektiivsete elektrospinnitud haavakatete ratsionaalsele disainimisele.

Käesoleva töö eesmärk oli erinevaid kandjapolümeere ning raviaineid kasutades välja töötada antibakteriaalsed elektrospinnitud ravimkandursüsteemid, mida saaks kasutada haavainfektsioonide ennetamiseks ning lokaalseks raviks. Põhiliseks hüpoteesiks oli, et erinevalt disainitud elektrospinnitud maatriksitel on erinevad füsikokeemilised ja biofarmatseutilised omadused, millest sõltub raviaine vabanemisprofiil ning antibakteriaalne efektiivsus. Läbi viidi fiibermaatriksite põhjalik karakteriseerimine, mõistmaks olulisimaid faktoreid, mis mõjutavad nende funktsionaalsust ja kvaliteeti. Uute analüütiliste meetodite väljatöötamisega püüti mõista ja selgitada raviaine vabanemisprotsesse elektrospinnitud fiibermaatriksitest ning nende antibakteriaalseid omadusi.

Eesmärgid

Töö eesmärgiks oli välja töötada erinevad antibakteriaalsed elektrospinnitud fiibermaatriksid, mida võiks kasutada haavainfektsioonide ennetuseks ja lokaalseks raviks; ning põhjalikult karakteriseerida neid fiibermaatrikseid, et mõista, millised faktorid mõjutavad nende funktsionaalsust ja kvaliteeti.

Täpsemad töö eesmärgid olid:

- disainida ja valmistada antibakteriaalsed elektrospinnitud fiibermaatriksid, kasutades selleks erinevaid kandjapolümeere ja antibiootikume (I, II);
- iseloomustada nende maatriksite füsikokeemilisi ja struktuurseid omadusi (I, II);
- hinnata võimalikke interaktsioone erinevate maatriksikomponentide vahel molekulaarsel tasemel ja maatriksi interaktsioone vesikeskkonnaga (I, II);
- töötada välja ja võrrelda omavahel erinevaid analüütilisi meetodeid, et hinnata raviaine vabanemist neist maatriksitest (I–IV);
- hinnata maatriksite antibakteriaalset ja biokilevastast aktiivsust, kasutades selleks nii olemasolevaid meetodeid kui ka töötada välja uusi meetodeid (I,II, IV);
- hinnata maatriksite ohutust *in vitro* rakukultuuridel (I, II);
- võrrelda erinevate desinfektsiooni/steriliseerimismeetodite mõju mitmesugustele maatriksi omadustele (III).

Materjalid ja meetodid

Fiibermaatriksid valmistati elektrospinnimise meetodil, kasutades kandjapolümeeridena hüdrofoobset polükaprolaktooni (PCL) ja hüdrofiilset polüetüleenoksiidi (PEO), ning mudelraviainetena antibiootikume: hüdrofoobset kloramfenikooli (CAM) ning hüdrofiilseid metronidasooli (MTZ) ja tsiprofloksatsiin (CIP) vesinikkloriid-hüdraati.

Saadud fiibermaatriksite morfoloogiat ja struktuurseid omadusi uuriti skaneeriva elektronmikroskoopia (SEM), elavhõbeda porosimeetria ning gaasi adsorptsiooni (Brunauer-Emmett-Teller, BET) meetodil. Fiibermaatriksite mehaanilisi omadusi hinnati läbistuskatsetega tekstuurianalüsaatoril. Elektrospinnimise protsessi ja erinevate desinfektsiooni/sterilisatsioonimeetodete mõju raviaine stabiilsusele uuriti kõrgefektiivse vedelikkromatograafia abil (HPLC). Samuti uuriti HPLC ja Ramani mikrospektroskoopia (RSM) abil raviaine jaotumise ühtlust maatriksitest. Raviaine tahke faasi analüüsiks kasutati röntgendifraktomeetriat (XRD), nõrgendatud täieliku sisepeegelduse Fourier' teisendatud infrapuna spektroskoopiat (ATR-FTIR) ning diferentsiaalset skaneerivat kalorimeetriat (DSC). Maatriksi märgumisomadusi uuriti kontaktnurga määramisel. Puhverlahuse imamisvõimet ja maatriksi paisumist ning kaalukadu puhverlahuses hinnati gravimeetrilistel meetoditel. Raviaine vabanemist uuriti modifitseeritud *in vitro* dissolutsioonitestiga puhverlahusesse (fosfaatpuhver pH 7,4) ning vabanenud raviaine koguste määramiseks kasutati ultraviolett(UV)-spektrofotomeetriat. Lisaks töötati raviaine vabanemise uurimiseks välja uudsed meetodid: HPLC-ga määratud raviaine vabanemine hüdrogeeli; bioreporteritega difusioonitest; ning UV-pildistamise meetodil määratud raviaine vabanemine hüdrogeeli. Fiibermaatriksite antibakteriaalseid omadusi uuriti traditsioonilise difusioonitestiga agarsöötmesse, bioreporteritega difusioonitestiga ning modifitseeritud ja prolongeeritud difusioonitestidega. Samuti töötati välja meetod fiibermaatriksitele biokile moodustumise uurimiseks. Fiibermaatriksite ohutust *in vitro* eukarüootsetele rakkudele uuriti vastavalt ISO juhistele (09993-5).

Elektrospinnitud fiibermaatriksite desinfitseerimiseks/steriliseerimiseks kasutati UV-kiirgust (15, 30 või 60 min mõlemalt küljelt), gammakiirgust (50 kGy), *in situ* tekitatud gaasilist kloori (töötluse aeg 1 või 2 h) ning madalatemperatuurilist argooniplasmat (0,5 kuni 30 min). Steriliseerimise efektiivsust hinnati Euroopa farmakopöa (9.0) meetodi alusel nii aeroobsetes kui ka anaeroobsetes tingimustes.

Tulemused ja arutelu

Elektrospinnimise meetodil õnnestus valmistada erinevate omadustega kandjapolümeere ning raviaineid sisaldavad fiibermaatriksid: 4%-lise (m/m) CAM-sisaldusega PCL ja PCL/PEO (suhtes 5:1 m/m) fiibermaatriksid; ja PCL fiibermaatriksid, kuhu oli viidud 5% (m/m) MTZ-i, 5% (m/m) CIP vesinikkloriid-hüdraati ning kombineeritult nii 2,5% (m/m) MTZ-i kui ka 2,5% (m/m) CIP vesinikkloriidhüdraati.

SEM analüüs näitas, et CAM-i inkorporeerimisel PCL ja PCL/PEO maatriksitesse saadi vastavalt nano- ja mikrofiibrid ning MTZ-i ja CIPi inkorporeerimisel eraldi või kombineeritult PCL maatriksisse saadi nanofiibrid. Peaaegu kõigil juhtudel olid fiibrid ühtlase pinnaga, kus puudusid tilgakesed, nähtavad poorid ja raviaine kristallid. Vaid PCL/CIP ja PCL/MTZ/CIP maatriksites oli fiibrite pinnal märgata kristalliseerunud raviaine osakesi. Poorsuse määramise tulemused näitasid, et kõik fiibermaatriksid on suure poorsusega (~76–89%), st fiibritevaheline ruum on suhteliselt suur, kuid fiibrid ise poorsed pole. Samuti selgus, et suurema diameetriga fiibrite puhul on ka fiibritevaheline kaugus ehk nö pooride suurus fiibermaatriksis suurem.

HPLC ja RSM tulemused näitasid, et CAM elektrospinnimise käigus olulisel määral ei lagune ning jaotub valmistatud fiibermaatriksites ühtlaselt. Tahke faasi analüüs näitas, et CAM oli elektrospinnimise käigus omandanud amorfse vormi, kusjuures nii MTZ kui ka CIP olid vähemalt osaliselt rekristalliseerunud. MTZ kristalliseerus oma algsesse vormi, kusjuures CIP-i kristallvorm muutus. Lähtuvalt SEMi tulemustest võib arvata, et MTZ kristalliseerub fiibrite sees ning CIP fiibrite pinnal. Tahke faasi analüüs aitas ka tuvastada muutusi polümeeride kristallilisuses ning näitas, et tõenäoliselt esines elektrospinnitud fiibermaatriksites interaktsioone PCL ja CAM molekulide vahel ning PCL ja PEO molekulide vahel, mida füüsikalistes segudes ei esinenud.

Fiibermaatriksite kontaktnurga suured väärtused näitasid, et kõik fiibermaatriksid, kus kandjapolümeeriks oli vaid PCL, olid hüdrofoobsed. Hüdrofiilse PEO lisamisel kontaktnurk vähenes ning maatriks muutus hüdrofiilseks. Täpsemaid interaktsioone vedelikega sai hinnata paisumistestiga, mis näitas, et hoolimata sarnastest märgumisomadustes imasid PCL/MTZ, PCL/CIP ja PCL/MTZ/CIP puhverlahust endasse väga erineval määral. Üheks põhjuseks võis olla hüdrofiilsete ja hügroskoopsete CIP-i kristallide esinemine PCL/CIP ja PCL/MTZ/CIP pinnal, mis soodustasid puhvri liikumist maatriksisse. Hüdrofoobne PCL/CAM maatriks praktiliselt vedelikku endasse ei imanud, samas kui hüdrofiilne PCL/PEO/CAM maatriks imas seda suurel määral.

Raviaine vabanemiskatsed näitasid, et kandjapolümeeride omadustel on oluline mõju raviaine vabanemisele. CAM vabanes hüdrofoobsest PCL/CAM fiibermaatriksist puhverlahusesse aeglaselt (~19% esimese tunni jooksul ja 78 h tunni jooksul ~60% raviainest), samas kui hüdrofiilsest PCL/PEO/CAM maatriksist oli vabanemine kiire (~92 % raviainest esimese 15 min jooksul). Tulemused kinnitasid ka, et fiibermaatriksite struktuursetel omadustel on oluline mõju raviaine vabanemisele mõnede raviaine-polümeer kombinatsioonide puhul. Fiibermaatriksi paksus oli kriitilise mõjuga raviaine vabanemisele PCL/MTZ maatriksitest, kuid mitte teistest maatriksitest. MTZ-i vabanemist kontrollis puhvri maatriksisse tungimise kiirus, mis oli seda aeglasem, mida paksem PCL/MTZ fiibermaatriks oli. Samas ei omanud fiibermaatriksi paksus tähtsust MTZ-i vabanemisele PCL/MTZ/CIP fiibermaatriksist, kuhu puhver tungis sõltumata maatriksi paksusest kiiresti. CIP-i vabanemisele fiibermaatriksi paksus mõju ei avaldanud.

Raviaine tahke faasi omaduste mõju raviaine vabanemisele oli töös uuritud maatriksite puhul kaudne. Amorfne raviaine paikneb suurema tõenäosusega fiibrite sisemuses, samas kui raviaine rekristalliseerub elektrospinnimise käigus, toimub see pigem fiibrite pinnal või selle läheduses. Kuna fiibermaatriksitel on suur eripind ning rekristalliseerunud raviaine kristallid väga väikesed, on raviaine vabanemine soodsam just kristallilise raviaine puhul, sest puhverlahus pääseb nendeni kiiremini. Lisaks võivad hüdrofiilse raviaine kristallid soodustada puhvri tungimist maatriksisse, mis omakorda võib kiirendada raviaine vabanemist, nagu oli näha MTZ-i vabanemisest PCL/MTZ/CIP maatriksist.

Lisaks raviaine vabanemisele puhverlahusesse, kasutati töös ka hüdrogeelidel põhinevaid vabanemiskeskkondi ning erinevaid vabanenud raviaine detekteerimise viise. Hüdrogeelid on võrreldes puhverlahustega sarnasem keskkond haavale, mistõttu võiks sellised meetodid olla biorelevantsemad, ning võimaldavad lisaks raviaine vabanemisele hinnata ka selle edasist difusiooni haavas. Samuti imiteerisid need meetodid paremini *in vitro* antibakteriaalse aktiivsuse testimise tingimusi. Ilmnes, et võrreldes CAM-i vabanemisega puhverlahusesse, olid erinevused PCL/CAM ja PCL/PEO/CAM maatriksitest raviaine vabanemises hüdrogeeli märksa tagasihoidlikumad ning raviaine vabanemine puhvrisse ülehindas suuresti esialgset kiiret vabanemisfaasi. Raviaine difusioon agargeelis oli küllaltki aeglane, mistõttu suurem osa vabanenud raviainest jäi esimeste tundide jooksul fiibermaatriksi alla või selle lähedusse. Vabanenud raviaine kontsentratsioonide määramiseks kasutati raviaine ekstraheerimist agarist ning järgnevat HPLC analüüsi, bioreportereid ja ka UV-pildistamist. Kõik meetodid olid võrreldava tundlikkusega, kuid UV-pildistamine kõige vähem töömahukas ning pakkus parimat ruumilist ja ajalist resolutsiooni. Samas võimaldas bioreporterite kasutamine samaaegselt hinnata ka fiibermaatriksite antibakteriaalset aktiivsust.

Difusioonitest agarsöötmes näitas, et vabanenud CAMi kontsentratsioonid olid piisavad, et inhibeerida *E. coli* MG1655 ning CFT073 kasvu, kusjuures erinevusi ei ilmnenud PCL/CAM ja PCL/PEO/CAM fiibermaatriksite tekitatud kasvuvabade tsoonide suurustes, kuid inhibitsioonitsoonid olid mõnevõrra suuremad *E. coli* MG1655 puhul võrreldes CFT073 tüvega. MTZ osutus efektiivseks anaeroobses keskkonnas *F. nucleatum*'i, *P. gingivalis*'e ja *A. actinomycetemcomitans*'i suhtes, samas kui CIP-i sisaldavad fiibermaatriksid olid efektiivsed kõigi testitud bakterite suhtes nii aeroobses kui ka anaeroobses keskkonnas. *A. actinomycetemcomitans* oli tundlikum CIP-i suhtes, samas kui *F. nucleatum* oli tundlikum MTZ-i suhtes. Fiibermaatriksid, mis sisaldasid nii MTZ-i kui ka CIP-i omasid kõige paremat antibakteriaalset aktiivsust võrreldes maatriksitega, kus kumbki raviaine sisaldus üksi.

Lisaks traditsioonilisele difusioonitestile viidi läbi ka modifitseeritud difusioonitest agarsöötmel, mis võimaldas tuvastada PCL/CAM ja PCL/PEO/CAM fiibermaatriksite antibakteriaalses aktiivsuses väikeseid erinevusi, mida oli näha ka erinevustena raviaine vabanemises agargeeli. Prolongeeritud difusioonitest näitas, et erineva paksusega ja seetõttu erineva vabanemiskineetikaga PCL/ MTZ fiibermaatriksite antibakteriaalne aktiivsus on sarnane esimese 24 h jooksul, kus

vabaneva raviaine hulk on väga suur, kuid hiljem omab efektiivsust vaid pika-ajalisemalt MTZ-i vabastav fiibermaatriks. Samas nägime, et MTZ ei avaldanud märgatavat antibakteriaalset aktiivsust 72 h ajapunktis, kuigi tulemused raviaine vabanemises puhverlahusesse oleks seda eeldanud.

Biokilekatse näitas, et raviainet aeglasemalt vabastav PCL/CAM fiibermaatriks omas suuremat inhibeerivat efekti biokile moodustumisele, võrreldes PCL/PEO/CAM fiibermaatriksiga. Samas aga tekkis biokile märksa paremini ilma raviaineta PCL fiibermaatriksile, võrreldes ilma raviaineta PCL/PEO fiibermaatriksiga. Üheks tõenäoliseks põhjuseks on maatriksite erinev hüdrofiilsus/hüdrofoobsus, mis mõjutab bakterite kinnitumist fiibritele.

Uuritud fiibermaatriksid olid eukarüootsetele rakkudele ohutud ning ei mõjutanud nende rakkude elulemust *in vitro* katsetes.

Elektrospinnitud fiibermaatriksite steriliseerimine oli efektiivne, kasutades gammakiirgust (doos 50 kGy), UV-kiirgust (30 minutit mõlemalt küljelt) ning *in situ* tekitatud gaasilist kloori (toimeaeg 1h). Erinevad töötlused avaldasid erinevat mõju raviaine sisaldusele fiibermaatriksis, kusjuures ilmnes, et raviaine lagunemine oli suurem PCL/PEO/CAM maatriksites, võrreldes PCL/CAM maatriksitega. Erinevad steriliseerimismeetodid ei omanud mõju fiibrite morfoloogiale, kuid olulisemaks osutus nende mõju polümeeride kristallilisusele ning sellest tulenevalt fiibermaatriksite mehaanilistele omadustele ja lagunemisele vesikeskkonnas. Plasmasteriliseerimine omas märkimisväärset mõju fiibermaatriksite pinnaomadustele, parandades nende märgumist ja puhverlahuse imamisvõimet. See tõi omakorda kaasa suured muutused PCL/CAM fiibermaatriksitest raviaine vabanemises, kus pärast plasmatöötlust vabastas fiibermaatriks raviainet puhverlahusesse väga kiiresti.

Järeldused

Elektrospinnimise teel oli võimalik valmistada erinevate omadustega nano- ja mikrofiibermaatrikseid, kasutades selleks erinevaid kandjapolümeere ja antibakteriaalseid raviaineid. Sõltuvalt raviaine ja polümeeri sobivusest, võis raviaine elektrospinnimise käigus minna amorfsesse vormi või rekristalliseeruda. Viimane võis toimuda nii fiibrite pinnal kui ka sisemuses. Elektrospinnimine mõjutas ka polümeeride kristallilisust ning tõi kaasa interaktsioone erinevate fiibermaatriksi komponentide vahel.

Raviaine vabanemine puhverlahustesse oli erinevalt disainitud fiibermaatriksitest erinev. Üheks olulisimaks faktoriks selles oli fiibermaatriksite erinev interakteerumine vesikeskkonnaga, st fiibermaatriksite märgumine ning puhverlahuse tungimine fiibermaatriksitesse. Vabanemiskeskkonna tungimist fiibermaatriksisse mõjutasid kandjapolümeeride hüdrofiilsus/hüdrofoobsus, maatriksi paksus, ning kaudselt ka raviaine tahke vorm. Samas ei kontrollinud maatriksi paksus ja puhverlahuse tungimine sellesse kõigi raviainete vabanemist, mistõttu pole tegu universaalse strateegiaga raviaine vabanemise kontrollimiseks.

Võrreldes raviaine vabanemisega puhverlahusesse, jäljendasid hüdrogeelid vabanemiskeskkonnana paremini *in vitro* antibakteriaalse aktiivsuse testimise tingimusi ning võib arvata, et ka raviaine vabanemist ja difusiooni haavakeskkonnas. Vabanemine puhvrisse ülehindas suuresti esialgset kiiret vabanemisfaasi. Väljatöötatud alternatiivsed meetodid raviaine vabanemise hindamiseks olid sarnase tundlikkusega, kuid erinevate eeliste ja puudustega.

Antibakteriaalse aktiivsuse määramisel võimaldas traditsiooniline difusioontest agarsöötmes kinnitada, kas vabanenud raviained ning nende kontsentratsioonid olid efektiivsed erinevate mudelmikroorganismide suhtes. Siiski ei suutnud need tuvastada erinevusi antibakteriaalses aktiivsuses erineva raviaine vabanemisprofiiliga fiibermaatriksite vahel, milleks sobisid paremini uudsed difusioonitestid. Prolongeeritud difusioonitest võimaldas hinnata fiibermaatriksist pikema aja jooksul vabaneva raviaine antibakteriaalset aktiivsust ning andis kinnitust, et raviaine vabanemine puhverlahusesse pole võrreldav selle vabanemisega hüdrogeeli.

Haavakatte disainil tuleb arvestada erinevate kandjapolümeeride mõjuga biokile moodustumisele. Samuti on oluline, et raviaine vabaneks fiibermaatriksist aeglaselt, mis aitab vältida sellele biokile teket, ning et esineks raviaine esmane kiire vabanemine, mis tagab kiire efektiivsete raviaine kontsentratsioonide saavutamise ja toime alguse.

Kõik valmistatud fiibermaatriksid olid *in vitro* tsütotoksilisuse katsetes ohutud, mistõttu võib jätkata edasiste põhjalikumate uuringutega, sh loomkatsetega, et jõuda lõppeesmärgini ehk haavakatete kasutamiseni kliinilises praktikas inimesel.

Elektrospinnitud fiibermaatrikseid on võimalik efektiivselt steriliseerida erinevatel meetoditel, kuid tuleb arvestada, et steriliseerimisprotsess võib muuta erinevaid fiibermaatriksi omadusi, sealhulgas raviaine sisaldust, fiibermaatriksi mehaanilisi omadusi ning käitumist vesikeskkonnas ja raviaine vabanemist. Võimalik mõju sõltub nii konkreetsest steriliseerimismeetodist kui ka maatriksi materjalidest ning raviaine omadustest.

ACKNOWLEDGEMENTS

This work was mainly carried out at the Institute of Pharmacy, Faculty of Medicine, University of Tartu, Estonia, and Institute of Technology, Faculty of Technology and Science, University of Tartu, Estonia during the years 2015–2019.

Estonian Research Council grants ETF7980, PUT1088, IUT-2-22, and PRG335, European Regional Development Fund through the Centre of Excellence for Molecular Cell Technology, Estonian Ministry of Education and Research and European Regional Development Fund (Kristjan Jaak Scholarship, Dora Pluss Programme and University of Tartu ASTRA project PER ASPERA) are acknowledged for research and mobility funding. L'ORÉAL Baltic "For Women In Science" fellowship 2018 (K. Kogermann) with the support of the Estonian National Commission for UNESCO and the Estonian Academy of Sciences and the L'ORÉAL–UNESCO international program "For Women In Science" is acknowledged.

I wish to thank all the persons that were involved with this study at the University of Tartu, Estonia, University of Helsinki, Finland, University of Ljubljana, Slovenia and University of Copenhagen, Denmark.

Most importantly, I want to express my deepest gratitude and appreciation to my supervisors Associate Professor Karin Kogermann, Professor Tanel Tenson and Associate Professor Andres Meos for their time and effort. I will always cherish the guidance, shared wisdom and support that has made my PhD journey easier and an enjoyable endeavor. I have been truely lucky to have You as my supervisors! I am especially grateful to Associate Professor Karin Kogermann whose kindness and encouragement throughout the years I will never forget. The positive, passionate, and diligent attitude towards science and life itself is remarkable and I aspire to come close to that one day. From the bottom of my heart, thank You! I am also sincerely thankful to PhD Marta Putrinš who has been like a supervisor to me and whose bright insights have been indispensable.

I am very thankful to my reviewers Associate professor Meeme Utt and Associate professor Niilo Kaldalu for their time and effort to read the thesis and provide valuable comments on how to improve it.

I wish to thank all my friends and colleagues from the Institute of Pharmacy and Institute of Technology for their help and guidance, and for creating a positive and nurturing work environment. I value the shared ideas and discussions that have helped me see things from a different perspective. It has been a pleasure to work with You!

Finally, I want to express my love and gratitude to my friends and family. I am ever grateful to my parents, who have unconditionally supported my decisions and given me a loving home to grow up in, and to my husband, whose constant love, patience and support I feel every day. At last, my love goes to my little daughter, whose sweet and curious questions remind me that the world is full of wonders for an inquisitive and unprejudiced mind.

PUBLICATIONS

CURRICULUM VITAE

Name:	Liis Preem (neé Saks)
Date of birth:	August 6, 1990
Address:	Institute of Pharmacy, University of Tartu, Nooruse 1, 50411, Tartu, Estonia
E-mail:	liis.preem@ut.ee

Education:

1997–2000	Jõhvi Gymnasium
2000–2006	Põltsamaa Co-Educational Gymnasium
2006–2009	Nõo Secondary Science Gymnasium (with a gold medal)
2009–2014	University of Tartu, Faculty of Medicine, Institute of Pharmacy (MSc, *cum laude*)
2015–…	University of Tartu, Faculty of Medicine, Institute of Pharmacy, PhD studies

Professional employment:

2014–2015	Tasku Pharmacy branch in Lõunakeskus, Pharmacist
2017–2018	University of Tartu, Faculty of Medicine, Institute of Pharmacy, Specialist (0,10)
01.2018–12.2018	University of Tartu, Faculty of Medicine, Institute of Pharmacy, Junior Research Fellow (0,50)
2018–2019	University of Tartu, Faculty of Medicine, Institute of Pharmacy, Assistant of Pharmaceutical Analysis (0,50)
2019–2021	Maternity leave
2021–…	University of Tartu, Faculty of Medicine, Institute of Pharmacy, Junior Lecturer of Pharmaceutical Analysis (0,5)

Research fields: Development, characterization and analysis of nanotechnological drug delivery systems, antimicrobial activity studies (CERCS classification: B740 Pharmacological sciences, pharmacognosy, pharmacy, toxicology, T410 Pharmaceuticals and related technologies; T490 Biotechnology)

Research projects:

2016–2019	Investigator in a Estonian Research Council research project “Design and Development of Multicomponent Antibacterial Nanofibrous Dressings for Advanced Wound Care“.

List of publications in international peer-reviewed journals:

1. Preem, Liis; Mahmoudzadeh, Mohammad; Putrinš, Marta; Meos, Andres; Laidmäe, Ivo; Romann, Tavo; Aruväli, Jaan; Härmas, Riinu; Koivuniemi, Artturi; Bunker, Alex; Tenson, Tanel; Kogermann, Karin (2017). Interactions between Chloramphenicol, Carrier Polymers, and Bacteria-Implications for Designing Electrospun Drug Delivery Systems Countering Wound Infection. Molecular Pharmaceutics, 14 (12), 4417−4430. DOI: 10.1021/acs.molpharmaceut.7b00524.
2. Zupančič, Špela; Preem, Liis; Kristl, Julijana; Putrinš, Marta; Tenson, Tanel; Kocbek, Petra; Kogermann, Karin (2018). Impact of PCL Nanofiber Mat Structural Properties on Hydrophilic Drug Release and Antibacterial Activity on Periodontal Pathogens. European Journal of Pharmaceutical Sciences, 122, 347−358. DOI: 10.1016/j.ejps.2018. 07.024.
3. Preem, Liis; Vaarmets, Ebe; Meos, Andres; Jõgi, Indrek; Putrinš, Marta; Tenson, Tanel; Kogermann, Karin (2019). Effects and Efficacy of Different Sterilization and Disinfection Methods on Electrospun Drug Delivery Systems. International Journal of Pharmaceutics, 567, 118450−118450. DOI: 10.1016/j.ijpharm.2019.118450.
4. Preem, Liis; Bock, Frederik; Hinnu, Mariliis; Putrins, Marta; Sagor, Kadi; Tenson, Tanel; Meos, Andres; Ostergaard, Jesper; Kogermann, Karin (2019). Monitoring of Antimicrobial Drug Chloramphenicol Release from Electrospun Nano- and Microfiber Mats Using UV Imaging and Bacterial Bioreporters. Pharmaceutics, 11 (9), ARTN 487. DOI: 10.3390/pharmaceutics11090487.
5. Lanno, Georg-Marten; Ramos, Celia; Preem, Liis; Putrinš, Marta; Laidmäe, Ivo; Tenson, Tanel; Kogermann, Karin (2020). Antibacterial Porous Electrospun Fibers as Skin Scaffolds for Wound Healing Applications. ACS Omega, 5 (46), 30011−30022. DOI: 10.1021/acsomega. 0c04402.

1 book chapter has been published:

Preem, Liis; Kogermann, Karin (2018). Electrospun Antimicrobial Wound Dressings: Novel Strategies to Fight Against Wound Infections. In: Recent Clinical Techniques, Results, and Research in Wounds (1−41). Springer. DOI: 10.1007/15695_2018_133

In addition, 3 oral talks and 8 posters have been presented at international scientific conferences.

ELULOOKIRJELDUS

Nimi:	Liis Preem (neé Saks)
Sünniaeg:	6. august 1990
Aadress:	Farmaatsia instituut, Tartu Ülikool, Nooruse 1, 50411, Tartu, Estonia
E-mail:	liis.preem@ut.ee

Haridus:

1997–2000	Jõhvi Gümnaasium
2000–2006	Põltsamaa Ühisgümnaasium
2006–2009	Nõo Reaalgümnaasium (kuldmedaliga)
2009–2014	Tartu Ülikool, Arstiteaduskond, farmaatsia instituut, proviisoriõpe (*cum laude*)
2015–…	Tartu Ülikool, Meditsiiniteaduste valdkond, farmaatsia instituut, doktorant farmaatsia erialal

Erialane teenistuskäik:

2014–2015	Tasku Apteegi haruapteek Lõunakeskuses, proviisor
2017–2018	Tartu Ülikool, Meditsiiniteaduste valdkond, Farmaatsia instituut, spetsialist (0,10)
01.2018–12.2018	Tartu Ülikool, Meditsiiniteaduste valdkond, farmaatsia instituut, nooremteadur (0,5)
2018–2019	Tartu Ülikool, Meditsiiniteaduste valdkond, farmaatsia instituut, farmatseutilise analüüsi assistent (0,50)
2019–2021	Lapsehoolduspuhkus
2021–…	Tartu Ülikool, Meditsiiniteaduste valdkond, farmaatsia instituut, farmatseutilise analüüsi nooremlektor (0,5)

Teadustöö suunad: Nanotehnoloogiliste ravimkandursüsteemide arendamine, karakteriseerimine ja analüüs, antimikroobse aktiivsuse uurimine. (CERCS klassifikaator: B740 Farmakoloogia, farmakognoosia, farmaatsia, toksikoloogia, T410 Farmaatsiatooted ja nende tehnoloogiad; T490 Biotehnoloogia)

Teadusprojektid:

2016–2019	Täitja Sihtasutus Eesti Teadusagentuuri projektis: “Haavaravis kasutatavate mitmeosaliste antibakteriaalsete nanofiiberkatete disain ja valmistamine”

Rahvusvahelistes eelretsenseeritud ajakirjades avaldatud artiklid:

1. Preem, Liis; Mahmoudzadeh, Mohammad; Putrinš, Marta; Meos, Andres; Laidmäe, Ivo; Romann, Tavo; Aruväli, Jaan; Härmas, Riinu; Koivuniemi, Artturi; Bunker, Alex; Tenson, Tanel; Kogermann, Karin (2017). Interactions between Chloramphenicol, Carrier Polymers, and Bacteria-Implications for Designing Electrospun Drug Delivery Systems Countering Wound Infection. Molecular Pharmaceutics, 14 (12), 4417−4430. DOI: 10.1021/acs.molpharmaceut.7b00524.
2. Zupančič, Špela; Preem, Liis; Kristl, Julijana; Putrinš, Marta; Tenson, Tanel; Kocbek, Petra; Kogermann, Karin (2018). Impact of PCL Nanofiber Mat Structural Properties on Hydrophilic Drug Release and Antibacterial Activity on Periodontal Pathogens. European Journal of Pharmaceutical Sciences, 122, 347−358. DOI: 10.1016/j.ejps.2018.07.024.
3. Preem, Liis; Vaarmets, Ebe; Meos, Andres; Jõgi, Indrek; Putrinš, Marta; Tenson, Tanel; Kogermann, Karin (2019). Effects and Efficacy of Different Sterilization and Disinfection Methods on Electrospun Drug Delivery Systems. International Journal of Pharmaceutics, 567, 118450−118450. DOI: 10.1016/j.ijpharm.2019.118450.
4. Preem, Liis; Bock, Frederik; Hinnu, Mariliis; Putrins, Marta; Sagor, Kadi; Tenson, Tanel; Meos, Andres; Ostergaard, Jesper; Kogermann, Karin (2019). Monitoring of Antimicrobial Drug Chloramphenicol Release from Electrospun Nano- and Microfiber Mats Using UV Imaging and Bacterial Bioreporters. Pharmaceutics, 11 (9), ARTN 487. DOI: 10.3390/pharmaceutics11090487.
5. Lanno, Georg-Marten; Ramos, Celia; Preem, Liis; Putrinš, Marta; Laidmäe, Ivo; Tenson, Tanel; Kogermann, Karin (2020). Antibacterial Porous Electrospun Fibers as Skin Scaffolds for Wound Healing Applications. ACS Omega, 5 (46), 30011−30022. DOI: 10.1021/acsomega.0c04402.

Avaldatud on 1 raamatupeatükk:

Preem, Liis; Kogermann, Karin (2018). Electrospun Antimicrobial Wound Dressings: Novel Strategies to Fight Against Wound Infections. In: Recent Clinical Techniques, Results, and Research in Wounds (1−41). Springer. DOI: 10.1007/15695_2018_133

Lisaks on rahvusvahelistel teaduskonverentsidel esinetud 3 suulise ettekandega ning 8 posterettekandega.

DISSERTATIONES MEDICINAE UNIVERSITATIS TARTUENSIS

1. **Heidi-Ingrid Maaroos**. The natural course of gastric ulcer in connection with chronic gastritis and *Helicobacter pylori*. Tartu, 1991.
2. **Mihkel Zilmer**. Na-pump in normal and tumorous brain tissues: Structural, functional and tumorigenesis aspects. Tartu, 1991.
3. **Eero Vasar**. Role of cholecystokinin receptors in the regulation of behaviour and in the action of haloperidol and diazepam. Tartu, 1992.
4. **Tiina Talvik**. Hypoxic-ischaemic brain damage in neonates (clinical, biochemical and brain computed tomographical investigation). Tartu, 1992.
5. **Ants Peetsalu**. Vagotomy in duodenal ulcer disease: A study of gastric acidity, serum pepsinogen I, gastric mucosal histology and *Helicobacter pylori*. Tartu, 1992.
6. **Marika Mikelsaar**. Evaluation of the gastrointestinal microbial ecosystem in health and disease. Tartu, 1992.
7. **Hele Everaus**. Immuno-hormonal interactions in chronic lymphocytic leukaemia and multiple myeloma. Tartu, 1993.
8. **Ruth Mikelsaar**. Etiological factors of diseases in genetically consulted children and newborn screening: dissertation for the commencement of the degree of doctor of medical sciences. Tartu, 1993.
9. **Agu Tamm**. On metabolic action of intestinal microflora: clinical aspects. Tartu, 1993.
10. **Katrin Gross**. Multiple sclerosis in South-Estonia (epidemiological and computed tomographical investigations). Tartu, 1993.
11. **Oivi Uibo**. Childhood coeliac disease in Estonia: occurrence, screening, diagnosis and clinical characterization. Tartu, 1994.
12. **Viiu Tuulik**. The functional disorders of central nervous system of chemistry workers. Tartu, 1994.
13. **Margus Viigimaa**. Primary haemostasis, antiaggregative and anticoagulant treatment of acute myocardial infarction. Tartu, 1994.
14. **Rein Kolk**. Atrial versus ventricular pacing in patients with sick sinus syndrome. Tartu, 1994.
15. **Toomas Podar**. Incidence of childhood onset type 1 diabetes mellitus in Estonia. Tartu, 1994.
16. **Kiira Subi**. The laboratory surveillance of the acute respiratory viral infections in Estonia. Tartu, 1995.
17. **Irja Lutsar**. Infections of the central nervous system in children (epidemiologic, diagnostic and therapeutic aspects, long term outcome). Tartu, 1995.
18. **Aavo Lang**. The role of dopamine, 5-hydroxytryptamine, sigma and NMDA receptors in the action of antipsychotic drugs. Tartu, 1995.
19. **Andrus Arak**. Factors influencing the survival of patients after radical surgery for gastric cancer. Tartu, 1996.

20. **Tõnis Karki**. Quantitative composition of the human lactoflora and method for its examination. Tartu, 1996.
21. **Reet Mändar**. Vaginal microflora during pregnancy and its transmission to newborn. Tartu, 1996.
22. **Triin Remmel**. Primary biliary cirrhosis in Estonia: epidemiology, clinical characterization and prognostication of the course of the disease. Tartu, 1996.
23. **Toomas Kivastik**. Mechanisms of drug addiction: focus on positive reinforcing properties of morphine. Tartu, 1996.
24. **Paavo Pokk**. Stress due to sleep deprivation: focus on $GABA_A$ receptor-chloride ionophore complex. Tartu, 1996.
25. **Kristina Allikmets**. Renin system activity in essential hypertension. Associations with atherothrombogenic cardiovascular risk factors and with the efficacy of calcium antagonist treatment. Tartu, 1996.
26. **Triin Parik**. Oxidative stress in essential hypertension: Associations with metabolic disturbances and the effects of calcium antagonist treatment. Tartu, 1996.
27. **Svetlana Päi**. Factors promoting heterogeneity of the course of rheumatoid arthritis. Tartu, 1997.
28. **Maarike Sallo**. Studies on habitual physical activity and aerobic fitness in 4 to 10 years old children. Tartu, 1997.
29. **Paul Naaber**. *Clostridium difficile* infection and intestinal microbial ecology. Tartu, 1997.
30. **Rein Pähkla**. Studies in pinoline pharmacology. Tartu, 1997.
31. **Andrus Juhan Voitk**. Outpatient laparoscopic cholecystectomy. Tartu, 1997.
32. **Joel Starkopf**. Oxidative stress and ischaemia-reperfusion of the heart. Tartu, 1997.
33. **Janika Kõrv**. Incidence, case-fatality and outcome of stroke. Tartu, 1998.
34. **Ülla Linnamägi**. Changes in local cerebral blood flow and lipid peroxidation following lead exposure in experiment. Tartu, 1998.
35. **Ave Minajeva**. Sarcoplasmic reticulum function: comparison of atrial and ventricular myocardium. Tartu, 1998.
36. **Oleg Milenin**. Reconstruction of cervical part of esophagus by revascularised ileal autografts in dogs. A new complex multistage method. Tartu, 1998.
37. **Sergei Pakriev**. Prevalence of depression, harmful use of alcohol and alcohol dependence among rural population in Udmurtia. Tartu, 1998.
38. **Allen Kaasik**. Thyroid hormone control over β-adrenergic signalling system in rat atria. Tartu, 1998.
39. **Vallo Matto**. Pharmacological studies on anxiogenic and antiaggressive properties of antidepressants. Tartu, 1998.
40. **Maire Vasar**. Allergic diseases and bronchial hyperreactivity in Estonian children in relation to environmental influences. Tartu, 1998.
41. **Kaja Julge**. Humoral immune responses to allergens in early childhood. Tartu, 1998.

42. **Heli Grünberg**. The cardiovascular risk of Estonian schoolchildren. A cross-sectional study of 9-, 12- and 15-year-old children. Tartu, 1998.
43. **Epp Sepp**. Formation of intestinal microbial ecosystem in children. Tartu, 1998.
44. **Mai Ots**. Characteristics of the progression of human and experimental glomerulopathies. Tartu, 1998.
45. **Tiina Ristimäe**. Heart rate variability in patients with coronary artery disease. Tartu, 1998.
46. **Leho Kõiv**. Reaction of the sympatho-adrenal and hypothalamo-pituitary-adrenocortical system in the acute stage of head injury. Tartu, 1998.
47. **Bela Adojaan**. Immune and genetic factors of childhood onset IDDM in Estonia. An epidemiological study. Tartu, 1999.
48. **Jakov Shlik**. Psychophysiological effects of cholecystokinin in humans. Tartu, 1999.
49. **Kai Kisand**. Autoantibodies against dehydrogenases of α-ketoacids. Tartu, 1999.
50. **Toomas Marandi**. Drug treatment of depression in Estonia. Tartu, 1999.
51. **Ants Kask**. Behavioural studies on neuropeptide Y. Tartu, 1999.
52. **Ello-Rahel Karelson**. Modulation of adenylate cyclase activity in the rat hippocampus by neuropeptide galanin and its chimeric analogs. Tartu, 1999.
53. **Tanel Laisaar**. Treatment of pleural empyema — special reference to intrapleural therapy with streptokinase and surgical treatment modalities. Tartu, 1999.
54. **Eve Pihl**. Cardiovascular risk factors in middle-aged former athletes. Tartu, 1999.
55. **Katrin Õunap**. Phenylketonuria in Estonia: incidence, newborn screening, diagnosis, clinical characterization and genotype/phenotype correlation. Tartu, 1999.
56. **Siiri Kõljalg**. *Acinetobacter* – an important nosocomial pathogen. Tartu, 1999.
57. **Helle Karro**. Reproductive health and pregnancy outcome in Estonia: association with different factors. Tartu, 1999.
58. **Heili Varendi**. Behavioral effects observed in human newborns during exposure to naturally occurring odors. Tartu, 1999.
59. **Anneli Beilmann**. Epidemiology of epilepsy in children and adolescents in Estonia. Prevalence, incidence, and clinical characteristics. Tartu, 1999.
60. **Vallo Volke**. Pharmacological and biochemical studies on nitric oxide in the regulation of behaviour. Tartu, 1999.
61. **Pilvi Ilves**. Hypoxic-ischaemic encephalopathy in asphyxiated term infants. A prospective clinical, biochemical, ultrasonographical study. Tartu, 1999.
62. **Anti Kalda**. Oxygen-glucose deprivation-induced neuronal death and its pharmacological prevention in cerebellar granule cells. Tartu, 1999.
63. **Eve-Irene Lepist**. Oral peptide prodrugs – studies on stability and absorption. Tartu, 2000.

64. **Jana Kivastik**. Lung function in Estonian schoolchildren: relationship with anthropometric indices and respiratory symptomas, reference values for dynamic spirometry. Tartu, 2000.
65. **Karin Kull**. Inflammatory bowel disease: an immunogenetic study. Tartu, 2000.
66. **Kaire Innos**. Epidemiological resources in Estonia: data sources, their quality and feasibility of cohort studies. Tartu, 2000.
67. **Tamara Vorobjova**. Immune response to *Helicobacter pylori* and its association with dynamics of chronic gastritis and epithelial cell turnover in antrum and corpus. Tartu, 2001.
68. **Ruth Kalda**. Structure and outcome of family practice quality in the changing health care system of Estonia. Tartu, 2001.
69. **Annika Krüüner**. *Mycobacterium tuberculosis* – spread and drug resistance in Estonia. Tartu, 2001.
70. **Marlit Veldi**. Obstructive Sleep Apnoea: Computerized Endopharyngeal Myotonometry of the Soft Palate and Lingual Musculature. Tartu, 2001.
71. **Anneli Uusküla**. Epidemiology of sexually transmitted diseases in Estonia in 1990–2000. Tartu, 2001.
72. **Ade Kallas**. Characterization of antibodies to coagulation factor VIII. Tartu, 2002.
73. **Heidi Annuk**. Selection of medicinal plants and intestinal lactobacilli as antimicrobil components for functional foods. Tartu, 2002.
74. **Aet Lukmann**. Early rehabilitation of patients with ischaemic heart disease after surgical revascularization of the myocardium: assessment of health-related quality of life, cardiopulmonary reserve and oxidative stress. A clinical study. Tartu, 2002.
75. **Maigi Eisen**. Pathogenesis of Contact Dermatitis: participation of Oxidative Stress. A clinical – biochemical study. Tartu, 2002.
76. **Piret Hussar**. Histology of the post-traumatic bone repair in rats. Elaboration and use of a new standardized experimental model – bicortical perforation of tibia compared to internal fracture and resection osteotomy. Tartu, 2002.
77. **Tõnu Rätsep**. Aneurysmal subarachnoid haemorrhage: Noninvasive monitoring of cerebral haemodynamics. Tartu, 2002.
78. **Marju Herodes**. Quality of life of people with epilepsy in Estonia. Tartu, 2003.
79. **Katre Maasalu**. Changes in bone quality due to age and genetic disorders and their clinical expressions in Estonia. Tartu, 2003.
80. **Toomas Sillakivi**. Perforated peptic ulcer in Estonia: epidemiology, risk factors and relations with *Helicobacter pylori*. Tartu, 2003.
81. **Leena Puksa**. Late responses in motor nerve conduction studies. F and A waves in normal subjects and patients with neuropathies. Tartu, 2003.
82. **Krista Lõivukene**. *Helicobacter pylori* in gastric microbial ecology and its antimicrobial susceptibility pattern. Tartu, 2003.

83. **Helgi Kolk**. Dyspepsia and *Helicobacter pylori* infection: the diagnostic value of symptoms, treatment and follow-up of patients referred for upper gastrointestinal endoscopy by family physicians. Tartu, 2003.
84. **Helena Soomer**. Validation of identification and age estimation methods in forensic odontology. Tartu, 2003.
85. **Kersti Oselin**. Studies on the human MDR1, MRP1, and MRP2 ABC transporters: functional relevance of the genetic polymorphisms in the *MDR1* and *MRP1* gene. Tartu, 2003.
86. **Jaan Soplepmann**. Peptic ulcer haemorrhage in Estonia: epidemiology, prognostic factors, treatment and outcome. Tartu, 2003.
87. **Margot Peetsalu**. Long-term follow-up after vagotomy in duodenal ulcer disease: recurrent ulcer, changes in the function, morphology and *Helicobacter pylori* colonisation of the gastric mucosa. Tartu, 2003.
88. **Kersti Klaamas**. Humoral immune response to *Helicobacter pylori* a study of host-dependent and microbial factors. Tartu, 2003.
89. **Pille Taba**. Epidemiology of Parkinson's disease in Tartu, Estonia. Prevalence, incidence, clinical characteristics, and pharmacoepidemiology. Tartu, 2003.
90. **Alar Veraksitš**. Characterization of behavioural and biochemical phenotype of cholecystokinin-2 receptor deficient mice: changes in the function of the dopamine and endopioidergic system. Tartu, 2003.
91. **Ingrid Kalev**. CC-chemokine receptor 5 (CCR5) gene polymorphism in Estonians and in patients with Type I and Type II diabetes mellitus. Tartu, 2003.
92. **Lumme Kadaja**. Molecular approach to the regulation of mitochondrial function in oxidative muscle cells. Tartu, 2003.
93. **Aive Liigant**. Epidemiology of primary central nervous system tumours in Estonia from 1986 to 1996. Clinical characteristics, incidence, survival and prognostic factors. Tartu, 2004.
94. **Andres, Kulla**. Molecular characteristics of mesenchymal stroma in human astrocytic gliomas. Tartu, 2004.
95. **Mari Järvelaid**. Health damaging risk behaviours in adolescence. Tartu, 2004.
96. **Ülle Pechter**. Progression prevention strategies in chronic renal failure and hypertension. An experimental and clinical study. Tartu, 2004.
97. **Gunnar Tasa**. Polymorphic glutathione S-transferases – biology and role in modifying genetic susceptibility to senile cataract and primary open angle glaucoma. Tartu, 2004.
98. **Tuuli Käämbre**. Intracellular energetic unit: structural and functional aspects. Tartu, 2004.
99. **Vitali Vassiljev**. Influence of nitric oxide syntase inhibitors on the effects of ethanol after acute and chronic ethanol administration and withdrawal. Tartu, 2004.

100. **Aune Rehema**. Assessment of nonhaem ferrous iron and glutathione redox ratio as markers of pathogeneticity of oxidative stress in different clinical groups. Tartu, 2004.
101. **Evelin Seppet**. Interaction of mitochondria and ATPases in oxidative muscle cells in normal and pathological conditions. Tartu, 2004.
102. **Eduard Maron**. Serotonin function in panic disorder: from clinical experiments to brain imaging and genetics. Tartu, 2004.
103. **Marje Oona**. *Helicobacter pylori* infection in children: epidemiological and therapeutic aspects. Tartu, 2004.
104. **Kersti Kokk**. Regulation of active and passive molecular transport in the testis. Tartu, 2005.
105. **Vladimir Järv**. Cross-sectional imaging for pretreatment evaluation and follow-up of pelvic malignant tumours. Tartu, 2005.
106. **Andre Õun**. Epidemiology of adult epilepsy in Tartu, Estonia. Incidence, prevalence and medical treatment. Tartu, 2005.
107. **Piibe Muda**. Homocysteine and hypertension: associations between homocysteine and essential hypertension in treated and untreated hypertensive patients with and without coronary artery disease. Tartu, 2005.
108. **Külli Kingo**. The interleukin-10 family cytokines gene polymorphisms in plaque psoriasis. Tartu, 2005.
109. **Mati Merila**. Anatomy and clinical relevance of the glenohumeral joint capsule and ligaments. Tartu, 2005.
110. **Epp Songisepp**. Evaluation of technological and functional properties of the new probiotic *Lactobacillus fermentum* ME-3. Tartu, 2005.
111. **Tiia Ainla**. Acute myocardial infarction in Estonia: clinical characteristics, management and outcome. Tartu, 2005.
112. **Andres Sell**. Determining the minimum local anaesthetic requirements for hip replacement surgery under spinal anaesthesia – a study employing a spinal catheter. Tartu, 2005.
113. **Tiia Tamme**. Epidemiology of odontogenic tumours in Estonia. Pathogenesis and clinical behaviour of ameloblastoma. Tartu, 2005.
114. **Triine Annus**. Allergy in Estonian schoolchildren: time trends and characteristics. Tartu, 2005.
115. **Tiia Voor**. Microorganisms in infancy and development of allergy: comparison of Estonian and Swedish children. Tartu, 2005.
116. **Priit Kasenõmm**. Indicators for tonsillectomy in adults with recurrent tonsillitis – clinical, microbiological and pathomorphological investigations. Tartu, 2005.
117. **Eva Zusinaite**. Hepatitis C virus: genotype identification and interactions between viral proteases. Tartu, 2005.
118. **Piret Kõll**. Oral lactoflora in chronic periodontitis and periodontal health. Tartu, 2006.
119. **Tiina Stelmach**. Epidemiology of cerebral palsy and unfavourable neurodevelopmental outcome in child population of Tartu city and county, Estonia Prevalence, clinical features and risk factors. Tartu, 2006.

120. **Katrin Pudersell**. Tropane alkaloid production and riboflavine excretion in the field and tissue cultures of henbane (*Hyoscyamus niger* L.). Tartu, 2006.
121. **Külli Jaako**. Studies on the role of neurogenesis in brain plasticity. Tartu, 2006.
122. **Aare Märtson**. Lower limb lengthening: experimental studies of bone regeneration and long-term clinical results. Tartu, 2006.
123. **Heli Tähepõld**. Patient consultation in family medicine. Tartu, 2006.
124. **Stanislav Liskmann**. Peri-implant disease: pathogenesis, diagnosis and treatment in view of both inflammation and oxidative stress profiling. Tartu, 2006.
125. **Ruth Rudissaar**. Neuropharmacology of atypical antipsychotics and an animal model of psychosis. Tartu, 2006.
126. **Helena Andreson**. Diversity of *Helicobacter pylori* genotypes in Estonian patients with chronic inflammatory gastric diseases. Tartu, 2006.
127. **Katrin Pruus**. Mechanism of action of antidepressants: aspects of serotoninergic system and its interaction with glutamate. Tartu, 2006.
128. **Priit Põder**. Clinical and experimental investigation: relationship of ischaemia/reperfusion injury with oxidative stress in abdominal aortic aneurysm repair and in extracranial brain artery endarterectomy and possibilities of protection against ischaemia using a glutathione analogue in a rat model of global brain ischaemia. Tartu, 2006.
129. **Marika Tammaru**. Patient-reported outcome measurement in rheumatoid arthritis. Tartu, 2006.
130. **Tiia Reimand**. Down syndrome in Estonia. Tartu, 2006.
131. **Diva Eensoo**. Risk-taking in traffic and Markers of Risk-Taking Behaviour in Schoolchildren and Car Drivers. Tartu, 2007.
132. **Riina Vibo**. The third stroke registry in Tartu, Estonia from 2001 to 2003: incidence, case-fatality, risk factors and long-term outcome. Tartu, 2007.
133. **Chris Pruunsild**. Juvenile idiopathic arthritis in children in Estonia. Tartu, 2007.
134. **Eve Õiglane-Šlik**. Angelman and Prader-Willi syndromes in Estonia. Tartu, 2007.
135. **Kadri Haller**. Antibodies to follicle stimulating hormone. Significance in female infertility. Tartu, 2007.
136. **Pille Ööpik**. Management of depression in family medicine. Tartu, 2007.
137. **Jaak Kals**. Endothelial function and arterial stiffness in patients with atherosclerosis and in healthy subjects. Tartu, 2007.
138. **Priit Kampus**. Impact of inflammation, oxidative stress and age on arterial stiffness and carotid artery intima-media thickness. Tartu, 2007.
139. **Margus Punab**. Male fertility and its risk factors in Estonia. Tartu, 2007.
140. **Alar Toom**. Heterotopic ossification after total hip arthroplasty: clinical and pathogenetic investigation. Tartu, 2007.

141. **Lea Pehme**. Epidemiology of tuberculosis in Estonia 1991–2003 with special regard to extrapulmonary tuberculosis and delay in diagnosis of pulmonary tuberculosis. Tartu, 2007.
142. **Juri Karjagin**. The pharmacokinetics of metronidazole and meropenem in septic shock. Tartu, 2007.
143. **Inga Talvik**. Inflicted traumatic brain injury shaken baby syndrome in Estonia – epidemiology and outcome. Tartu, 2007.
144. **Tarvo Rajasalu**. Autoimmune diabetes: an immunological study of type 1 diabetes in humans and in a model of experimental diabetes (in RIP-B7.1 mice). Tartu, 2007.
145. **Inga Karu**. Ischaemia-reperfusion injury of the heart during coronary surgery: a clinical study investigating the effect of hyperoxia. Tartu, 2007.
146. **Peeter Padrik**. Renal cell carcinoma: Changes in natural history and treatment of metastatic disease. Tartu, 2007.
147. **Neve Vendt**. Iron deficiency and iron deficiency anaemia in infants aged 9 to 12 months in Estonia. Tartu, 2008.
148. **Lenne-Triin Heidmets**. The effects of neurotoxins on brain plasticity: focus on neural Cell Adhesion Molecule. Tartu, 2008.
149. **Paul Korrovits**. Asymptomatic inflammatory prostatitis: prevalence, etiological factors, diagnostic tools. Tartu, 2008.
150. **Annika Reintam**. Gastrointestinal failure in intensive care patients. Tartu, 2008.
151. **Kristiina Roots**. Cationic regulation of Na-pump in the normal, Alzheimer's and CCK_2 receptor-deficient brain. Tartu, 2008.
152. **Helen Puusepp**. The genetic causes of mental retardation in Estonia: fragile X syndrome and creatine transporter defect. Tartu, 2009.
153. **Kristiina Rull**. Human chorionic gonadotropin beta genes and recurrent miscarriage: expression and variation study. Tartu, 2009.
154. **Margus Eimre**. Organization of energy transfer and feedback regulation in oxidative muscle cells. Tartu, 2009.
155. **Maire Link**. Transcription factors FoxP3 and AIRE: autoantibody associations. Tartu, 2009.
156. **Kai Haldre**. Sexual health and behaviour of young women in Estonia. Tartu, 2009.
157. **Kaur Liivak**. Classical form of congenital adrenal hyperplasia due to 21-hydroxylase deficiency in Estonia: incidence, genotype and phenotype with special attention to short-term growth and 24-hour blood pressure. Tartu, 2009.
158. **Kersti Ehrlich**. Antioxidative glutathione analogues (UPF peptides) – molecular design, structure-activity relationships and testing the protective properties. Tartu, 2009.
159. **Anneli Rätsep**. Type 2 diabetes care in family medicine. Tartu, 2009.
160. **Silver Türk**. Etiopathogenetic aspects of chronic prostatitis: role of mycoplasmas, coryneform bacteria and oxidative stress. Tartu, 2009.

161. **Kaire Heilman**. Risk markers for cardiovascular disease and low bone mineral density in children with type 1 diabetes. Tartu, 2009.
162. **Kristi Rüütel**. HIV-epidemic in Estonia: injecting drug use and quality of life of people living with HIV. Tartu, 2009.
163. **Triin Eller**. Immune markers in major depression and in antidepressive treatment. Tartu, 2009.
164. **Siim Suutre**. The role of TGF-β isoforms and osteoprogenitor cells in the pathogenesis of heterotopic ossification. An experimental and clinical study of hip arthroplasty. Tartu, 2010.
165. **Kai Kliiman**. Highly drug-resistant tuberculosis in Estonia: Risk factors and predictors of poor treatment outcome. Tartu, 2010.
166. **Inga Villa**. Cardiovascular health-related nutrition, physical activity and fitness in Estonia. Tartu, 2010.
167. **Tõnis Org**. Molecular function of the first PHD finger domain of Autoimmune Regulator protein. Tartu, 2010.
168. **Tuuli Metsvaht**. Optimal antibacterial therapy of neonates at risk of early onset sepsis. Tartu, 2010.
169. **Jaanus Kahu**. Kidney transplantation: Studies on donor risk factors and mycophenolate mofetil. Tartu, 2010.
170. **Koit Reimand**. Autoimmunity in reproductive failure: A study on associated autoantibodies and autoantigens. Tartu, 2010.
171. **Mart Kull**. Impact of vitamin D and hypolactasia on bone mineral density: a population based study in Estonia. Tartu, 2010.
172. **Rael Laugesaar**. Stroke in children – epidemiology and risk factors. Tartu, 2010.
173. **Mark Braschinsky**. Epidemiology and quality of life issues of hereditary spastic paraplegia in Estonia and implemention of genetic analysis in everyday neurologic practice. Tartu, 2010.
174. **Kadri Suija**. Major depression in family medicine: associated factors, recurrence and possible intervention. Tartu, 2010.
175. **Jarno Habicht**. Health care utilisation in Estonia: socioeconomic determinants and financial burden of out-of-pocket payments. Tartu, 2010.
176. **Kristi Abram**. The prevalence and risk factors of rosacea. Subjective disease perception of rosacea patients. Tartu, 2010.
177. **Malle Kuum**. Mitochondrial and endoplasmic reticulum cation fluxes: Novel roles in cellular physiology. Tartu, 2010.
178. **Rita Teek**. The genetic causes of early onset hearing loss in Estonian children. Tartu, 2010.
179. **Daisy Volmer**. The development of community pharmacy services in Estonia – public and professional perceptions 1993–2006. Tartu, 2010.
180. **Jelena Lissitsina**. Cytogenetic causes in male infertility. Tartu, 2011.
181. **Delia Lepik**. Comparison of gunshot injuries caused from Tokarev, Makarov and Glock 19 pistols at different firing distances. Tartu, 2011.
182. **Ene-Renate Pähkla**. Factors related to the efficiency of treatment of advanced periodontitis. Tartu, 2011.

183. **Maarja Krass**. L-Arginine pathways and antidepressant action. Tartu, 2011.
184. **Taavi Lai**. Population health measures to support evidence-based health policy in Estonia. Tartu, 2011.
185. **Tiit Salum**. Similarity and difference of temperature-dependence of the brain sodium pump in normal, different neuropathological, and aberrant conditions and its possible reasons. Tartu, 2011.
186. **Tõnu Vooder**. Molecular differences and similarities between histological subtypes of non-small cell lung cancer. Tartu, 2011.
187. **Jelena Štšepetova**. The characterisation of intestinal lactic acid bacteria using bacteriological, biochemical and molecular approaches. Tartu, 2011.
188. **Radko Avi**. Natural polymorphisms and transmitted drug resistance in Estonian HIV-1 CRF06_cpx and its recombinant viruses. Tartu, 2011, 116 p.
189. **Edward Laane**. Multiparameter flow cytometry in haematological malignancies. Tartu, 2011, 152 p.
190. **Triin Jagomägi**. A study of the genetic etiology of nonsyndromic cleft lip and palate. Tartu, 2011, 158 p.
191. **Ivo Laidmäe**. Fibrin glue of fish (*Salmo salar*) origin: immunological study and development of new pharmaceutical preparation. Tartu, 2012, 150 p.
192. **Ülle Parm**. Early mucosal colonisation and its role in prediction of invasive infection in neonates at risk of early onset sepsis. Tartu, 2012, 168 p.
193. **Kaupo Teesalu**. Autoantibodies against desmin and transglutaminase 2 in celiac disease: diagnostic and functional significance. Tartu, 2012, 142 p.
194. **Maksim Zagura**. Biochemical, functional and structural profiling of arterial damage in atherosclerosis. Tartu, 2012, 162 p.
195. **Vivian Kont**. Autoimmune regulator: characterization of thymic gene regulation and promoter methylation. Tartu, 2012, 134 p.
196. **Pirje Hütt**. Functional properties, persistence, safety and efficacy of potential probiotic lactobacilli. Tartu, 2012, 246 p.
197. **Innar Tõru**. Serotonergic modulation of CCK-4- induced panic. Tartu, 2012, 132 p.
198. **Sigrid Vorobjov**. Drug use, related risk behaviour and harm reduction interventions utilization among injecting drug users in Estonia: implications for drug policy. Tartu, 2012, 120 p.
199. **Martin Serg**. Therapeutic aspects of central haemodynamics, arterial stiffness and oxidative stress in hypertension. Tartu, 2012, 156 p.
200. **Jaanika Kumm**. Molecular markers of articular tissues in early knee osteoarthritis: a population-based longitudinal study in middle-aged subjects. Tartu, 2012, 159 p.
201. **Kertu Rünkorg**. Functional changes of dopamine, endopioid and endocannabinoid systems in CCK2 receptor deficient mice. Tartu, 2012, 125 p.
202. **Mai Blöndal**. Changes in the baseline characteristics, management and outcomes of acute myocardial infarction in Estonia. Tartu, 2012, 127 p.

203. **Jana Lass**. Epidemiological and clinical aspects of medicines use in children in Estonia. Tartu, 2012, 170 p.
204. **Kai Truusalu**. Probiotic lactobacilli in experimental persistent *Salmonella* infection. Tartu, 2013, 139 p.
205. **Oksana Jagur**. Temporomandibular joint diagnostic imaging in relation to pain and bone characteristics. Long-term results of arthroscopic treatment. Tartu, 2013, 126 p.
206. **Katrin Sikk**. Manganese-ephedrone intoxication – pathogenesis of neurological damage and clinical symptomatology. Tartu, 2013, 125 p.
207. **Kai Blöndal**. Tuberculosis in Estonia with special emphasis on drug-resistant tuberculosis: Notification rate, disease recurrence and mortality. Tartu, 2013, 151 p.
208. **Marju Puurand**. Oxidative phosphorylation in different diseases of gastric mucosa. Tartu, 2013, 123 p.
209. **Aili Tagoma**. Immune activation in female infertility: Significance of autoantibodies and inflammatory mediators. Tartu, 2013, 135 p.
210. **Liis Sabre**. Epidemiology of traumatic spinal cord injury in Estonia. Brain activation in the acute phase of traumatic spinal cord injury. Tartu, 2013, 135 p.
211. **Merit Lamp**. Genetic susceptibility factors in endometriosis. Tartu, 2013, 125 p.
212. **Erik Salum**. Beneficial effects of vitamin D and angiotensin II receptor blocker on arterial damage. Tartu, 2013, 167 p.
213. **Maire Karelson**. Vitiligo: clinical aspects, quality of life and the role of melanocortin system in pathogenesis. Tartu, 2013, 153 p.
214. **Kuldar Kaljurand**. Prevalence of exfoliation syndrome in Estonia and its clinical significance. Tartu, 2013, 113 p.
215. **Raido Paasma**. Clinical study of methanol poisoning: handling large outbreaks, treatment with antidotes, and long-term outcomes. Tartu, 2013, 96 p.
216. **Anne Kleinberg**. Major depression in Estonia: prevalence, associated factors, and use of health services. Tartu, 2013, 129 p.
217. **Triin Eglit**. Obesity, impaired glucose regulation, metabolic syndrome and their associations with high-molecular-weight adiponectin levels. Tartu, 2014, 115 p.
218. **Kristo Ausmees**. Reproductive function in middle-aged males: Associations with prostate, lifestyle and couple infertility status. Tartu, 2014, 125 p.
219. **Kristi Huik**. The influence of host genetic factors on the susceptibility to HIV and HCV infections among intravenous drug users. Tartu, 2014, 144 p.
220. **Liina Tserel**. Epigenetic profiles of monocytes, monocyte-derived macrophages and dendritic cells. Tartu, 2014, 143 p.
221. **Irina Kerna**. The contribution of *ADAM12* and *CILP* genes to the development of knee osteoarthritis. Tartu, 2014, 152 p.

222. **Ingrid Liiv**. Autoimmune regulator protein interaction with DNA-dependent protein kinase and its role in apoptosis. Tartu, 2014, 143 p.
223. **Liivi Maddison**. Tissue perfusion and metabolism during intra-abdominal hypertension. Tartu, 2014, 103 p.
224. **Krista Ress**. Childhood coeliac disease in Estonia, prevalence in atopic dermatitis and immunological characterisation of coexistence. Tartu, 2014, 124 p.
225. **Kai Muru**. Prenatal screening strategies, long-term outcome of children with marked changes in maternal screening tests and the most common syndromic heart anomalies in Estonia. Tartu, 2014, 189 p.
226. **Kaja Rahu**. Morbidity and mortality among Baltic Chernobyl cleanup workers: a register-based cohort study. Tartu, 2014, 155 p.
227. **Klari Noormets**. The development of diabetes mellitus, fertility and energy metabolism disturbances in a Wfs1-deficient mouse model of Wolfram syndrome. Tartu, 2014, 132 p.
228. **Liis Toome**. Very low gestational age infants in Estonia. Tartu, 2014, 183 p.
229. **Ceith Nikkolo**. Impact of different mesh parameters on chronic pain and foreign body feeling after open inguinal hernia repair. Tartu, 2014, 132 p.
230. **Vadim Brjalin**. Chronic hepatitis C: predictors of treatment response in Estonian patients. Tartu, 2014, 122 p.
231. **Vahur Metsna**. Anterior knee pain in patients following total knee arthroplasty: the prevalence, correlation with patellar cartilage impairment and aspects of patellofemoral congruence. Tartu, 2014, 130 p.
232. **Marju Kase**. Glioblastoma multiforme: possibilities to improve treatment efficacy. Tartu, 2015, 137 p.
233. **Riina Runnel**. Oral health among elementary school children and the effects of polyol candies on the prevention of dental caries. Tartu, 2015, 112 p.
234. **Made Laanpere**. Factors influencing women's sexual health and reproductive choices in Estonia. Tartu, 2015, 176 p.
235. **Andres Lust**. Water mediated solid state transformations of a polymorphic drug – effect on pharmaceutical product performance. Tartu, 2015, 134 p.
236. **Anna Klugman**. Functionality related characterization of pretreated wood lignin, cellulose and polyvinylpyrrolidone for pharmaceutical applications. Tartu, 2015, 156 p.
237. **Triin Laisk-Podar**. Genetic variation as a modulator of susceptibility to female infertility and a source for potential biomarkers. Tartu, 2015, 155 p.
238. **Mailis Tõnisson**. Clinical picture and biochemical changes in blood in children with acute alcohol intoxication. Tartu, 2015, 100 p.
239. **Kadri Tamme**. High volume haemodiafiltration in treatment of severe sepsis – impact on pharmacokinetics of antibiotics and inflammatory response. Tartu, 2015, 133 p.

240. **Kai Part**. Sexual health of young people in Estonia in a social context: the role of school-based sexuality education and youth-friendly counseling services. Tartu, 2015, 203 p.
241. **Urve Paaver**. New perspectives for the amorphization and physical stabilization of poorly water-soluble drugs and understanding their dissolution behavior. Tartu, 2015, 139 p.
242. **Aleksandr Peet**. Intrauterine and postnatal growth in children with HLA-conferred susceptibility to type 1 diabetes. Tartu. 2015, 146 p.
243. **Piret Mitt**. Healthcare-associated infections in Estonia – epidemiology and surveillance of bloodstream and surgical site infections. Tartu, 2015, 145 p.
244. **Merli Saare**. Molecular Profiling of Endometriotic Lesions and Endometria of Endometriosis Patients. Tartu, 2016, 129 p.
245. **Kaja-Triin Laisaar**. People living with HIV in Estonia: Engagement in medical care and methods of increasing adherence to antiretroviral therapy and safe sexual behavior. Tartu, 2016, 132 p.
246. **Eero Merilind**. Primary health care performance: impact of payment and practice-based characteristics. Tartu, 2016, 120 p.
247. **Jaanika Kärner**. Cytokine-specific autoantibodies in AIRE deficiency. Tartu, 2016, 182 p.
248. **Kaido Paapstel**. Metabolomic profile of arterial stiffness and early biomarkers of renal damage in atherosclerosis. Tartu, 2016, 173 p.
249. **Liidia Kiisk**. Long-term nutritional study: anthropometrical and clinico-laboratory assessments in renal replacement therapy patients after intensive nutritional counselling. Tartu, 2016, 207 p.
250. **Georgi Nellis**. The use of excipients in medicines administered to neonates in Europe. Tartu, 2017, 159 p.
251. **Aleksei Rakitin**. Metabolic effects of acute and chronic treatment with valproic acid in people with epilepsy. Tartu, 2017, 125 p.
252. **Eveli Kallas**. The influence of immunological markers to susceptibility to HIV, HBV, and HCV infections among persons who inject drugs. Tartu, 2017, 138 p.
253. **Tiina Freimann**. Musculoskeletal pain among nurses: prevalence, risk factors, and intervention. Tartu, 2017, 125 p.
254. **Evelyn Aaviksoo**. Sickness absence in Estonia: determinants and influence of the sick-pay cut reform. Tartu, 2017, 121 p.
255. **Kalev Nõupuu**. Autosomal-recessive Stargardt disease: phenotypic heterogeneity and genotype-phenotype associations. Tartu, 2017, 131 p.
256. **Ho Duy Binh**. Osteogenesis imperfecta in Vietnam. Tartu, 2017, 125 p.
257. **Uku Haljasorg**. Transcriptional mechanisms in thymic central tolerance. Tartu, 2017, 147 p.
258. **Živile Riispere**. IgA Nephropathy study according to the Oxford Classification: IgA Nephropathy clinical-morphological correlations, disease progression and the effect of renoprotective therapy. Tartu, 2017, 129 p.

259. **Hiie Soeorg**. Coagulase-negative staphylococci in gut of preterm neonates and in breast milk of their mothers. Tartu, 2017, 216 p.
260. **Anne-Mari Anton Willmore**. Silver nanoparticles for cancer research. Tartu, 2017, 132 p.
261. **Ott Laius**. Utilization of osteoporosis medicines, medication adherence and the trend in osteoporosis related hip fractures in Estonia. Tartu, 2017, 134 p.
262. **Alar Aab**. Insights into molecular mechanisms of asthma and atopic dermatitis. Tartu, 2017, 164 p.
263. **Sander Pajusalu**. Genome-wide diagnostics of Mendelian disorders: from chromosomal microarrays to next-generation sequencing. Tartu, 2017, 146 p.
264. **Mikk Jürisson**. Health and economic impact of hip fracture in Estonia. Tartu, 2017, 164 p.
265. **Kaspar Tootsi**. Cardiovascular and metabolomic profiling of osteoarthritis. Tartu, 2017, 150 p.
266. **Mario Saare**. The influence of AIRE on gene expression – studies of transcriptional regulatory mechanisms in cell culture systems. Tartu, 2017, 172 p.
267. **Piia Jõgi**. Epidemiological and clinical characteristics of pertussis in Estonia. Tartu, 2018, 168 p.
268. **Elle Põldoja**. Structure and blood supply of the superior part of the shoulder joint capsule. Tartu, 2018, 116 p.
269. **Minh Son Nguyen**. Oral health status and prevalence of temporomandibular disorders in 65–74-year-olds in Vietnam. Tartu, 2018, 182 p.
270. **Kristian Semjonov**. Development of pharmaceutical quench-cooled molten and melt-electrospun solid dispersions for poorly water-soluble indomethacin. Tartu, 2018, 125 p.
271. **Janne Tiigimäe-Saar**. Botulinum neurotoxin type A treatment for sialorrhea in central nervous system diseases. Tartu, 2018, 109 p.
272. **Veiko Vengerfeldt**. Apical periodontitis: prevalence and etiopathogenetic aspects. Tartu, 2018, 150 p.
273. **Rudolf Bichele**. TNF superfamily and AIRE at the crossroads of thymic differentiation and host protection against *Candida albicans* infection. Tartu, 2018, 153 p.
274. **Olga Tšuiko**. Unravelling Chromosomal Instability in Mammalian Preimplantation Embryos Using Single-Cell Genomics. Tartu, 2018, 169 p.
275. **Kärt Kriisa**. Profile of acylcarnitines, inflammation and oxidative stress in first-episode psychosis before and after antipsychotic treatment. Tartu, 2018, 145 p.
276. **Xuan Dung Ho**. Characterization of the genomic profile of osteosarcoma. Tartu, 2018, 144 p.
277. **Karit Reinson**. New Diagnostic Methods for Early Detection of Inborn Errors of Metabolism in Estonia. Tartu, 2018, 201 p.

278. **Mari-Anne Vals**. Congenital N-glycosylation Disorders in Estonia. Tartu, 2019, 148 p.
279. **Liis Kadastik-Eerme**. Parkinson's disease in Estonia: epidemiology, quality of life, clinical characteristics and pharmacotherapy. Tartu, 2019, 202 p.
280. **Hedi Hunt**. Precision targeting of intraperitoneal tumors with peptide-guided nanocarriers. Tartu, 2019, 179 p.
281. **Rando Porosk**. The role of oxidative stress in Wolfram syndrome 1 and hypothermia. Tartu, 2019, 123 p.
282. **Ene-Ly Jõgeda**. The influence of coinfections and host genetic factor on the susceptibility to HIV infection among people who inject drugs. Tartu, 2019, 126 p.
283. **Kristel Ehala-Aleksejev**. The associations between body composition, obesity and obesity-related health and lifestyle conditions with male reproductive function. Tartu, 2019, 138 p.
284. **Aigar Ottas**. The metabolomic profiling of psoriasis, atopic dermatitis and atherosclerosis. Tartu, 2019, 136 p.
285. **Elmira Gurbanova**. Specific characteristics of tuberculosis in low default, but high multidrug–resistance prison setting. Tartu, 2019, 129 p.
286. **Van Thai Nguyeni**. The first study of the treatment outcomes of patients with cleft lip and palate in Central Vietnam. Tartu, 2019, 144 p.
287. **Maria Yakoreva**. Imprinting Disorders in Estonia. Tartu, 2019, 187 p.
288. **Kadri Rekker**. The putative role of microRNAs in endometriosis pathogenesis and potential in diagnostics. Tartu, 2019, 140 p.
289. **Ülle Võhma**. Association between personality traits, clinical characteristics and pharmacological treatment response in panic disorder. Tartu, 2019, 121 p.
290. **Aet Saar**. Acute myocardial infarction in Estonia 2001–2014: towards risk-based prevention and management. Tartu, 2019, 124 p.
291. **Toomas Toomsoo**. Transcranial brain sonography in the Estonian cohort of Parkinson's disease. Tartu, 2019, 114 p.
292. **Lidiia Zhytnik**. Inter- and intrafamilial diversity based on genotype and phenotype correlations of Osteogenesis Imperfecta. Tartu, 2019, 224 p.
293. **Pilleriin Soodla**. Newly HIV-infected people in Estonia: estimation of incidence and transmitted drug resistance. Tartu, 2019, 194 p.
294. **Kristiina Ojamaa**. Epidemiology of gynecological cancer in Estonia. Tartu, 2020, 133 p.
295. **Marianne Saard**. Modern Cognitive and Social Intervention Techniques in Paediatric Neurorehabilitation for Children with Acquired Brain Injury. Tartu, 2020, 168 p.
296. **Julia Maslovskaja**. The importance of DNA binding and DNA breaks for AIRE-mediated transcriptional activation. Tartu, 2020, 162 p.
297. **Natalia Lobanovskaya**. The role of PSA-NCAM in the survival of retinal ganglion cells. Tartu, 2020, 105 p.

298. **Madis Rahu**. Structure and blood supply of the postero-superior part of the shoulder joint capsule with implementation of surgical treatment after anterior traumatic dislocation. Tartu, 2020, 104 p.
299. **Helen Zirnask**. Luteinizing hormone (LH) receptor expression in the penis and its possible role in pathogenesis of erectile disturbances. Tartu, 2020, 87 p.
300. **Kadri Toome**. Homing peptides for targeting of brain diseases. Tartu, 2020, 152 p.
301. **Maarja Hallik**. Pharmacokinetics and pharmacodynamics of inotropic drugs in neonates. Tartu, 2020, 172 p.
302. **Raili Müller**. Cardiometabolic risk profile and body composition in early rheumatoid arthritis. Tartu, 2020, 133 p.
303. **Sergo Kasvandik**. The role of proteomic changes in endometrial cells – from the perspective of fertility and endometriosis. Tartu, 2020, 191 p.
304. **Epp Kaleviste**. Genetic variants revealing the role of STAT1/STAT3 signaling cytokines in immune protection and pathology. Tartu, 2020, 189 p.
305. **Sten Saar**. Epidemiology of severe injuries in Estonia. Tartu, 2020, 104 p.
306. **Kati Braschinsky**. Epidemiology of primary headaches in Estonia and applicability of web-based solutions in headache epidemiology research. Tartu, 2020, 129 p.
307. **Helen Vaher**. MicroRNAs in the regulation of keratinocyte responses in *psoriasis vulgaris* and atopic dermatitis. Tartu, 2020, 242 p.
308. **Liisi Raam**. Molecular Alterations in the Pathogenesis of Two Chronic Dermatoses – Vitiligo and Psoriasis. Tartu, 2020, 164 p.
309. **Artur Vetkas**. Long-term quality of life, emotional health, and associated factors in patients after aneurysmal subarachnoid haemorrhage. Tartu, 2020, 127 p.
310. **Teele Kasepalu**. Effects of remote ischaemic preconditioning on organ damage and acylcarnitines' metabolism in vascular surgery. Tartu, 2020, 130 p.
311. **Prakash Lingasamy**. Development of multitargeted tumor penetrating peptides. Tartu, 2020, 246 p.
312. **Lille Kurvits.** Parkinson's disease as a multisystem disorder: whole transcriptome study in Parkinson's disease patients' skin and blood. Tartu, 2021, 142 p.
313. **Mariliis Põld.** Smoking, attitudes towards smoking behaviour, and nicotine dependence among physicians in Estonia: cross-sectional surveys 1982–2014. Tartu, 2021, 172 p.
314. **Triin Kikas**. Single nucleotide variants affecting placental gene expression and pregnancy outcome. Tartu, 2021, 160 p.
315. **Hedda Lippus-Metsaots**. Interpersonal violence in Estonia: prevalence, impact on health and health behaviour. Tartu, 2021, 172 p.

316. **Georgi Dzaparidze.** Quantification and evaluation of the diagnostic significance of adenocarcinoma-associated microenvironmental changes in the prostate using modern digital pathology solutions. Tartu, 2021, 132 p.
317. **Tuuli Sedman.** New avenues for GLP1 receptor agonists in the treatment of diabetes. Tartu, 2021, 118 p.
318. **Martin Padar.** Enteral nutrition, gastrointestinal dysfunction and intestinal biomarkers in critically ill patients. Tartu, 2021, 189 p.
319. **Siim Schneider.** Risk factors, etiology and long-term outcome in young ischemic stroke patients in Estonia. Tartu, 2021, 131 p.
320. **Konstantin Ridnõi.** Implementation and effectiveness of new prenatal diagnostic strategies in Estonia. Tartu, 2021, 191 p.
321. **Risto Vaikjärv.** Etiopathogenetic and clinical aspects of peritonsillar abscess. Tartu, 2021, 115 p.